EFFECT OF A NATURAL COMPOUND MALABARICONE C, ON CARDIOVASCULAR DISEASE AND REMODELING

By

Jitesh Singh Rathee

(LIFE01200804010)

Bhabha Atomic Research Centre, Mumbai

A thesis submitted to the

Board of Studies in Life Sciences

In partial fulfillment of requirements

For the Degree of

DOCTOR OF PHILOSOPHY

of

HOMI BHABHA NATIONAL INSTITUTE

December, 2015

Homi Bhabha National Institute

Recommendations of the Viva Voce Board

As members of the Viva Voce Board, we certify that we have read the dissertation prepared by Mr. Jitesh Singh Rathee entitled "Effect of a natural compound malabaricone C, on cardiovascular disease and remodeling" and recommend that it may be accepted as fulfilling the dissertation requirement for the Degree of Doctor of Philosophy.

K. Indira Priyadarshini Date: 22.4.16

Chairman – **Dr. K. Indira Priyadarshini**

Date: 22.04.2016

Guide / Convener - **Dr. B. S. Patro**

Date: 22/4/16

Member 1 – **Dr. S Santosh Kumar**

B.N. Pandey Date: 22/4/16

Member 2 - **Dr. B N Pandey**

Date: 22.4.16

External examiner: **Dr. Shyamal K Goswami**

Final approval and acceptance of this dissertation is contingent upon the candidate's submission of the final copies of the dissertation to HBNI.

I hereby certify that I have read this dissertation prepared under my direction and recommend that it may be accepted as fulfilling the dissertation requirement.

Date: 22.04.2016

Place: Mumbai

Dr. B. S. Patro (Guide)

STATEMENT BY AUTHOR

This dissertation has been submitted in partial fulfillment of requirements for an advanced degree at Homi Bhabha National Institute (HBNI) and is deposited in the Library to be made available to borrowers under rules of the HBNI.

Brief quotations from this dissertation are allowable without special permission, provided that accurate acknowledgement of source is made. Requests for permission for extended quotation from or reproduction of this manuscript in whole or in part may be granted by the Competent Authority of HBNI when in his or her judgment the proposed use of the material is in the interests of scholarship. In all other instances, however, permission must be obtained from the author.

Jitesh Singh Rathee

DECLARATION

I, hereby declare that the investigation presented in the thesis has been carried out by me. The work is original and has not been submitted earlier as a whole or in part for a degree / diploma at this or any other Institution / University.

Jitesh Singh Rathee

List of Publications arising from the thesis

Journal

1. Mechanism of the anti-hypertensive property of the naturally occurring phenolic, malabaricone C in DOCA-rats. Jitesh S. Rathee, Birija S. Patro, Lindsay Brown, and Subrata Chattopadhyay. *FRR Volume 50, Issue 1, 2016, DOI: 10.3109/10715762.2015 .1112005*

2 Cardiovascular remodulatory effect of a naturally occurring phenolic, malabaricone C in DOCA-rats. Jitesh S. Rathee, Lindsay Brown, and Subrata Chattopadhyay. Manuscript communicated to *Pharmacology Research*

Conferences

1. Targeting cardiovascular disease with a novel dietary molecule, malabaricone C. INVITED Lecture. Jitesh Rathee and S. Chattopadhyay. *International Conference on Cardiovascular Translational Research and the 13th Annual Conference of ISHR (Indian Section).* Jan 22-24, 2016, IIT Madras, Chennai, India.

2. Cardiovascular remodeling property of a malabaricone C in DOCA-salt hypertensive rats. Jitesh Rathee and S. Chattopadhyay. in *International Symposium on Advances In Free Radicals, Redox Signaling And Translational Antioxidant Research (SFRR-STAR).* Lucknow (Jan 2013)

3. Antihypertensive activity of a natural phenolic malabaricone C in DOCA-salt rats. Jitesh Rathee and S. Chattopadhyay. in *International Conference on Recent Advances In Free Radical Research, Natural Products, Antioxidants & Radio-protectors In Health*. Hydrabad (Jan 2010)

In Loving Memory

Of

My father (Late Ch. B S Rathee)

and my

mother (Mrs. Krishna Rathee)

ACKNOWLEDGEMENTS

First of all, I feel highly privileged to express my heartfelt sincere gratitude to Professor Subrata Chattopadhyay, HBNI and Associate Director (B), Bio-science group, BARC, Mumbai. I am appreciative of his constant motivation and endeavor to extract best out of me through his guidance, advice, patience, time and support. It's my fortune and I am proud to have him as my mentor. His parental affection, infectious optimism, bright spirits, never say die attitude and belief in me were invaluable at every stumble or wrong turn in both personal and professional life. I will remain indebted forever to him.

Words are not enough to thank Professor Lindsay Brown University of Southern Queensland, Australia, for introducing me into the wonderful world of cardio vascular system. From my first steps in the vast maize of intricacies in the system to the more assured strides, he was always there, showing the way with his, constant encouragement and support. I would also like to thank his lab members for helping me to learn the surgical techniques and other intricacies of the subject.

I wish to express my deep gratitude to my guide Dr. B. S. Patro, Associate Professor, HBNI, and Scientific officer 'G', BOD, BARC for providing me an opportunity to work under his guidance for Ph.D. I am appreciative of his guidance, advice, patience and time. It's my fortune and I am proud to have him as my guide. Indeed, I am honored to be one of his students.

I would like to take this opportunity to thank Dr. H. D Sarma, Head Animal House Facility, BARC, for his constant support and help, especially allowing me the opportunity to use animal house facilities in thick and thin.

I would also like to express my deep gratitude to Dr. K. Indira Priyadarshini, Chairman of my doctoral committee and the members Dr. S Santosh Kumar and Dr. B N Pandey for their kind support, encouragement, constructive criticisms, and suggestions for the improvement of the doctoral work. They are always available for helping and supporting me during my thesis work. I would also like to specially acknowledge Dr Anubha Sharma, Associate Professor HBNI and Scientific Officer 'H', BARC for her constant moral and emotional support anytime I needed. She was always there in all the situations. I also wish to thank my lab colleagues Mr Mrityunjay, Mr Saikat, and Ms Pooja, for providing constructive suggestions throughout the work and cordial environment in the lab. I would also like to thank all the BOD staff for their constant support and encouragement. I take this opportunity to thank Dr. Hema, Dean, Lifesciences, HBNI, for her constant support during all the submissions and also being approachable.

I am deeply indebted to my parents who enlighten the way of my life with their painstaking efforts and hard work, care, love, and contribution for shaping and moulding my scientific career. I wish to acknowledge my continued debt to my sisters and jija ji for their moral support, kind help, encouragement and fruitful nature which make me to share all the things with them. I would also like to thank my wife for her constant encouragement for doing the good work. I am at a loss of words to thank 'Nachiket' and 'Sparsh' my bundles of joy who has brought so much sunshine in our lives. Their smile and sweet innocent talks are the best stress busters I can ever wished. My thesis could never have seen the light of the day without them.

Date **22.12.2015** **Jitesh Singh Rathee**

INDEX

CONTENTS PAGE NOS.

List of figures

List of tables

SYNOPOSIS

Chapter I will be **introduction** to the topic

Cardiovascular disease (CVD) is a medical complication affecting heart, kidney and blood vessels, accounting for about 31% of human death worldwide in 2012. By 2020, CVD is likely to become the single leading cause of death and disability in India (1). Chronic hypertension (HT) is the insidious culprit and one of the major risk factors of CVD prevalence. Uncontrolled HT leads to a pathological process to the heart and vasculature, known as cardiovascular remodeling that involves change in the size, shape and function of the heart and vessels as a physiological response to metabolic or hormonal changes in the body. These lead to hypertrophy, necrosis and apoptosis of the myocyte and vascular tissues, and fibrosis in the vessels along with cardiac interstitial and perivascular regions (2). Eventually vascular endothelial and smooth muscle dysfunction leads to abnormalities in systolic and diastolic cardiac function including impaired contractility and relaxation, diminished cardiac pump function, decreased myocyte electrical conduction pattern, dilatation and increased sphericity of the heart. The clinically used drugs against HT and CVD have side effects, warranting search for newer alternatives.

The deoxycorticosterone acetate (DOCA) salt-rat is a renin-independent, volume overload HT model widely-used for drug development. The model induces HT with extensive cardiovascular remodeling and endothelial dysfunction. Electrical conduction abnormalities are also manifested in this, as revealed from the changes in action potential durations, and electrocardiogram changes (ECG). The DOCA-salt rat hearts show restrictive chamber filling, decreased cardiac output, contractile and relaxation measurements, increased diastolic stiffness and vascular hypertrophy with prominent thickening of the media. The increased arg^8-vasopressin (AVP) and endothelin-1 (ET-1) levels in this model increases oxidative stress (OS), fibrosis, vasoconstriction, and HT.

Consumption of vegetables and fruit-rich diets can lower BP, due to the constituent polyphenolic antioxidants. The diarylnonanoid, malabaricone C (mal C, chemical structure shown in **Fig. 1**), present in the Indian spice, *Myristica malabarica* possess excellent antioxidant and anti-inflammatory activities (3). Hence, the present study was aimed to examine if chronic oral administration of mal C to DOCA-salt hypertensive rats attenuates HT and pathogenic cardiovascular remodeling. The well-known antioxidant, curcumin (4) and the anti-hypertensive drug atenolol were used as the positive controls.

Fig. 1 Chemical structure of mal C

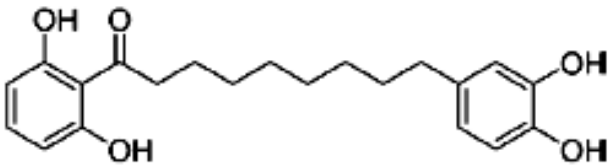

Malabaricone C

Chapter II will describe the **Material and methods**

All chemicals and biochemical assays kits were purchased from reputed manufacturers. Male Wistar rats (6-10 weeks, 300-330 g) were uninephrectomyzed (UNX) and used for the experiments, strictly following the international and institutional ethical guidelines. The UNX rats were subcutaneously injected with DOCA solution (24 mg/0.4 ml in dimethylformamide) every fourth day and given drinking water containing 1% NaCl for 28 days to develop the model. The normal and UNX groups were given an oral dose of vehicle (1% DMSO in PEG, 0.4 ml) only. The treatment groups received mal C (various doses), curcumin (60 mg/kg) or atenolol (10 mg/kg) by oral gavage every day during 15-28 days and the systolic blood pressure (SBP) were non-invasively measured on the 28^{th} day. The invasive SBP and diastolic blood pressure (DBP) as well as histopathological and biochemical parameters of the control, mal C (10 mg/kg, optimized dose) and curcumin (60

mg/kg) groups were measured at the end of the experiments. The parameters *viz*. total nitrates, TBARS, PGI2, AVP, big ET, ET-1, total antioxidant status (TAS), Na^+ and K^+ and Ca^{2+} levels were assayed using the tissue extracts and/or plasma, using commercially available kits according to manufacturer's protocols. The collagen depositions, inflammatory cell infiltrations and aortic superoxide in different tissues were carried out by confocal microscopy after staining with picrosirius red, haematoxylin and eosin (H&E) and dihydroethidium (DHE) respectively. The cardiac infarction was visualized using histology.

The organ bath studies were carried out with thoracic aortic rings in the presence of noradrenaline (NA), acetylcholine (ACh) + NA and sodium nitroprusside (SNP) + NA. The cardiac functions and outputs were assessed by ECG and 2D-Echo *in vivo* (under light sedation) as well as using isolated Langendorf heart preparation (5) and microelectrode studies (6) on isolated LV papillary muscles. The renal and hepatic functions were assessed from the biochemical analysis of plasma. The data of the DOCA-salt group was compared to that of the UNX group, while those of the treatment groups were compared to that of the DOCA-salt group. All data are presented as mean ± S. E. M. of three independent experiments with similar results, carried out with 8 rats/group. The data were analyzed by paired t-test and one-way analysis of variance (ANOVA). A *p*-value of < 0.05 was considered statistically significant.

Chapter III will present **Results and Discussion**

III.1 Toxicity of mal C

Mal C (100 mg/kg/day × one month) was non-toxic, but showed a minor hepatic toxicity at an acute single dose (500 mg/kg). Its plasma bioavailability peaked at 3 h after oral gavaging, but was negligible after 24 h, requiring daily oral dose for these studies. The SBP of the UNX rats, used as the as the control throughout the studies was similar to that of the normal rats.

III.2 Mal C lowers SBP and DBP of the DOCA-salt rats and increases their survival

DOCA-salt administration progressively elevated the SBP of the rats, reaching 228±7 mm Hg on the 28th day. The increased HT in the DOCA-salt rats was not due to salt stress, because the UNX and UNX + salt rats did not show significant changes in SBP, compared to the normal rats. Mal C dose-dependently reduced the DOCA-salt induced SBP, with best potency at 10 mg/kg. Similar anti-hypertensive effect of mal C was also observed in the invasive measurement of SBP and DBP on the 28th day. Mal C (10 mg/kg) was more potent than curcumin (60 mg/kg), and showed comparable SBP reduction as that of atenolol (10 mg/kg). Mal C also improved the survival of rats that was drastically reduced by DOCA-salt. Curcumin (60 mg/kg) and atenolol (10 mg/kg) also increased rat survival, but less than that by mal C. Hence, all subsequent studies were carried out with mal C (10 mg/kg) and the results are presented below. The BP data are shown in table 1.

III.3 Mal C reduces organ hypertrophy of DOCA-salt rats

DOCA-salt administration increased the water intakes of the UNX rats without any gain in body weights. Mal C, but not curcumin decreased the water intakes of the DOCA-salt rats. The increased water intake and volumetric load in the animal is an outcome of excess salt intake, DOCA administration and reduced renal mass (UNX) (7) and reflected organ

Table 1. **Non-invasive SBP of different groups of rats**[a]

days	UNX (mm Hg)	DOCA (mm Hg)	Mal C 2.5 mg/kg (mm Hg)	Mal C 5 mg/kg (mm Hg)	Mal C 10 mg/kg (mm Hg)	Mal C 15 mg/kg (mm Hg)	Mal C 20 mg/kg (mm Hg)	Curcumin 60 mg/kg (mm Hg)
0	121±2.1	122±2.1	123±3.0	125±4.2	122±3.2	118±4.1	125±3.0	118±2.6
15	120±3.1	161±3.1*	158±4.0	160±6.0	162±6.0	165±7.0	160±6.1	161±3.4
28	125±1.3	227±7.3*	210±1.0**	195±7.1**	178±6.3**	175±5.1**	176±4**	183±4.4**

[a]The experimental details are provided in Chapter II. $^{*}P<0.05$ compared to UNX group; $^{**}P<0.05$ compared to the DOCA-salt group.

hypertrophy, often associated with HT (8). Consistent with this, the DOCA-salt rats showed marked right and left ventricles (RV and LV respectively) and kidney hypertrophy, as reflected from the increased wet weights of the organs relative to the body weights. Mal C attenuated the increase in the weights of all these organs indicating decreased hypertrophy. This may reduce the cardiac load and improve cardiac and kidney functions to reduce SBP (9).

III.4 The antioxidant action of mal C may be responsible for its anti-hypertensive property

Oxidative stress is believed to be primarily responsible for HT, vascular disease progression and endothelial dysfunction (10). The results of the OS in the DOCA-salt and treated groups are presented in **Table 2**. As reported earlier (11), the DOCA-salt rats showed reduced plasma TAS and high MDA levels in the LV and aorta, confirming OS. However, mal C treatment brought the plasma TAS nearly to that of the UNX groups, and reduced the MDA levels in different organs. Mal C also dissipated aortic superoxide generation in the DOCA-salt rats, as revealed by DHE staining, and xanthine oxidase (XO) and NADPH oxidase assay. These radicals cause endothelial dysfunction and contributes to hypertrophy and fibrosis. These suggested that mal C may exert its anti-HT action through its antioxidant property.

III.5 Mal C reduces vasoconstriction in DOCA-salt rats

Since narrowing of blood vessels increases SBP (12), the status of the vasoconstrictors (AVP, Big ET and ET-1) and a vasodilator (NO) in the different groups of rats were assessed. The plasma AVP and Big ET levels of the DOCA-salt group were 2.9 and 5.0. folds respectively, compared to that in the UNX rats. Mal C and curcumin treatments reduced such an increase of the plasma AVP level by 68.3% and 46.6% respectively. Mal C and curcumin also reduced the big ET level of the DOCA-salt rats by 45.2% and 37.5% respectively. DOCA-salt increased the aortic ET-1 level of the UNX rats to 4.4 folds, which

was significantly reduced by mal C (56.8%) and curcumin (42.3%). Compared to the UNX rats, total nitrate level in the DOCA-salt rats was reduced by 14.9%. Mal C restored it to that

Table 2 Oxidative stress markers in different groups of rats[a]

Parameter	UNX	DOCA-salt	Mal C-treated	Curcumin-treated
LV TBARS level (µmol MDA/l)	14.1 ± 3.2	61.7 ± 5.3*	24.3 ± 3.1**	33.9 ± 4.2**
Aorta TBARS level (µmol MDA/l)	10.3 ± 2.3	24.4 ± 1.5*	11.3 ± 1.2**	19.3 ± 1.2**
Liver TBARS level (µmol MDA/l)	19.4 ± 2.4	33.8 ± 3.3*	23.3±2.4**	26.4±1.8**
Plasma TAS level (mM Trolox® equivalent)	2.4 ± 0.3	1.1 ± 0.2*	2.1 ± 0.1**	1.5 ± 0.2**
Plasma xanthine oxidase (mU/ml)	17.5 ± 2.0	89.3 ± 8.1*	43.7 ± 5.1**	71.7 ± 6.2**

[a]The experimental details are provided in Chapter II. $^{*}P<0.05$ compared to UNX group; $^{**}P<0.05$ compared to the DOCA-salt group.

of the UNX group, while curcumin augmented it even further. Since vasoconstriction can enhance PGI2 production, we assessed the effect of mal C on PGI2 levels in the DOCA-salt rats. The PGI2 levels in the plasma, LV and aorta of the DOCA-salt group were 1.8, 1.5 and 2.4 folds respectively, compared to the UNX rats. Mal C treatment reduced such increases in these parameters by 13.4%, 18.7% and 55.1% respectively. Curcumin reduced the plasma and aorta PGI2 levels of the DOCA-salt group by 10.6% and 14.4% respectively, without changing the PGI2 level in LV. The results are summarized in **Table 3**.

Collagen depositions and fibrosis are adaptive response to the increased physical stress because of the volumetric load, but can lead to HT (9). Presently, mal C markedly attenuated the excessive cardiac and vascular collagen depositions of the DOCA-salt rats. It also reduced the scar tissue formation and inflammatory insult in the ventricle, as revealed from the less extravasation of leukocytes and scar tissue in the ventricle **(Figs. 2.A-E)**. All these may improve vascular and endothelial dysfunction, a key factor for HT (13). Owing to dynamic volumetric load conditions, the isolated thoracic aorta rings of the DOCA-salt rats

showed reduced contraction force of the aortic tissues to noradrenaline (NA) and reduced relaxation responses to SNP and ACh, implying smooth muscle and endothelial dysfunction. This was significantly improved by mal C **(Figs. 3.A-C)**, possibly due to its ability to reduce the aortic ET-1 level.

Table 3. **Plasma biochemical markers**[a]

Parameter	UNX	DOCA-salt	Mal C-treated	Curcumin-treated
Plasma PGI2 level (pg/ml)	401.3 ± 16.5	718.3 ± 86.6*	622.0 ± 66.6**	642.1 ± 78.6**
LV PGI2 level (pg/ml)	306.7 ± 48.6	460.1 ± 68.6*	374.2 ± 25.8**	453.9 ± 55.3**
Aorta PGI2 level (pg/ml)	520.4 ± 67.6	1228.7 ± 153.8*	551.6 ± 74.6**	1051.2 ± 103.8**
Plasma AVP level (pg/ml)	52.7 ± 3.7	153.4 ± 13.5*	66.2 ± 7.4**	88.5 ± 8.3**
Plasma Big ET level (pg/ml)	7.6 ± 0.9	38.2 ± 5.2*	12.1 ± 1.5**	20.0 ± 2.1**
Aorta Big ET level (pg/ml)	5.9 ± 0.8	26.11 ± 2.5*	14.3 ± 1.5**	16.3 ± 3.2**
Aorta Et-l level (pg/ml)	2.3 ± 0.6	15.6 ± 1.8*	9.4 ± 1.6**	13.3 ± 2.1**
Plasma nitrate level (µM)	634.8 ± 55.4	540.3 ± 42.6*	628.7 ± 51.4**	666.6 ± 51.5**

[a]The experimental details are provided in Chapter II. $^{*}P<0.05$ compared to UNX group; $^{**}P<0.05$ compared to the DOCA-salt group.

III.6 Mal C corrects the electrical conduction pattern of DOCA-salt rats cardiomyocytes

Rhythmicity and electric conduction of the heart are important features of the cardiac function. This is controlled by relative intracellular and plasma levels of the Na^{+}, K^{+} and Ca^{2+} ions (**Table 4**). Higher extracellular Na^{+} and Ca^{2+} levels, coupled with lower K^{+} level can alter the cardiac action potential by changing the myocyte membrane potential gradients (14). Treatment with mal C reduced the DOCA-salt induced plasma Na^{+} and Ca^{2+} levels, but increased the plasma K^{+} levels. Consistent with these, our microelectrode analysis with the papillary muscles revealed that the action potential durations (APDs) at 20%, 50% and 90% of repolarization were markedly increased to 6.5 fold, 4.0 fold and 3.0 fold, compared to the respective values of the UNX rats. Mal C reduced the DOCA-salt induced increase in resting potential along with the depolarization intervals at 20%, 50% and 90% repolarization **(Figs.**

4.A-D). This would improve excitability of the muscles, and repolarization / depolarization cycles leading to increased muscular functioning and better valve movement, as papillary muscles control the valve movement in the heart.

Fig 2. Detection of collagen (2 A-C) and inflammation (2 D-E) in rat groups

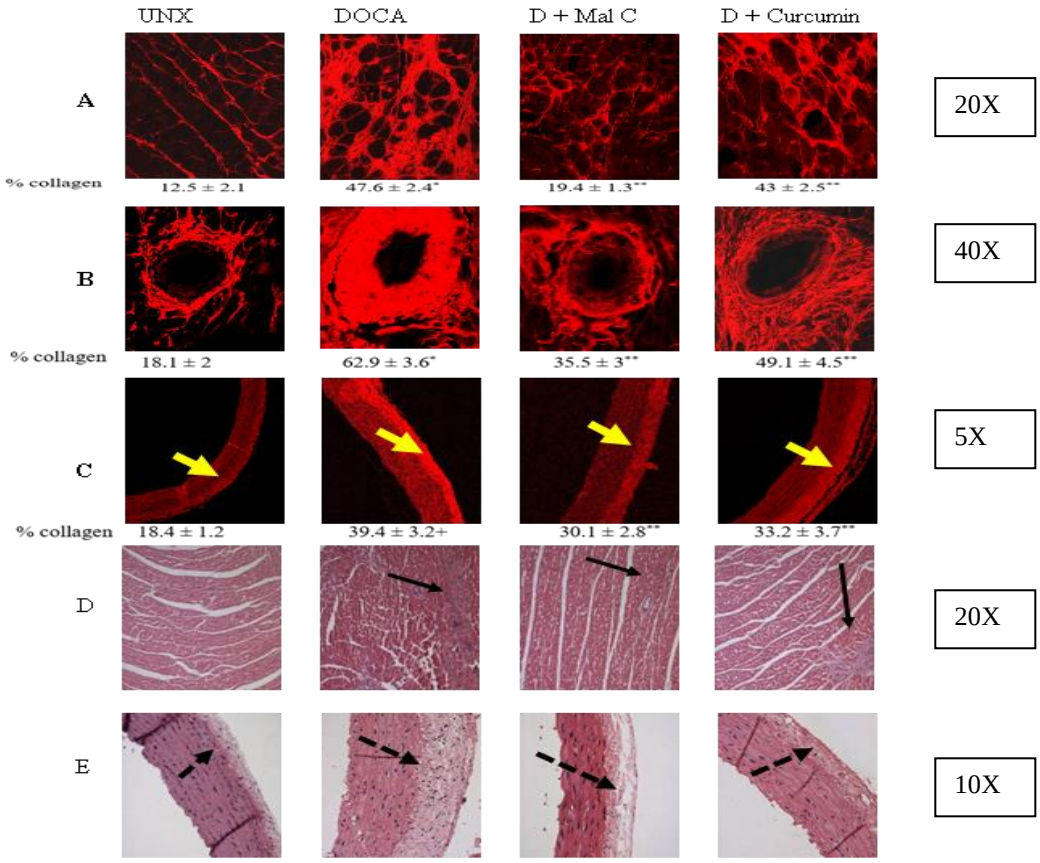

[a]The experimental details are provided in Chapter II.

In the ECG analyses, DOCA-salt rats showed increased P wave duration and amplitude, suggesting atrial hypertrophy and valve stenosis. Mal C reduced both these parameters as well as long PR interval of the DOCA-salt rats to reduce atrial hypertrophy and first degree AV block. Mal C also reduced the DOCA-salt induced QRS interval, indicating reduction in ventricular hypertrophy that would help in proper contraction of the ventricle in DOCA-salt rats. The mal C-mediated reduction of the ST segment height in DOCA-salt rats indicated reduction of infarction that was verified by histology. Moreover, the DOCA-salt rats showed increased heart rate (tachycardia) that was corrected by mal C for better heart rhythms.

Finally, as evident from the heart rate variability (HRV) analysis, mal C shifted the DOCA-salt-induced sympathovagal balance from sympathetic to parasympathetic tones. This might contribute to the slowing down of heart rate by mal C thus allowing heart to relax. The ECG data are shown in **Table 5**.

III.7 Mal C reduces structural modification of cardiovascular system of DOCA-salt rats

Mal C reduced the DOCA induced passive diastolic stiffness constant almost to the UNX levels. This would decrease hypertrophy and improve heart functioning. This also corroborated our earlier results indicating reduction in hypertrophy, increased functioning of heart and better rthymicity of the heart in mal C treated groups. Next, the functional, structural and fluid dynamic characteristics of the heart were assessed by echocardiography. DOCA administration increased the ventricle wall thickness, inter-ventricular septum thickness and LV posterior wall thickness both in diastole and systole, indicating ventricular hypertrophy.

Fig 3. Cumulative concentration–response curves for thoracic aortic rings of different rats.

Fig 3A **Fig 3B** **Fig 3C**

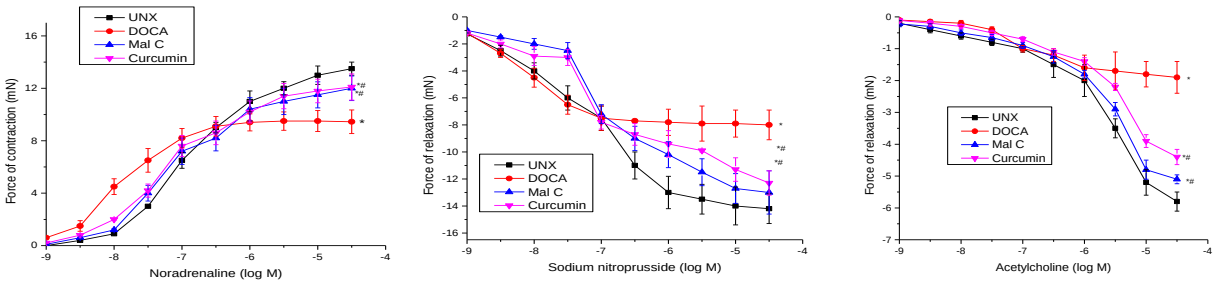

[a]The experimental details are provided in Chapter II. $^{*}P<0.05$ compared to UNX group; $^{**}P<0.05$ compared to the DOCA-salt group.

Mal C treatment decreased these changes resulting in reduced ventricular hypertrophy. As a direct consequence, mal C also increased the DOCA-salt-induced reduction in LV internal diameter in systole and diastole, thereby increasing the space for more blood pumping. These

improved the diastolic filling and allowed efficient cardiac contraction and expulsion of blood, as evident by the increased cardiac output in the mal C-treated rats.

DOCA-salt caused restrictive filling pattern of ventricle in rats, indicating impaired atrial and mitral valve functions. Besides improving the valve functions, mal C also prevented the

Table 4 Plasma ions levels in different groups of rats[a]

Parameters	UNX	DOCA (D)	D + Mal C	D + Curcumin
Na^+ mEq/l	143.91 ± 7.8	232.17 ± 10.9*	170.5 ± 8.6**	178.26 ± 9.7**
K^+ mEq/l	5.37 ± 0.76	4.09 ± 0.59*	4.34 ± 0.86**	3.87 ± 0.58**
Ca^{2+} mEq/l	3.07 ± 0.32	4.48 ± 0.61*	3.87 ± 0.58**	2.95 ± 0.38**

[a]The experimental details are provided in Chapter II. *P<0.05 compared to UNX group; **P<0.05 compared to the DOCA-salt group.

increase in ascending and descending aortic flows, aortic arch and descending aorta diameters

Fig 4. Membrane potential (4A) and action potential durations (4B-D) of papillary muscles[a]

Fig 4A

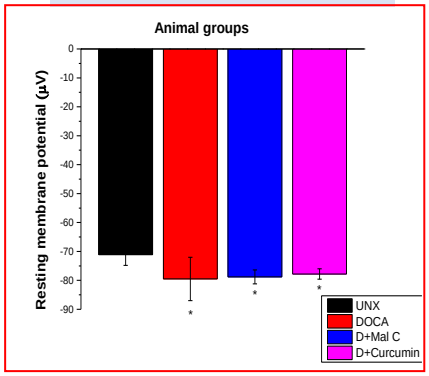

Fig 4B

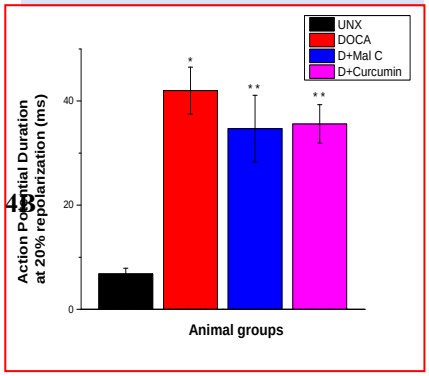

Fig 4C

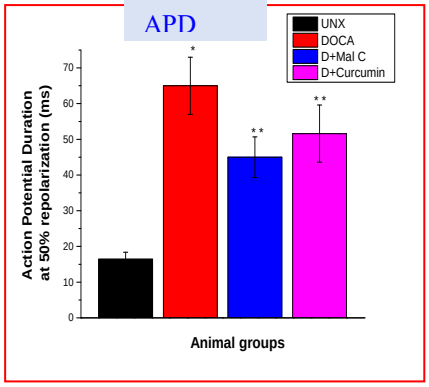

Fig 4D

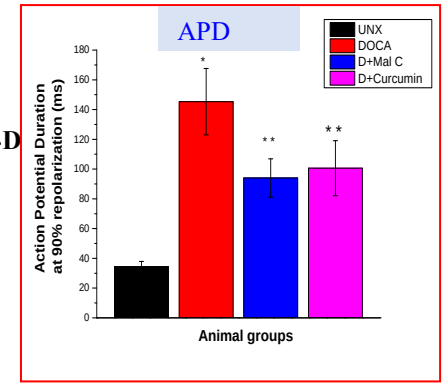

[a]The experimental details are provided in Chapter II. *P<0.05 compared to UNX group; **P<0.05 compared to the DOCA-salt group.

of the DOCA-salt rats to reduce blood pressure. Both systolic and diastolic volumes were

increased by mal C that might be a direct effect of increased LV internal diameter in systole and diastole. This along with reduction in LV mass significantly increased cardiac functioning in the mal C group.

Table 5. ECG parameters of different groups of rats[a]

Parameters	UNX	DOCA	Mal C + DOCA	Curcumin+ DOCA
RR Interval (ms)	213.4 ± 16.1	167.5 ± 13.4*	196.4 ± 20.3**	201.3 ± 19.4**
Heart rate (beats /min)	285.3 ± 20.8	398.3 ± 47.7*	320.4 ± 81.5**	277.7 ± 20.4**
PR Interval (ms)	61.2 ± 2.3	70.3 ± 5.3*	53.4 ± 3.1**	63.1 ± 5.3**
P Duration (ms)	16.3 ± 1.3	19.4 ± 2.2*	16.1 ± 4.2**	21.5 ± 1.2**
QRS Interval (ms)	15.2 ± 2.4	20.3 ± 1.3*	16.4 ± 2.3**	23.2 ± 1.1**
QTc (ms)	101.4 ± 4.2	205.3 ± 14.1*	172.4 ± 16.6**	189.5 ± 15.3**
Tpeak Tend Interval (s)	12.3 ± 1.0	26.4 ± 7.1*	21.5 ± 4.2**	34.2 ± 5.3**
P Amplitude (µV)	60.91 ± 6.5	102.5 ± 20.1*	64.1 ± 6.3**	79.13 ± 9.7**
R Amplitude (µV)	564.1 ± 60.4	431.3 ± 40.7*	449.8 ± 29.3**	464.73 ± 34.5**
ST Height (µV)	15.9 ± 4.6	49.96 ± 4.6*	33.07 ± 5.9**	56.41 ± 8.6**

[a]The experimental details are provided in Chapter II. $^{*}P<0.05$ compared to UNX group; $^{**}P<0.05$ compared to the DOCA-salt group.

Chapter IV will describe the **Conclusions** as follows:

1. The non-toxic phenolic, mal C is a potential anti-HT agent as revealed from the noninvasive and invasive measurements of SBP and DBP of the DOCA-salt rats. The anti-HT property of mal C (10 mg/kg) was similar to that of atenolol (10 mg/kg), amlodipine (15 mg/kg) and superior to that of curcumin (60 mg/kg).
2. Mal C reduced the DOCA-induced hypertrophy, fibrosis and inflammation in vascular and cardiac tissues resulting in better functioning of the cardio-vascular system. The strong antioxidant and anti-inflammatory property of mal C may be responsible for these.
3. Mal C administration reduced the ventricular stiffness and functioning, while decreasing the ventricular lumen diameter and cardiac wall thickness. These improved cardiac

output and increased blood volumes and flow.

4. Mal C corrected the electric imbalances of the cardiomyocytes including P and PR, QTc as well as ST waves, which are clinical makers for future heart failure. Its ability to reduce plasma Na^{+}/Ca^{+2} and hypokalemia contributed to better electrical conduction of the heart. These led to higher survival rates of the animals.
5. Mal C also corrected the DOCA-salt-induced changes in the papillary muscles electrophysiology thereby improving the heart valve system. This was also confirmed by echocardiography, that showed better rhythmicity of the heart
6. Mal C improved the endothelial layer functioning of the aorta and other vessels leading to better vascular reactivity under hemodynamic load as revealed in the organ bath studies. Mal C shifted the sympathovagal balance towards parasympathetic from sympathetic tones to decrease the stress response of the animals.

Overall, mal C appears to be a good cardio-protective agent, and may be taken up for further pre-clinical and clinical evaluations.

Chapter V will provide the collated list of **Bibliography**

Bibliography

1. O'Donnell, M. J.; Xavier. (2002). The World Health Report: Reducing Risk, Promoting Healthy Life. Geneva, Switzerland: *World Health Organization* (WHO).
2. Iyer, A.; Chan, V.; Brown, L. (2010). The DOCA-Salt Hypertensive Rat as a Model of Cardiovascular Oxidative and Inflammatory Stress. *Current Cardiology Reviews*. 6: 291-297
3. Banerjee, D.; Bauri, A. K.; Guha, R. K.; Bandyopadhyay, S. K.; Chattopadhyay, S. (2008) Healing properties of malabaricone B and malabaricone C against indomethacin-induced gastric ulceration and mechanism of action. *Eur. J. Pharmacol*. 578:300–312.

4. Wongcharoen, W and Phrommintikul, A. (2009). The protective role of curcumin in cardiovascular diseases. *Int. J. Cardiol*. 133: 145-151.
5. Brilla, C.G.; Janicki, J.S.; Weber, K.T. (1991). Impaired diastolic function and coronary reserve in genetic hypertension. *Circ. Res*. 69:107-115
6. Mirkovic, S.; Seymour, A. M. L.; Fenning, A.; Strachan, A.; Margolin, S. B.; Taylor, S. M.; Brown, L. (2002). Attenuation of cardiac fibrosis by pirfenidone and amiloride in DOCA-salt hypertensive rats. *British Journal of Pharmacology* 135:961-968.
7. Tomaschitz, A, Pilz, S.; Ritz, E.; Pietsch, B.; Pieber, T. R. (2010) Aldosterone and arterial hypertension. *Nat. Rev. Endocrinol.* 6:83–93.
8. Yu, M.; Gopalakrishnan, V.; McNeill, J. R. (2001) Role of endothelin and vasopressin in DOCA-salt hypertension. *Br. J. Pharmacol*. 132:1447–1454.
9. Chan, V.; Hoey, A.; Brown, L. (2006) Improved cardiovascular function with aminoguanidine in DOCA-salt hypertensive rats. *Br. J. Pharmacol*. 148:881–883.
10. Zhu, Z. (2009) Window period for oxidative stress attenuating intervention (WPOS Theory). *Am. J. Biomed. Sci*. 1:250–259.
11. Manning, R. D.; Tian, N.; Meng, S. (2005) Oxidative stress and antioxidant treatment in hypertension and the associated renal damage. *Am. J. Nephrol*. 25:311–317.
12. Vane, J. R.; Anggard, E. E.; Botting, R. M. (1990) Regulatory functions of the vascular endothelium. *N. Engl. J. Med*. 323:27–36.
13. Perez-Vizcaino, F.; Duarte, J.; Andriantsitohaina, R. (2006) Endothelial function and cardiovascular disease: effects of quercetin and wine polyphenols. *Free Radic. Res*. 40:1054–1065.
14. Diercks, D. B.; Shumaik, G. M.; Harrigan, R. A.; Brady, W. J.; Chan, T. C. (2004) Electrocardiographic manifestations: electrolyte abnormalities. *J. Emergency Medicine* 27:153–160.

Publications in Refereed Journal:

a. Published One

b. Accepted: - One, Mechanism of the anti-hypertensive property of the naturally occurring phenolic, malabaricone C in DOCA-salt rats. Jitesh S. Rathee, Birija S. Patro, Lindsay Brown, and Subrata Chattopadhyay. *Free Radical Research DOI:10.3109/10715762.2015.1112005*

c. Communicated:

d. Other Publications: Conferences

1. Antihypertensive activity of a natural phenolic malabaricone C in DOCA-salt rats. *Jitesh Rathee and S. Chattopadhyay*. in International Conference on *Recent Advances In Free Radical Research, Natural Products, Antioxidants & Radioprotectors In Health*. Hyderabad (Jan 2010)
2. Cardiovascular remodeling property of a malabaricone C in DOCA-salt hypertensive rats. *Jitesh Rathee and S. Chattopadhyay*. in International Symposium on *Advances In Free Radicals, Redox Signaling And Translational Antioxidant Research* (SFRR-STAR). Lucknow (Jan 2013)

Signature of Student:

Date:

Doctoral Committee:

S. No.	Name	Designation	Signature	Date
1	**Dr K. Indira Priyadarshini**	Chairman		
2	**Dr. B. S. Patro**	Guide & Convener		
3	**Dr S Santosh Kumar**	Member		
4	**Dr. B N Pandey**	Member		

CHAPTER - I

INTRODUCTION

I.1 Cardiovascular Disease – Preamble

Cardiovascular disease (CVD) affects heart, kidney, brain and blood vessels, accounting for 1.5 million deaths annually in India and is estimated to be the largest cause of mortality and morbidity in India by 2020 [1,2]. In 2003 alone, it contributed to about 29% of human death worldwide, with an upward trend in urban population in the last 5 years [2]. Currently Indians experience CVD deaths at least a decade earlier than their counterparts in countries with established market economies (EME). Compared to ~52% of CVD deaths occurring below the age of 70 years in India, those in the EME countries stand as 23%, resulting in a profound adverse impact on the economy. Coronary heart disease, stroke, heart failure, peripheral vascular disease and kidney failure are the five major contributors to the unacceptably high rates of CVD in India. Thus, understanding and addressing this problem is very important and relevant, both from health and economic perspectives. For better appreciation of the pathological processes, particularly the causes of disease induction and progression, a brief review of the anatomy and function of heart is provided below. This is followed by an analysis of the current treatment options for CVD as well as their drawbacks to rationalize the need of the present investigations.

I.2 Anatomy and function of cardiovascular system

The heart is a muscular organ consisting of a range of tissues that help it to function as the body's circulatory pump for transporting blood throughout the body. It takes in deoxygenated blood through the veins and delivers it to the lungs for oxygenation before pumping it into the various arteries. This is essential for the supply of oxygen and nutrients to the body tissues, and is achieved by the remarkable abilities of the heart components to contract and relax in a rhythmic fashion. The heart consists of four chambers: right and left atria above right and left ventricles (RV and LV respectively), each of which has defined

functions as discussed below. Distortion/damage of any the components may lead to heart malfunction with dangerous consequences including CVD.

***I.2.1 Cardiovascular architecture*:** The atria act as the receiving chambers for blood, and are connected to the veins that carry blood to the heart. The ventricles are the pumping chambers, connected to the arteries to send blood out of the heart. The right side of the heart maintains pulmonary circulation to the nearby lungs while the left side of the heart pumps blood all the way to the extremities of the body in the systemic circulatory loop. The backwards blood flow into the heart is prevented through the one-way atrioventricular (AV) and semilunar valves. The AV valves, located between the atria and ventricles allow blood to flow from the atria into the ventricles only. Those on the right and left sides of the heart are known as tricuspid and mitral valves respectively, and are attached on the ventricular side by chordae tendineae that holds each valve firmly and prevent them from folding backwards. The semilunar valves lie between the ventricles and the arteries, and carry blood away from the heart. The semilunar valves *viz*. pulmonary and aortic valves, present on the right and left sides of the heart respectively, prevent the blood backflow into RV and LV.

I.2.2 Cardiovascular function: As explained above, the role of heart is to ensure continuous movement of blood around the body, collecting and supplying vital substances to cells as well as removing waste from them. This is achieved by a cyclical combination of systole (contractions) and diastole (relaxation) operation of the chambers in the following sequence.

In the first stage (ventricular diastole, atrial systole), the ventricles relax simultaneously to result in lower pressure in them compared to each atrium above. This is followed by partial opening of the AV valves and contraction of the atria, which forces blood through the AV valves. It also closes the valves in the vena cava and pulmonary vein to prevent backflow of blood. In the next stage **(**ventricular systole, atrial diastole), both the atria relax along with simultaneous contraction of LV and RV. The resultant higher pressure

in the ventricles compared to the atria above closes each AV valve to prevent backflow of blood into each atrium. At the same time, the higher ventricular pressure (compared to the aorta and pulmonary artery) opens the semi-lunar valves, and blood is ejected into these arteries. So blood flows through the systemic circulatory system via the aorta and vena cava and through the lungs via the pulmonary vessels.

Immediately thereafter, both ventricles and atria relax for a short time in the next stage **(**ventricular and atrial diastole). Due to the higher pressure in the aorta and pulmonary artery than in the ventricles, the semi-lunar valves close to prevent the backflow of blood. The higher pressure in the vena cava and pulmonary vein than in the atria results in the refilling of the atria. The whole sequence above is one *cardiac cycle* or *heart beat* and takes less than one second. The number of heartbeats /min varies to suit the activity of an organism as is evident from the increased heart rate during vigorous exercise, but low heart rate during sleep. The function of heart is controlled by its own inherent rhythm and the efficient conduction system that is coordinated by pacemakers.

The conduction system starts with the sinoatrial (SA) node, a pacemaker structure in the wall of the right atrium inferior to the superior vena cava. The SA node is responsible for setting the pace of the heart as a whole and directly signals the atria to contract. The electrical activity then reaches a second pacemaker, the AV node (located in the right atrium in the inferior portion of the interatrial septum) and gets transmitted through the AV bundle, a strand of conductive tissue that runs through the interatrial septum and into the interventricular septum. The AV bundle splits into left and right branches in the interventricular septum and runs through the septum up to the apex of the heart. The electrical signal is carried through the Purkinje fibres (Pfs), which pass through the septum of the heart deep into the walls of LV and RV. Eventually both the ventricles undergo contraction from the apex (base) upwards, stimulating the cardiac muscle cells to contract in a coordinated

manner to efficiently pump blood out of the heart. The activity of the pacemaker can be altered by the electrical stimulation from the brain in the medulla oblongata. This leads to the change in the rate and strength of the heartbeat. The sympathetic nerve stimulates heart rate, while vagus nerve decreases it.

I.3 Risk factors of CVD

Chronic hypertension (HT) is the insidious culprit that is known to be one of the major risk factors of high CVD prevalence, as uncontrolled HT leads to a pathological process to the heart and vasculature, known as cardiovascular remodeling [3]. The other contributing risk factors are primarily dyslipidemia, diabetes, overweight or obesity, physical inactivity and tobacco use. Studies have shown a genetic component for HT, type 2 diabetes and abnormal blood lipids that can lead to the development of CVD. Familial hypercholesterolemia is one of the genetic factors, while inherited HT from first-degree relatives is a key factor in the familial link of ischemic stroke. Despite intensive research including genome-wide association (GWA) studies and very large cohorts of patients, not a single genetic risk factor provided any clue for risk assessment [4]. Interestingly, much of the burden caused by CVD is preventable if the associated risk factors are adequately controlled.

India has the dubious distinction of being known as the coronary and diabetes capital of the world. According to Indian Heart Watch [5], urban social development is also playing a role in the development of CVD risk factors. Risk factors such as smoking, high fat intake and low fruit/vegetable intake were shown to be more common in less developed cities, while physical inactivity was seen to be more prevalent in highly-developed cities. Accordingly, metabolic risk factors such as obesity, high blood pressure (BP) and high cholesterol were seen to be more prevalent in highly developed cities. Thus, government must develop public health strategies to change the lifestyles, if these risk factors are to be controlled.

On its own, HT increase the chance of CVD by 2-4 times. It induces cardiac, vascular and renal damages by cardiovascular remodeling that contributes to cardiovascular mortality and morbidity immensely. Endothelial dysfunction and neurohormonal activation, which effects remodeling also contribute to HT and heart failure. Although countering HT is of prime importance, equal importance should be given to the control the HT-induced pathological cardiovascular remodeling. Following is a brief account of HT and pathological cardiovascular remodeling.

I.4 Hypertension (HT)

HT is defined as an elevation in BP with a systolic blood pressure (SBP) of 140 mm Hg or a diastolic blood pressure (DBP) of 90 mm Hg. BPs above this range are strong predictors for CVD. The rise in BP increases the incidence of cardiovascular, cerebrovascular and renal diseases. HT not only contributes to the pathogenesis, but also to the progression of cardiac dysfunction and ultimately heart failure. At an underestimate, there are 31.5 million hypertensives in rural and 34 million in urban Indian populations. It is directly responsible for 57% of all stroke deaths and 24% of all coronary heart disease deaths in India.

Although there are a few recognizable causes of HT, such as steroid-secreting tumors of the adrenal cortex or renal artery stenosis, most patients have essential HT where no specific cause can be determined. High BP was reported in 33% of men and 30% of women, while high cholesterol was found in one-quarter of all men and women. In human HT, possible triggers are various environmental influences such as salt intake, obesity, physical exercise and excessive alcohol acting on a genetic predisposition [6**]**. Incidence of HT dramatically increases with the increase in age. Fortunately, HT is a controllable disease as is reflected by the fact that the antihypertensive medications topped the list for the most dispensed medicinal type for cardiovascular treatment. A population-wide decrease in BP by 2 mm Hg can prevent 151,000 stroke and 153,000 coronary heart disease deaths in India. [7].

According to another estimate, a reduction of BP by 5 mm Hg can decrease the risk of stroke by 34%, of ischemic heart disease by 21%, and also reduce the likelihood of dementia, heart failure, and mortality from CVD [8].

I.5 Pathological cardiovascular remodeling

Cardiovascular remodeling is defined as a process of genomic, molecular, cellular and interstitial changes that are manifested clinically in terms of changes in size, shape and function of the heart, after a cardiac load or injury [9]. It can be beneficial or pathological, and results as a physiological response to metabolic or hormonal changes in the body. The positive physiological remodeling includes changes due to intensive exercise by athletes. However, the pathological remodeling is central to the progression of HT to heart failure [9]. It leads to the development of hypertrophy, necrosis and apoptosis of the myocyte and vascular tissues, and fibrosis in the vessels along with cardiac interstitial and perivascular regions [3]. Eventually these lead to myocardial function abnormalities such as (i) impaired contractility and relaxation, (ii) diminished cardiac pump function, (iii) decreased myocyte electrical conduction pattern, and (iv) dilatation and increased sphericity of heart. These result in dysfunction of vascular endothelial and smooth muscles and diminished vascular reactivity.

HT results in left atrial structural and electrophysiological changes, which, in turn, predispose to development of atrial fibrillation and risk for thromboembolic and stroke. The structural and mechanical changes include left atrial enlargement [10,11], atrial fibrosis and impairment of left atrial function [12]. The electyrophysiological changes in hypertensive patients include prolonged atrial conduction [13] and heterogenous decrease in atrial refractoriness. These changes are associated with development of atrial fibrillation [14]. Ultimately, these lead to systolic and diastolic cardiac dysfunction, which form the basis of heart failure and death. There are many types of remodeling events like necrosis, apoptosis

cardiovascular hypertrophy, cardiac fibrosis and endothelial dysfunction that lead to the disease progression. The latter three are most studied and discussed here.

***I.5.1 Cardiac hypertrophy*:** It is defined as the increase in mass of contractile and ancillary proteins of the heart to levels greater than normal for the given stage of its maturation growth, rather than an increase in cell numbers [15]. The increased myocardial mass results in change in the heart shape. Since adult cardiac myocytes are terminally differentiated, they increase their cell size (hypertrophy) rather than the number (hyperplasia) under stress or during growth [16].

Cardiac hypertrophy is of three major morphological types: (1) *concentric remodeling*, which has a normal LV mass but a reduced end-diastolic diameter and cardiac output; (2) *concentric hypertrophy*, which is pressure-dependent, and results in an increased LV mass, but normal or decreased end-diastolic diameter and cardiac output; and (3) *eccentric hypertrophy*, which is volume-dependent, and results in an increase in LV mass, end-diastolic diameter and cardiac output. In *concentric hypertrophy*, the septum and posterior walls thicken throughout the heart at the expense of chamber volume. Usually, an increase in the number of sarcomeres is present where the contractile-protein units are assembled in parallel, resulting in a relative increase in the width of individual cardiac myocytes. In contrast, *eccentric hypertrophy* involves thickening of the chamber wall (not consistently throughout the heart) with concomitant chamber dilatation. In this case, the sarcomeres are increased longitudinally and assembled in series. The myocytes undergo a relative greater increase in the length than in width [17].

LV hypertrophy (LVH) is generally accepted as the physiological adaptation of the heart to the increased physio-mechanical workload on the circulatory system [18]. Here, the pressure overload is distributed over a larger surface area of the myocardium, keeping the systolic wall stress, fibre shortening, and stroke volume to normal values, but reducing the

ventricular function [16]. To compensate this, the heart responds by multiplying the contractile units and reducing wall stress according to Laplace's law [19]. Despite the adaptive benefits, chronic LVH has been a strong BP-independent risk factor responsible for a number of clinical manifestations of coronary artery disease, myocardial infarction, stroke, arrhythmias and heart failure [18,20,21]. LVH results in impaired oxygen supply, while an increased muscle mass increases the oxygen demand significantly [22]. Also, the growth of capillary beds in the hypertrophied myocardium does not keep up with the increasing ventricular mass, resulting in more ischemic heart problems [23]. Because myocardial relaxation and diastolic function with LVH is sensitive to hypoxia and ischemia, changes in LVH may worsen the diastolic filling properties [24].

It is known that hypertensive patients with LVH have a higher prevalence of severe cardiac arrhythmias than those without LVH [25]. Cardiac electrophysiological abnormalities may also be responsible for the adverse outcome of patients with LVH. Myocardial ischemia, excessive myocardial collagen (fibrosis) and distorted myocardial architecture, all contribute to rhythm disturbances in LVH. LVH has been shown to influence the quantity and quality of the extracellular matrix (ECM) directly, and cardiac hypertrophy results in an increased expression of collagen mRNA [26]. During LVH, remodeling of the matrix network must occur in order to accommodate the increase in muscle mass, indicating a close relationship between LVH and fibrosis. Increases in fibrillar collagen during hypertrophy would increase tensile strength and three-dimensional delivery of force to the myocardium. Ventricular hypertrophy alone may contribute to increased stiffness of the heart. Diastolic function and stiffness depend more on myocardial collagen than on myocardial mass [27].

Impaired inotropic responsiveness and impaired Ca^{2+} regulation are also features of the hypertrophied heart. Hypertrophied rat hearts show impaired response to β-adrenoceptor stimulation that may be due to a defect within the transduction and impaired cAMP

production [28] Altered intracellular Ca^{2+} cycling such as changes to the release and uptake of Ca^{2+}, changes to ryanodine receptors and Ca^{2+} transport proteins can all contribute to excitation-contraction coupling abnormalities in hypertrophy and failure [29]. During hypertensive cardiac disease progression, the hypertrophied heart can't compensate for the increased afterload, resulting in a dilated and failing heart with reduced-outputs. In pressure-overload hypertrophic rats, hypertrophic remodeling is the main contributor to decompensation. This type of remodeling, rather than the depressed myocardial function plays a major role in the development and progression of heart failure [30].

Neurohormones such as noradrenaline (NA), endothelin (ET) and angiotensin (Ang) II, growth factors (like transforming growth factor (TGF- β) and fibroblast growth factor (FGF)), inflammatory cytokines (such as TNF-α and IL-1 β), oxidative stress (OS) and mechanical stretch have all been implicated as potential stimuli for myocytic hypertrophy [31]. These factors increase protein synthesis and gene expression in cardiac myocytes, thereby increasing the mass of contractile and ancillary proteins. In hypertrophy, abnormalities in the function and growth of myocytes may be because of induction of the expressions of proto-oncogenes (for example *c-myc*, *c-fos*, and *c-ras*) and other genes that regulate cell growth [16]. An overview of myocardial remodeling from the stimulus to the disease progression [31] is shown in **Fig. I.1**.

***I.5.2 Vascular hypertrophy*:** Blood vessels can also alter their geometry as an adaptive response to changes in hemodynamic load and humoral factors. The vascular remodeling contributes to the pathophysiology of vascular diseases and circulatory disorders as well as HT [32]. Furthermore, mechanical and humoral factors responsible for hypertensive heart disease may also be associated with vascular disease, and consequently with morbidity [33]. Moreover, vascular smooth muscle cells (VSMC) can undergo both hypertrophy and hyperplasia resulting in structural changes to the vasculature. During HT, vasculature can

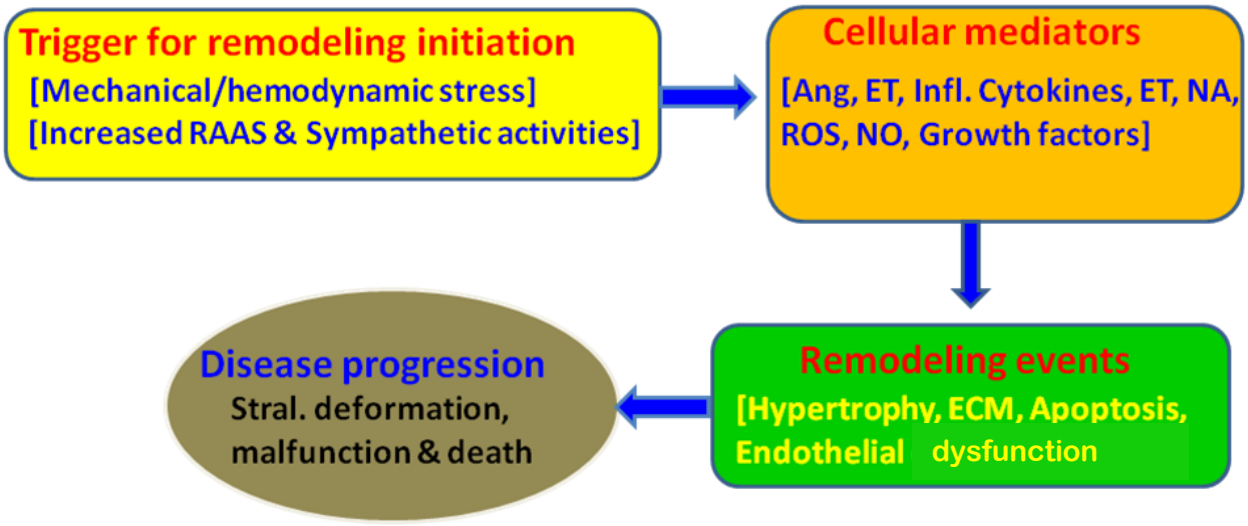

RAAS = Renin Angiotensin Aldosterone System; Ang = Angiotensin; ET = Endothelin; NA = Noradrenaline; NO = Nitric Oxide; ROS = Reactive Oxygen Species; ECM = Extracellular Matrix.

Fig. I.1. Schematic overview of myocardial remodeling to disease progression

undergo two changes: (1) an inward eutrophic remodeling; and/or (2) a hypertrophic remodeling [34]. In the former, the outer and lumen diameters are decreased with an increase in the media/lumen ratio, but the cross-sectional area of the media is unaltered. This type of vascular remodeling is often seen in the spontaneously hypertensive rat (SHR) model [34]. In hypertrophic remodeling, the media thickens to reduce the lumen, resulting in increased media cross-sectional area and media/lumen ratio. This type of remodeling predominates in severe HT such as in the deoxycorticosterone acetate (DOCA)-salt rat model [35].

Increased intimal-medial thickness in hypertensive patients indicates vascular hypertrophy. A correlation between the intimal-medial thickness of the carotid artery and LV mass exists [36]. Hypertrophy and proliferation of VSMC are responsible for the changes in structure and thickness of coronary and systemic vascular walls [37]. Increased vascular wall size can reduce dilatory capacity along with the wall-lumen ratio, which increases diffusion time across the vessel and total peripheral resistance [38]. Many triggers can stimulate VSMC growth. Growth factors like TGF, EGF and FGF, neurohormones like Ang II, ET and NA as

well as inflammatory cytokines like IL-1 and IL-6 are known to trigger vascular hypertrophy [32].

***I.5.3 Cardiac fibrosis*:** Cardiac fibrosis is defined as the pathological increase in LV mass, accompanied by a disproportional proliferation of cardiac fibroblasts and deposition of ECM proteins, especially collagen [39]. Cardiac fibroblasts, representing greater than 90% of the non-myocyte component of heart, are the cells responsible for the production and deposition of ECM in the heart. Cardiac ECM is defined as a network surrounding and supporting myocardial constitutive cells: cardiac myocytes, cardiac fibroblasts, and blood vessel endothelial and smooth muscle cells. The main components of ECM include (1) structural proteins such as collagen and elastin; (2) adhesive proteins such as laminin, fibronectin and type IV collagen; (3) anti-adhesive proteins such as tenascin, thrombospondin and osteopontin; and (4) proteoglycans [40]. The ECM, which is the structural and protective framework of the heart, is essential for the functional integrity of the heart as it connects myocytes, aligns contractile elements, prevent overextending and disruption of myocytes, transmits force and provide tensile strength to prevent rupture [41]. It represents a major determinant of myocardial stiffness (or myocardial compliance) because of its alignment, location, configuration and tensile strength relative to cardiac myocytes [42]. The quality, but not the quantity of myocardium accounts for ventricular dysfunction in diseases such as HT [39,41].

Five collagen types (I, III, IV, V and VI) have been identified in the adult heart [40], but the major components of the ECM are collagens type I and III and fibronectin [41]. Collagen I, which comprises of 80% of the total collagens in the heart, is a heterotrimer triple helix constituted by repeating hydroxyproline-glycine-proline units to provide tensile strength. Collagen III, which comprises of 12% of the total collagens, is a homotrimer forming a fine network of fibrils to provide compliance. The dimeric glycoprotein,

fibronectin serves as a bridge between cells and the interstitial collagen network to influence cell growth, adhesion, migration and wound repair. The quality of collagen is an important factor in determining the degree of cardiac stiffness [43]. It is the collagen cross-linking rather than the increased collagen *per se* that is responsible for the myocardial stiffness [44].

Excessive interstitial and perivascular collagen deposition is a critical component of cardiac fibrosis and cardiac remodeling in various cardiovascular diseases. Numerous studies have reported fibrosis together with an increased stiffness or decreased compliance of the heart [41,45,46]. Interstitial fibrosis may also alter the mechanical properties of the myocardium to impair relaxation and restrict delivery of nutrients to myocytes. The cardiac fibrosis plays an important role in the progressive deterioration of coronary hemodynamics. Fibrosis is commonly divided into reparative fibrosis and reactive fibrosis [19]. Reparative fibrosis (scar formation) occurs following loss of myocardial material due to necrosis or apoptosis, and is mainly interstitial. In contrast, reactive fibrosis is observed in the absence of cell loss as a reaction to inflammation or other stimuli, and is primarily perivascular, but can extend into the neighboring interstitial spaces [47,19]. Myocardial fibrosis in pressure-overload rats resulted in normal systolic function, but impaired diastolic function, implying altered diastolic properties of the heart [48]. Moreover, fibrosis is known to have an association with cardiac arrhythmias [18,49], further contributing to the risk of adverse cardiovascular events such as diastolic and systolic ventricular dysfunction, myocardial infarction and ultimately heart failure [50-52].

Taken together, several studies suggest that the relationship between cardiac collagen deposition, cardiac stiffness and contractile function of the heart is of significance and worth investigating. As stiffness is the functional correlate of fibrosis, the Langendorf isolated heart preparation can be used to establish the relationship between fibrosis, diastolic stiffness and contractility [53]. Staining of the organs with picrosirius red, a specific stain for collagen, but

non-selective for the fibrillar collagen subtypes, followed by a confocal scanning laser microscopy is a useful technique to study depositions of collagen fibers and its 3D arrangement within the myocardium [54-56]. The anionic dye reacts with the sulphonic acid groups in the collagen, and the stained collagen displays auto fluorescence under green light excitation to give a red emission. It has been shown that the accuracy of quantifying picrosirius red staining is very similar to results obtained from biochemical assay and immuno-localization techniques [57].

Collagen synthesis and degradation are closely coordinated, and an imbalance in this normally balanced process results in fibrosis. Like hypertrophy, the pathogenesis of cardiac fibrosis is complex and not completely understood. However, it also involves a complicated cascade of triggers and stimuli activating multiple pathways and signaling cascades eventually leading to fibrosis [40]. Fibroblasts are the primary cells responsible for the synthesis of collagen and insoluble fibronectin, while soluble fibronectin is mainly produced by the hepatocytes. Collagen synthesis in the heart may be increased by an increase in synthesis per fibroblast and/or an increase in fibroblast number. It is likely that both mechanisms are involved in the enhanced collagen production in the heart [58].

To a large extent, the stimuli and pathways leading to the development of fibrosis are quite comparable to those responsible for hypertrophy. NA, ET, Ang II and the mineralocorticoid aldosterone are all known potent triggers for collagen synthesis in cardiac fibroblasts [50,59]. Importantly, Ang II increases the activities of ET and TGF-β_1 [60], while inhibiting collagenases. These would create an imbalance in the synthesis-degradation processes of collagenases to promote fibrosis [59]. Hypertrophy may induce TGF-β_1 activity [61], and its high levels have been demonstrated to inhibit collagen breakdown by deactivating matrix metallo-proteinases (MMPs) [62]. Nitric oxide (NO) and bradykinin may also have inhibitory effects on ECM production, presumably through a cyclic GMP

mechanism [63]. Also, NO-generating compounds inhibited total protein and collagen synthesis in VSMCs, implying positive role of NO in fibrosis [64]. The growth factors and mechanical stretch have also been implicated as potential stimuli for cardiac fibrosis [65,40]. Further, there is a close relationship between inflammatory cells and myocardial fibrosis, because lymphocytes and macrophages are co-localized with myocardial fibroblasts, and that fibroblastic activity closely correlates to the presence of these inflammatory cells [66]. Inflammation may play a causal role in fibrosis and the process of pressure-overload alone is enough to induce accumulation of macrophages in perivascular areas and fibroblast proliferation [48]. Thus, fibrosis is not a single pathological process, but rather due to excesses in inflammatory response that are involved in normal tissue repair also [67]. Numerous inflammatory cytokines and mediators can cause fibrosis by both increasing fibroblast activity as well as decreasing MMP function [68]. However, both proinflammatory cytokines and reactive oxygen species (ROS) appear to play key roles in both promoting and inhibiting collagen synthesis and breakdown. Similar to hypertrophy, once the triggering signals are present, collagen gene expression and transcription in fibroblasts can be increased to increase collagen production and deposition [65].

The breakdown of mature collagen involves a complex interplay between proteinases (which break down collagen), their inhibitors (which modulate proteinase activity) and their regulators [69]. Mature collagens are cleaved into two unequal fragments by the MMPs, especially MMPs-1, -2 and -8 (collagenases). Fibronectins are also degraded by the MMPs, especially MMP-3 and -9 [70-72]. The tissue inhibitors of metalloproteinases (TIMPs) are believed to be the major players controlling MMP activity [69]. These processes are altered by common cardiovascular diseases such as heart failure [72]. Nevertheless, increased activation of MMPs has been shown to contribute to matrix breakdown and progression of LV dilatation following myocyte slippage [73].

***I.5.4 Endothelial dysfunction*:** Endothelial dysfunction is defined as a pathological disease state in which homeostatic functions of endothelial cells are disturbed [74]. One of the main components of endothelial dysfunction is the loss of endothelial and NO-dependent vasorelaxation. While endothelial dysfunction *per se* is not a physical or structural change unlike hypertrophy or fibrosis, it is often described as an inevitable part of HT and heart failure, and thus, constitutes a major component of pathological remodeling. Vascular endothelium plays an important role in cardiovascular regulation by producing a number of vasoactive agents and their alterations can detrimentally affect the cardiovascular homeostasis.

Due to its strategic position, vascular endothelium plays a dynamic role in cardiovascular control by actively performing multiple functions including regulation of coagulation, leukocyte and platelet adhesion, vascular tone, vascular smooth muscle cell function and growth, as well as acting as a barrier to transvascular flux of liquids and solutes [75]. Further, the endothelium has been described as an endocrine, paracrine and even autocrine organ with multiple functions in addition to its role as a permeable and physical barrier protecting vascular smooth muscle cells [76]. Thus, it is clear that a functional endothelium is of great importance, both in health and disease.

The large number of regulatory substances produced from the endothelium includes vasodilators such as NO, and endothelium-derived hyperpolarizing factor (EDHF), as well as vasoconstrictors such as thromboxane A_2 and ET [77]. Further, the endothelium is also known to produce prostaglandins, natriuretic peptides, steroids and receptors for numerous substances [76]. Amongst these, NO and ET have been studied the most due to their multiple roles in the cardiovascular system, as well as the fact that these two are heavily implicated in HT [77,78].

The mechanisms controlling the release of vasoactive substances from the

endothelium are complex. Under normal physiological conditions, a precise and balanced release of contracting and relaxing factors contributes to appropriate vascular control and organ perfusion. However, this fine balance is altered in a number of cardiovascular disorders such as HT, atherosclerosis, diabetes, coronary artery disease and chronic heart failure [74]. As HT is usually characterized by increased peripheral vascular resistance, decreased vasorelaxation or increased vasoconstriction may contribute to or even cause elevated BP. Considerable evidence in hypertensive animal models [79-82] as well as in human HT [83,84] suggest that defects in endothelium-dependent relaxation results in HT. Studies have shown that if endothelium-dependent vasodilation to acetylcholine (ACh) is impaired, the *in vitro* vasodilatory response to endothelium-independent NO donors, such as nitroprusside and nitroglycerin are unaffected. This suggested abnormal NO production rather than decreased smooth muscle responsiveness causes endothelial dysfunction [85,86]. Overall, endothelial dysfunction, observed during HT is likely to be due to defective NO production and its release [74,77].

ET is one of the most potent vasoconstrictor that increases BP [87,88]. ET system is activated in most of the animal models of HT, specifically in the DOCA-salt hypertension model [78,3], and in some, but not all human hypertensive patients [89,90]. Although plasma ET levels are normal in most patients with essential HT, the hypertensive blood vessel wall may contract more profoundly to ET-1 stimulation [91]. ET-1 is formed by proteolytic cleavage of big-ET-1 in rats. In addition, its synthesis and release from the endothelial cells is also enhanced by the neurohypophysial hormone, arg^8-vasopressin (AVP). Interestingly AVP also constricts blood vessels and retains water in the body, thereby increasing BP [92]. In summary, by synthesizing and releasing a number of vasoactive substances, the vascular endothelium plays a crucial role in the maintenance of the cardiovascular system and endothelial integrity. It also plays a role in many disorders such as HT and heart failure. A

better strategy for reversal of endothelial dysfunction may help in combating CVD.

I.6 Role of oxidative stress (OS) in cardiac remodeling and CVD

It is now well appreciated that OS plays an important role in the pathogenesis of cardiovascular remodeling, vascular endothelial dysfunction and heart failure [93,94]. OS is defined as an imbalance between the antioxidant defence system and the production of reactive oxidants (predominantly free radicals), in favour of the latter. The addition or removal of an electron in a redox reaction results in the production of free radicals that are highly reactive due to the presence of one or more unpaired electron in them. Oxygen has two electrons with parallel spins in its outermost shell, and is classed as a biradical that requires four electrons for its complete reduction to water. The sequential univalent reduction of oxygen results in the formation of a battery of ROS [94]. Addition of a single electron to oxygen results in the production of superoxide anion radical ($O_2^{\cdot -}$), which on further addition of another electron gets converted to the peroxide anion and eventually forms hydrogen peroxide (H_2O_2) via protonation and dismutation. While H_2O_2 is not a radical *per se*, it may undergo Fenton reaction with transition metals such as iron (II) or copper (I) ions to form highly reactive hydroxyl radicals ($^{\cdot}OH$) that induce cell damage. The lower-valent transition metals are regenerated from their oxidized forms by the Haber-Weiss reaction wherein various reducing agents such as NADPH, ascorbate, GSH and even $O_2^{\cdot -}$ contribute.

The oxidizing agents *viz*. $O_2^{\cdot -}$, H_2O_2,$^{\cdot}OH$ and even singlet oxygen ($^1O_2$) are collectively known as ROS, and their uncontrolled generation is detrimental for various organs including heart [95,96]. Mitochondria have long been considered as a major source of ROS due to electron leakage from the respiratory chain to oxygen to form superoxide. Other sources of ROS may include xanthine oxidase (XO), cytochrome P450-based enzymes, dysfunctional NO synthases (NOS) and infiltrating inflammatory cells such as neutrophils [97,98]. These ROS can disrupt the cell membranes, as well as damage DNA by direct

reactions and/or covalent modifications [99,100] or through endogenous genotoxins like the ROS-derived lipid-hydroperoxide breakdown products [101]. Besides these, nicotinamide adenine dinucleotide 3-phosphate (NADPH) oxidase is the major source of ROS [102] in cardiovascular cells. It is found to be present in both pressure and volume overload rat models and in human myocardium. Its increased activity plays an important role in the progression of hypertrophy to heart failure [97,103]. Moreover, factors that are implicated in heart failure, such as Ang II, ET, NA, TNF-α and various growth factors also activate NADPH oxidase and potentially increase ROS production [102,104]. During hypertrophy, when haemodynamic function is maintained, the antioxidant reserve is high, resulting in low OS. However, at the stage of decompensated failure, significant OS exists [105]. ROS have been shown to mediate the hypertrophic effects of several extracellular stimuli such as β-adrenergic receptor stimulation, Ang, ET and TNF-α on cardiac myocytes that may possibly involve activation of several kinases by NADPH oxidase [106-108].

ROSs are implicated in various aspects of cardiac remodeling and apoptosis, to lead to heart failure [94,98,109]. Patients with heart failure were found to have significantly higher levels of OS and decreased levels of endogenous antioxidants [110]. OS can regulate the quantity and quality of ECM by decreasing fibrillar collagen synthesis as well as activating the matrix metalloproteinases (MMPs) [111]. This would contribute to the process of cardiac dilatation seen in severe heart failure. Moreover, $O_2^{\cdot -}$ upregulates TGF-β_1 resulting in proliferation of cardiac fibroblasts [112]. Excessive production of superoxide anions can reduce vascular NO bioavailability via oxidative inactivation or biodegradation resulting in impaired endothelium-dependent vasorelaxation in HT [113]. Furthermore, interaction of superoxide anions and nitric oxide results in the production of peroxynitrite anion ($OONO^-$) in the vascular walls, which is a strong oxidant, and can further cause oxidative injury to the endothelium for its dysfunction [109,113]. All these provide strong support for the

involvement of OS in the pathogenesis of heart failure.

I.7 Cardiac electrophysiology

***I.7.1 Electrical remodeling*:** As mentioned previously, a normal heart functions incessantly at a constant rate through its special excitatory and contractile systems. The cardiac action potential (AP) is governed by the difference of potentials between the interior and exterior of a cardiac cell. The APs in various portions of the heart differs significantly, allowing their different electrical characteristics. For example, the heart excitatory system has the special property of spontaneous depolarization through a slow, but positive increase in the pacemaker potential across the cell membrane. Once the threshold potential is reached, the next pacemaker potential undergoes a rhythmic firing.

The cardiac APs or electrical stimulations are generated by the movement of ions through the transmembrane ion channels in the cardiac cells. The K^+ ions, phosphate anions and the conjugate bases of organic acids dominate inside the cells, while Na^+ and Cl^- ions are the major contributors outside the cells. In the resting state, a cardiac myocyte has a negative membrane potential. Ca^{2+} influx into the cardiac myocytes releases further Ca^{2+} ions from the sarcoplasmic reticulum through voltage-gated Ca^{2+} channels causing muscle contraction. After a delay, the K^+ channels reopen and the resulting flow of K^+ ions out of the cell causes repolarization. The voltage-gated Ca^{2+} channels in the cardiac sarcolemma are generally triggered by an influx in Na^+ ions during this phase of AP. Thus, fluxes of three ions: Na^+, K^+ and Ca^{2+} across the cardiac cell membranes generate the electrical potentials that are essential for cardiac contraction or activation the heart [114]. The AP in typical cardiomyocytes is composed of 5 phases (0-4), beginning and ending with phase 4. This is required for synchronous contraction of the atria and ventricles. Phase 0 is the phase of rapid depolarization, wherein the membrane potential shifts into positive voltage range. This phase is central to rapid propagation of the cardiac impulse (conduction velocity, 1 m/s). Phase 1

contributes to a rapid repolarization, and sets the potential for the next phase of AP. Phase 2, the longest plateau phase is unique among excitable cells and marks the phase of Ca^{2+} entry into the cells (conduction velocity, 0.3 m/s). Phase 3 induces rapid repolarization to restore the membrane potential to its resting value of normal working myocardial cells in phase 4 (conduction velocity, 0.8 m/s).

The depolarization phase (phase 0) is mediated by a rapid influx of Na^+ through voltage-gated Na^+ channels. This is followed by a rapid but incomplete repolarization in phase 1 via K^+ efflux through transiently activated K^+ channels (also known as the transient outward potassium current I_{to}). This early outward current set the initial plateau potential, influencing the behavior of subsequently-activated ion channels and AP duration [115]. The plateau of AP (phase 2) is characterized by minimal net ion flow due to the balance of an inactivating L-type Ca^{2+} inward current (I_{Ca}) and K^+ efflux through slowly activating voltage-gated channels (delayed rectifier K^+ current I_k). The K^+ permeability increases with time in phase 3 and ultimately results in complete repolarization. Phase 4 represents the time period between APs, where the pacemaker current is crucial [115]. The Na^+- and K^+-ATPase also play important roles in returning the Na^+ and K^+ ions to the initial values. The inward rectifying K^+ current I_{k1} is primarily responsible for maintaining the negative resting membrane potential (RMP) [114,115]. The I_{k1} gets inactivated after depolarization to prevent repolarization. The RMP has also been shown to be regulated by I_{k1ACh} (the K^+ current modulated by the muscarinic ACh receptor) and I_{k1ATP} (ATP-sensitive K^+ channel) [115]. I_{t0} and I_k are believed to be the major currents involved in controlling repolarization, and thus, duration of AP.

Electrical remodeling refers to electrical changes to the heart in response to various pressure and volume overload conditions, and encompasses changes such as delayed repolarization, prolonged AP duration, increased dispersion of refractoriness and

electrophysiological heterogeneity [116]. The Ca^{2+}-independent transient outward current I_{t0} is important in the early phase of repolarization while the delayed outward rectifying current I_k plays a major role in the later phases of repolarization [114,117,118]. Prolongation of the AP duration can result either from an increase in inward current, a decrease in outward current, or both [119]. Prolonged AP or other electrical abnormalities in heart, observed in spontaneously hypertensive rat (SHR) [117] and the DOCA-salt hypertensive rat [119] might cause conduction problems such as ventricular ectopy and arrhythmias. Moreover, development of cardiac hypertrophy is attributed to the abnormalities in the cardiac myocytes electrophysiological properties such as AP [117,120].

***I.7.2 Measurement of electrical activity*:** The cardiac myocyte contraction mechanics are studied *in vitro* by examining the behavior of an isolated muscle strip. Electrophysiological techniques such as single-cell microelectrode technique are of clinical importance for understanding and measuring electrical changes in the hearts of hypertensive and heart failure rats. This is achieved by anchoring the papillary muscle strip at both ends and stimulating under an initial tension or preload to undergo isometric contraction. The tension, generated during isometric contraction increases with increasing initial length. Alteration in initial fibre length is analogous to preload. This technique also allows understanding of the reversibility of the electrical changes, associated with cardiac remodeling due to pharmacological interventions.

Electrocardiography (ECG) is a noninvasive technique for transthoracic interpretation of the electrical activity of the heart over a period that is externally recorded by skin electrodes and captured by an ECG device. ECG works mostly by detecting and amplifying the tiny electrical changes on the skin that are caused when the heart muscle depolarizes during each heartbeat. At rest, the cardiomyocyte has a negative charge across sarcolemma. For a healthy heart, reducing this charge towards zero (depolarization) activates the

mechanisms for contracting a myocyte during each heartbeat. The systematic progression of a depolarization wave triggered by the cells in the SA node spreads out through the atrium, passes through the intrinsic conduction pathways and then spreads all over the ventricles. This is detected as tiny rises and falls in the voltages between two electrodes, placed on either side of the heart. This provides information on the overall rhythm and weaknesses in different parts of the heart.

A typical and normally visible (in 50 to 75% cases) ECG tracing of the cardiac cycle consists of a P wave, a QRS complex, and a T wave. A U wave is also seen sometimes. The baseline voltage of the ECG is known as the isoelectric line and the potential as RMP. The RR interval, the interval between two successive R waves is the inverse of the heart rate (HR). HR is usually calculated from the time elapsed between two ventricular contractions and typically expressed as beats per minute (bpm). The normal resting HRs of humans and rats are 60-80 bpm and 250-300 bpm respectively. HR is regulated mainly by neural factors like autonomic control on the sinus node, hormonal factors such as the renin-angiotensin peptides, and mechanical factors such as right auricular wall stretch. Since HR is a determinant of stroke volume and cardiac output, it plays a major role in the regulation of arterial BP [121].

Heart rate variability (HRV) is the physiological phenomenon of variation in the time interval between heart beats. HRV analysis relies on the assessment of fluctuations on the intervals among the successive R waves of ECG. Its rapid fluctuations show that the structure generating the signal also involves nonlinear contributions. Hence, these may specifically reflect changes of sympathetic and vagal activities. It is a powerful tool to assess cardiac autonomic control [122,123] and a strong, independent predictor of mortality after an acute myocardial infarction [124]. In rats, power spectral and frequency spectral analyses of HRV have been shown to be effective methods of detecting disturbances in cardiac autonomic

control in some experimental pathologic models, such as myocardial infarction and diabetic neuropathy [125,126]. The frequency domain methods assign bands of frequency ranges. In rats, the bands are typically high frequency (HF): 0.15-0.4 Hz, low frequency (LF): 0.04-0.15 Hz, and very low frequency (VLF): < 0.04 Hz. The LF/HF ratio is an important marker of sympathovagal balance on HRV control [121].

Although cardiac automaticity is intrinsic to various pacemaker tissues, heart rate and rhythm are largely under the control of the autonomic nervous system [127]. The autonomous control over the heart is governed by sympathovagal system. Its two components, the sympathetic and the vagal or parasympathetic systems constantly interact under normal conditions and maintain a balance. The parasympathetic nerves are distributed mainly to the SA and AV nodes, to a lesser extent to the muscle of the two atria, and very little to the ventricular muscle directly. The sympathetic nerves, conversely, are distributed to all parts of the heart, with strong representation in the ventricular muscle as well as in other areas. The parasympathetic activity is a major contributor to the HF component of HRV, as seen in clinical and experimental observations of autonomic maneuvers such as electrical vagal stimulation, muscarinic receptor blockade, and vagotomy. Thus, HF denotes prevalence of parasympathetic or vagal activity. During prevalence of parasympathetic tones, acetylcholine (ACh) is released at the vagal nerve endings to greatly increase the permeability of the fiber membranes to K^+ ions. This allows rapid leakage of K^+ out of the conductive fibers, leading to increased negative charge inside the fibers. This reduces the excitability of the tissues and RMP in the SA node. Thus, the initial rise of the sinus nodal membrane potential because of inward Na^+ and Ca^{+2} leakage requires much longer time to reach the threshold potential for excitation, slowing rhythmicity rate of these nodal fibers. Moreover, reduced electricity production by the atrial fibers entering the AV node reduces the nodal fibers excitability, and thus, delays conduction of the impulse. The parasympathetic responses are usually relaxation

responses [128]. The LF denotes the prevalence of sympathetic tones. It increases the rate of sinus nodal discharge along with the rate of conduction as well as the level of excitability in all portions of the heart. It also increases the force of contraction of all the cardiac musculature, both atrial and ventricular. Sympathetic nerves release the hormone norepinephrine at the nerve endings that increases the permeability of the fiber membrane to Na^+ and Ca^{2+} ions. In the SA node, an increase in Na^+ and Ca^{2+} permeability results in more positive resting potential to increase the rate of upward drift of the diastolic membrane potential toward the threshold level for self-excitation. These accelerate self-excitation and, therefore, increase HR. In the AV node and bundles, increased Na^+-Ca^{2+} permeability causes the excitation of each succeeding portion of the conducting fiber bundles by the AP, thus decreasing the conduction time from the atria to the ventricles. The increased permeability to the Ca^{2+} ions is responsible for the increase in contractile strength of the cardiac muscle under the influence of sympathetic stimulation. Sympathetic response is usually a stress-related response, which becomes active during the stress condition to fight. It is important to consider that HRV measures fluctuations in autonomic inputs to the heart rather than the mean level of autonomic inputs. There is a significant relationship between the autonomic nervous system and cardiovascular mortality, including sudden cardiac death [129]. Experimental evidence for an association between propensity for lethal arrhythmias and signs of either increased sympathetic or reduced vagal activity has spurred efforts to develop quantitative markers of autonomic activity [130]. HRV represents one of the most promising such markers.

The P wave in the ECG is the main electrical vector directed from the SA node towards the AV node, spreading from the right to the left atria. The P wave duration is a measure of atrial hypertrophy, as more muscle mass leads to increased time of atria depolarization. This also indicates the increase in active flow from atria to ventricle. The PR

interval is the interval measured from the beginning of the P wave to the beginning of the QRS complex, and reflects the time taken by the electrical impulse to travel from the sinus node through AV node and enter the ventricles. The PR segment coincides with the electrical conduction from the AV node to the bundle of His to the bundle branches and then to the PFs. Without causing any myocyte contraction, this electrical activity simply moves towards the ventricles and appears as a flat region on the ECG. However, the PR interval is clinically more relevant as it provides important information of AV node function. The QRS complex reflects the rapid depolarization of RV and LV. The ventricles have a large muscle mass compared to the atria and so the QRS complex usually has a much larger amplitude than the P-wave.

The QT interval, the time between the start of the Q wave and the end of the T wave, represents electrical depolarization and repolarization of RV and LV. A prolonged QT interval is a biomarker for ventricular tachyarrhythmia and a risk factor for sudden death. But since it varies with HR, QT is corrected according to the Bazett method to obtain QTc that is used clinically. The QT interval is adjusted with HR to improve the detection of patients at increased risk of ventricular arrhythmia. It is the most clinically relevant parameter. The ST segment connects the QRS complex and the T wave, and represents the period when the ventricles are depolarized. It also gives the measure of infarction in the myocytes. The T wave, representing repolarization (or recovery) of the ventricles has two periods. The beginning of the QRS complex to the apex of the T wave is the absolute refractory period and the last half of the T wave is referred to as the relative refractory period (or vulnerable period).

The APs of the pacemaker cells in the SA and AV nodes are significantly different from those in working myocardium. The characteristics of the AP change across the myocardial wall from endocardium to mid myocardium to epicardium. Epicardial cells have a

prominent phase 1 and the shortest AP. The AP duration is longest in the mid myocardial region. The average value of the ventricular AP duration is reflected in the QT interval in the ECG. The membrane potential at the onset of phase 4 of cardiac AP cycle is more depolarized, undergoes slow diastolic depolarization, and gradually merges into phase 0. The rate of depolarization in phase 0 is much slower than that in the working myocardial cells and results in slow propagation of the cardiac impulse in the nodal regions. Cells in the His-Purkinje system also show phase 4 depolarization under special circumstances.

ECG is a remarkable tool to measure and diagnose abnormal rhythms of the heart, caused by damage to the conductive tissue that carries electrical signals or electrolyte imbalances [131]. It gives many parameters that are well-validated prognostic indicators of cardiac risk in patients suffering from a number of cardiomyopathies. Increased HR, decreased HRV, and increased duration and variability of cardiac ventricular electrical activity (QT interval) are all indicative of enhanced cardiac risk. Lethal cardiac arrhythmias contribute to mortality in a number of pathological conditions. It can also reveal the specific infarcted area. Some key ECG parameters, their implications and values for normal humans are listed in **Table I.1**.

This technique is also used in various animal models, in particular to assess the electrochemical modulatory effects of new drugs on cardiovascular system [132,133]. In rat models, the ECG-derived measures of cardiac electrical activity can provide information on the susceptibility of ventricular arrhythmias in seizure disorders, or any pathology associated with increased risk of sudden cardiac death. It is used to determine the drug-induced electrochemical disturbances in rats [134]. ECG is often used to study cardiac autonomous control allowing extraction of HRV parameters in rats [131]. However, ECG cannot reliably measure the pumping ability of heart. Hence, the ultrasound-based echocardiography or nuclear medicine tests (^{99m}Tc Sestmibi.) are used.

Table I.1 ECG components and their interpretations

ECG parameter	Normal period	Implication
P wave	80 ms	depolarization of atria and preparation for contraction
RR interval	0.12 - 0.2 sec	time for impulse to spread from atria to ventricles
QRS complex	15 ms	depolarization of the ventricles
ST segment	-0.5 and +1.0 mm below and above the baseline	completion of ventricles depolarization
QT interval	101 ms	electrical systole
T wave	<5 mm in amplitude	repolarization of ventricle

I.8 Assessment of cardiac functioning

Besides electrophysiology, myocardial functioning also depends on the size and shape of the heart, its pumping capacity, location of its components and conditions of its tissues. These are routinely assessed *in vitro* by the isolated perfused heart technique, developed by Oscar Langendorf; and more precisely by *in vivo* echocardiography (Echo), as are discussed below.

***1.8.1 Isolated heart preparations-Langendorf method*:** The simple and relatively inexpensive method is highly reproducible for broad spectrum of measurements of various parameters, especially the diastolic stiffness of the heart. Hence it is extensively used in modern cardiovascular and pharmacological research, despite its few shortcomings. In this, blood or other perfusates are delivered into the heart through a cannula inserted in the ascending aorta, either at a constant pressure or a constant flow. Perfusion can be done at a

constant pressure, but more frequently this is achieved at a constant flow, mostly with oxygenated saline solutions. The retrograde flow in the aorta closes the leaflets of the aortic valve. As a consequence, the entire perfusate enters the coronary arteries via the ostia at the aortic root. After passing through the coronary circulation the perfusate drains into the right atrium via the coronary sinus. With the insertion of intraventricular balloon in the ventricles, the ventricle can contract isovolumetrically to measure various parameters providing maximum information about the condition of the myocardium and the coronary vessels. These include mechanical parameters (contractile force, volume, ventricular diameter) of the working myocardium, mean coronary flow, bioelectrical parameters (ECG, monophasic injury potentials), and cardiac rhythm. The functional parameters are intact function of the working myocardium and the coronary vessels. In the Langendorf-heart of normal or pretreated animals, inotropic, chronotropic, antiarrhythmic or vasoactive substances can be investigated in the steady state or by means of specific stress tests. In addition, the preparation is particularly suitable for biochemical studies of myocardial metabolism. As stiffness is the functional correlate of fibrosis, the Langendorf isolated heart preparation is also used to establish the relationship between fibrosis, diastolic stiffness and contractility [53].

***1.8.2 Echocardiographic examination*:** Echo is a noninvasive technique that uses standard two-dimensional, three-dimensional, and Doppler ultrasound to image two-dimensional slices of the heart for diagnostic tests in cardiology. It can provide a wealth of helpful information, such as the size and shape of the heart, and key heart function parameters such as pumping capacity, cardiac output, ejection fraction, and relaxation function. In humans, use of this safe and painless procedure usually consists of a comprehensive two-dimensional (2-D) examination complemented by additional M-mode (motion-mode), spectral and colour flow Doppler modalities [135]. The Doppler echo relies on the Doppler effect *i. e*., if the object is

moving towards the sound source then the reflected frequency is higher than the transmitted one, while if the object is moving away then the reflected frequency is lower than the transmitted one. This gives excellent measures of blood flow, velocity, volumes and direction to assay the cardiovascular functions. [140]. It is especially useful for assessing diseases of the heart valves (area and function). It can detect abnormalities in the pattern of blood flow, such as the backward flow of blood through partly closed heart valves, known as regurgitation. By assessing the motion of the heart wall, echocardiography can help to detect the presence and assess the severity of coronary artery disease. It also helps to determine whether any chest pain is related to heart disease. Echo can help to detect hypertrophic cardiomyopathy, in which the walls of the heart thicken to compensate for heart muscle weakness. It can also detect any abnormal communications between the left and right side of the heart and help calculation of the cardiac output as well as the ejection fraction. It can measure diastolic function, fluid status and dys-synchrony [136].

Although commonly performed in humans, the use of echo in cardiovascular studies on rats and small rodents is sporadic, due to the technical difficulties of their small heart sizes and rapid heart rates relative to humans. Nevertheless, improved echo equipment and techniques, digital processing, higher frame rates and improved resolution have triggered its use in small animal research [137]. The echo machines use piezo electric transducers. For rats, generally a high frequency 12 MHz probe is used for detection at a depth of 3 cm to focal zones. It's utility as a reliable measure of the LV structure and function [138] and reproducibility in studying cardiac geometry and function in post-infarction LV remodeling in rats have been demonstrated [139]. Moreover, feasibility of performing serial echo measurements in rats permits tracking of structural and functional changes longitudinally [139,140].

I.9 Rat models of hypertension and cardiovascular remodeling

Animal models are invaluable tools to study CVD at various stages, the mechanisms of the pathogenesis and also the effects of drug interventions. An ideal animal model for human CVD should (i) mimic the disease; (ii) allow studies in chronic and stable disease states; (iii) produce predictable and controllable symptoms; (iv) allow measurement of relevant cardiac, biochemical and hemodynamic parameters; and (v) strictly satisfy animal welfare considerations. Although the rat models are extensively used in CVD, these can't integrate neurohumoral adaptations, encountered in human CVDs. Moreover, the use of young adult rats truly does not mimic human CVDs. Nevertheless, these models are acceptable from the economical viewpoint since a large sample size can be produced in a relatively short period of time [141,142]. To this end, several genetically-induced, surgically-induced or drug-induced models of HT and heart failure are widely used. Amongst these, those for systemic HT include: (i) spontaneously hypertensive rat (SHR); (ii) stroke-prone SHR (SHR-SP); (iii) two kidney one clip model (iv) mineralocorticoids (deoxycorticosterone acetate (DOCA)-salt); (v) NO synthase inhibition (L-NAME administration) and (vi) diabetic hypertensive rats (STZ-SHR). All models have their *pros* and *cons* but the SHR and DOCA-salt hypertensive models are most commonly used. SHR is a genetically induced model, wherein animals are born normotensive but develop HT at 4-5 months of age. After 18 months, heart failure develops and animal start dying. This model requires long term experiments to assess the relevant parameters. An overview of the presently used DOCA-salt HT model is given below.

1.9.1 DOCA-salt hypertensive rats: In this model, DOCA is administered to uninephrectomized (UNX) rats together with salt (NaCl) loading to induce HT rapidly, mimicking human volume overload-induced HT [53]. This model develops HT with increases in cardiac and renal weights. Interestingly, more severe HT is developed in male

than female rats [143]. Administration of DOCA or NaCl alone does not change the BP significantly [144]. It is regarded as an angiotensin-independent model as the renin-angiotensin system (RAS) is depressed in it [141]. Studies show that compounds, inhibiting RAS do not have any effect on the increased BP of DOCA-salt rats [145]. The volume overload is achieved because of renal mass loss (due to uninephrectomy), and administration of salt retaining hormone, DOCA as well as NaCl in drinking water. The excessive Na^+ retention stimulates the vasopressin V2 receptor, which increases the basal BP and accelerates the organ damage and mortality [146]. The DOCA-salt rats also show elevated ET system, specifically ET-1 [147,148]. The predominant sympathetic over parasympathetic tones in these animals [149], reflected by elevated levels of serum catecholamines [144,150] play an important role in HT and increased HR. Additional features of this model including its suitability and limitations in studying CVD are elaborated in Chapter III.

I.10 Current clinical antihypertensive drugs and their limitations

The antihypertensive drugs are the mainstay of treating any form of CVD. These drugs lower BP by different means. The most widely used drugs are the (i) thiazide diuretics (*e. g*., epitizide); (ii) calcium channel blockers (*e. g*., amlodipine); (iii) angiotensin-converting enzyme (ACE) inhibitors (*e. g*., lisinopril); (iv) angiotensin II receptor antagonists (ARBs) (*e. g*., losartan); and (v) β-blockers (*e. g*., atenolol). The fundamental goal of treatment is the prevention of the important endpoints of HT, such as heart attack, stroke, heart failure and mortality. The diuretics help the kidneys to eliminate excess salt and water from the body's tissues and blood. The calcium channel blockers prevent entry of calcium ions into muscle cells in artery walls to avoid their contraction. The ACE inhibitors prevent conversion of angiotensin I into angiotensin II, a potent vasoconstrictor, while the angiotensin II receptor antagonists work by antagonizing the activation of the angiotensin receptors. The β-blockers act on the β-adregenic receptors to block neurotransmitters in the brain, so that the message to

constrict doesn't reach smooth muscles. On the other hand, vasodilators like sodium nitroprusside (SNP) act directly on the smooth muscle of arteries to relax their walls facilitating easy movement of blood through them.

Despite lowering BP, many of these drugs show several limitations including several side effects. The thiazide diuretics are usually the first-line treatment of choice for high BP [151] because of their vasodilatory effect. However, they increase the chances of onset of new diabetes, and can also cause hypokalemia [152]. The β-blockers do not have a positive benefit on endpoints like some other antihypertensive drugs like the calcium channel blockers [153]. A systematic review of 63 trials with over 35,000 participants indicated that use of β-blockers increased the risk of mortality, compared to other antihypertensive therapies [154]. The α-blockers also have similar limitations and are no longer recommended as a first-line choice in the treatment of HT [155]. There are also conflicting views on angiotensin II receptor antagonists. The CHARM-alternative trial showed a significant + 52% (p = 0.025) increase in myocardial infarction with candesartan (versus placebo) despite a reduction in BP [156]. In the VALUE trial, valsartan produced a statistically significant 19% (p = 0.02) relative increase in the pre-specified secondary end point of myocardial infarction (fatal and non-fatal) compared to amlodipine [157]. Vasodilators like SNP are only used in hypertensive emergencies or when other drugs have failed, and are rarely given alone. The AASK trial showed that ACE inhibitors are more effective in slowing down the decline of renal function compared to the calcium channel and β-blockers [158]. However, the ACE inhibitors were less effective in reducing BP and had a 51% higher risk of stroke in African-Americans, when used as the initial therapy compared to a calcium channel blocker [159]. On the other hand, another trial showed that the thiazide-type diuretics and calcium channel blockers were both more effective as monotherapy in improving cardiovascular outcomes

compared to the ACE inhibitors for this subgroup [160]. The calcium channel blockers could not reduce mortality, but show multiple side effects [161].

I.11 Natural compounds as CVD modulators

From the forgoing, it is apparent that the clinical reports on the outcome of using many of the antihypertensive drugs are far from satisfactory. They target only one stage or pathway, and do not work in a multi-factorial manner to show the desired results. Further, many of these are often expensive and show side effects. These warrant search for drugs that are affordable, have no or less side effect, and act on different targets to manage the HT as well as its important end points. Both terrestrial and marine natural sources have provided several of the clinically used drugs or provided their leads. Moreover, the traditional or folklore medicinal systems, primarily based on plants/herbs are being extensively used by the people of several countries (including India) to cure various ailments. These factors as well as the limitations of the currently used synthetic drugs have evoked great interest in natural drugs.

Given the crucial role of OS in various stages of CVD, the natural antioxidants, especially the polyphenolics appear to be potential targets for developing better cardio-protective drugs. This is also substantiated by several epidemiological as well as randomized intervention studies with regard to consumption of vegetables and fruit-rich diets, containing high amounts polyphenolics antioxidants [162,163]. Extensive research with dietary antioxidants is being carried out for cardioprotection [164,165]. Polyphenols are a wide and complex group of secondary metabolites, produced by plants and microorganisms via the shikimic acid pathway. These are used by the hosts for their own defense against fungal infection, but don’t have any nutritional value [166,167]. Amongst the >8000 polyphenols identified, majority of the dietary polyphenols are the flavonoids. Their chemical structures range from simple molecules such as phenolic acids, to highly polymerized compounds like

proanthocyanidins. The richest sources are fruits, berries, vegetables, cereals, legumes, nuts, and beverages such as wine, tea, coffee and cocoa. However, the types and amounts of compounds may vary greatly between different foods. In general, the bioavailability of most polyphenols is relatively poor. Their absorption is considered to be dose-dependent and mainly occurs through small intestine and colon. The absorption is quite rapid and the peak concentrations in plasma are attained at 12 h after ingestion. The plasma concentrations usually vary between 0 to 4 μM after polyphenol supplementation. However, very little is known about the tissue uptake of polyphenols in humans. The polyphenols are excreted either in urine or bile after being conjugated (methylated, sulfated or glucuronidated) in the small intestine, or later in the liver to restrict their potential toxic properties. Evaluation of the clinical potential of polyphenols against CVD was seriously initiated after the *in vitro* finding that red wine polyphenols inhibited the oxidation of low density lipoprotein (LDL) [168] and provided a plausible explanation for the "French paradox"). Subsequently, the Zutphen Elderly Study showed found that high intake of flavonoids protected against coronary heart disease [169].

Despite showing some inconsistency, the results from various cohort studies with long follow-up as well as case control studies suggest that flavonoids may modestly decrease the risk of CHD [170]. Numerous *in vivo* studies have provided relatively strong and consistent evidence of the antioxidant and cardioprotective effects of polyphenols. In particular, the monomeric and polymeric flavan-3-ols, present in green and black teas, red wine and cocoa were found effective in treating the symptoms of CVD. More importantly, besides lowering BP, the polyphenols showed antithrombotic and anti-inflammatory properties as well as vasodilatory effects on endothelial function. These factors truly reflected their cardio-protective action. However, due to the short duration of the animal experiments and the shorter life span of animals *vis-à-vis* humans, too much clinical evidence is not expected.

Nevertheless, application of scaling equations based on different metabolic rate in humans and animals, and a body surface area-based conversion may provide valuable correlation. The present studies were conducted using the natural phenolic, malabaricone C, while another polyphenol, curcumin was used as the positive control. Hence, a brief account of these phenolics is provided below. The chemical structures of curcumin and mal C are shown in **Fig. I.2**.

***Curcumin*:** It is the principal ingredient of turmeric (*Curcuma longa*), an Indian spice extensively used all over the world in various food preparations, and also valued for its medicinal attributes. The cardio-protective property of curcumin has been studied by various groups that has been reviewed [171,172]. More recently, treatment with curcumin (100 mg/kg/day) reduced the BP in L-NG-nitroarginine methyl ester hypertensive rats [173]. Besides reducing surgically-induced myocardial infarction, curcumin (50 mg/kg/day) improved ventricular dimensions and functions in salt-sensitive Dahl rats by attenuating cardiac hypertrophy and fibrosis [174]. In a phase I clinical trial, its (8 g/day) oral administration for 3 months did not show any side-effect or toxicity [175]. It (500 mg/day) also decreased the serum lipid peroxides and total cholesterol concentration while increasing serum HDL cholesterol concentrations in healthy individuals [176]. Curcumin (10 mg twice a day, for 30 days) also reduced serum LDL cholesterol and increased serum HDL cholesterol in atherosclerosis patients [177]. However, its poor bioavailability limits its use in clinical scenario.

***Malabaricone C*:** The fruit rind of the plant *Myristica malabarica* (Myristicaceae) (popularly known as rampatri or false nutmeg) is an exotic Indian spice that is credited with hepatoprotective and antithrombotic properties. It is also an ingredient in the Ayurvedic preparation, pasupasi [178]. The diarylnonanoids, malabaricone C (designated as mal C) is one of its major antioxidant constituent, as revealed from both *in vitro* [179] and *in vivo*

studies, carried out with indomethacin-treated mice [180,181]. Its anti-cancer property has also been demonstrated using human lung and breast cancer cell models [182,183].

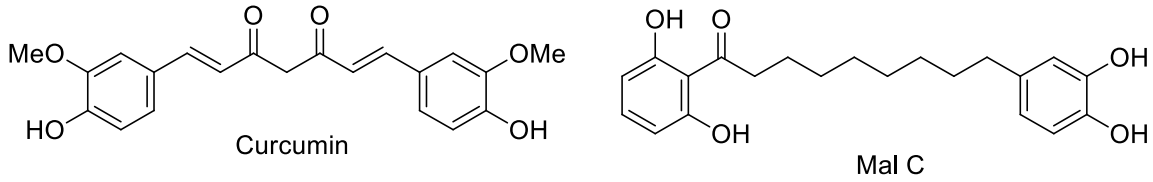

Fig. I.2 Chemical structures of curcumin and mal C.

I.12 Aims and hypothesis of the present investigation

Herbs and spices are usually considered to add sumptuous richness to many recipes in terms of improving color and aroma of foods with less contribution to nutrition. However, more recently, their positive impact on human health has been appreciated. Spices are one of the most important targets to search for natural antioxidants, and many have antioxidant levels comparable to several popular "super foods". Hence, the overall aim of this study was to examine the cardiovascular remodulatory potential of mal C using the DOCA-salt hypertensive rat model. The consensus belief is that HT results in cardiovascular remodeling, which leads to cardiovascular dysfunction ultimately resulting in heart failure. Hence, it was hypothesized that mal C may show cardio-protection due to its antioxidant and anti-inflammatory properties. Moreover, as a spice-component, it may also be non-toxic to humans even up to a significantly high dose. The specific aims of the present work were to:

(i) establish the non-toxicity and bioavailability of mal C in rats;

(ii) examine the BP-lowering efficacy of mal C in the chosen hypertensive model, and standardize the dose *vis-à-vis* a few clinically used antihypertensive drugs as well as a polyphenol, curcumin;

(iii) evaluate the ability of mal C to reduce OS and correlate with the alteration in the vaso-dilator/ vaso-constrictor ratio;

(iv) examine the effect of mal C on cardiac remodeling parameters such as hypertrophy,

collagen deposition and fibrosis; and finally,

(v) evaluate performance of mal C in improving cardiovascular structure and function, using *in viv*o and *ex vivo* systems.

CHAPTER-II

MATERIALS & METHODS

II.1 Chemicals and reagents

DOCA, heparin, aprotonin, leupeptin, PMSF, PEG, Triton X-100, ascorbic acid, EDTA, curcumin, dihydroethidium (DHE), noradrenaline (NA), acetylcholine (AC) and sodium nitroprusside (SNP) were purchased from Sigma Chemicals (St. Luois, MO). Other chemicals used were: ketamine (Themis Medicare Ltd., Mumbai, India), diazepam (Svizera Health Care, Mumbai, India), thiopentone (Neon Lab. Ltd., Mumbai, India), xylazine (Indian Immunologicals Ltd., Hydrabad, India.), atenolol (Ipca Lab. Ltd., Mumbai, India), amlodipine (Cipla Ltd., Uttrakhand, India), type II phosphatase inhibitor (New England Biolabs, UK), sirius red F3BA, haemotoxylin and eosin (Fluka, Germany), carbogen gas (AA Traders, Mumbai, India), NaCl, KCl, MgCl2, CaCl2, NaHCO3, NaH2PO4, glucose, formaldehyde and phosphomolybdic acid (Thomas Baker, Mumbai India), assay kits for total nitrate/nitrite (R&D Systems, Inc. MN, USA), TBARS, total antioxidant status (TAS) (Cayman Chemical Company, MI, USA), ET-1 immunoassay kit (R&D Systems, Inc. MN, USA) and EIA kits for PGI2 (Antibodies-Online, Georgia USA), AVP and big ET (Enzo Life Sciences, PA, USA). Mal C was isolated from *M. malab*arica fruit rinds as described previously [179].

II.2 Instrumentations

The UV-Vis absorption spectrophotometry was carried out with a JASCO spectrophotometer, model V670. The Atomic absorption spectroscopy (AAS) was carried out with an ANALYTIK JENA atomic absorption spectrometer, model ContrAA 301. The high performance liquid chromatography (HPLC) analyses were carried out with JASCO 2080 equipment. The HPLC separation was achieved using a C-18 reverse phase column of dimensions 4.6 mm × 250 mm, mobile phase: acetonitrile/water (60:40) at a flow rate of 1 ml/min, and detection at λ_{max} 354 nm. The retention time of mal C was 7.7 min under these conditions.

***II.2.1 Electro-cardiography (ECG)*:** ECG is an important diagnostic tool to assess the electrical and muscular functions of the heart. Usually more than 2 electrodes are used and combined into a number of pairs such as left arm (LA), right arm (RA) and left leg (LL) electrodes forms the LA + RA, LA + LL and RA + LL pairs. The output from each pair is called lead. Each lead looks at the different area of the heart from a different angle. Different types of ECGs can be referred to by the number of leads that are recorded, for example 3-lead, 5-lead or 12-lead ECGs. In a conventional 12 lead ECG profile, ten electrodes are placed on the patient's limbs and on the surface of the chest. The overall magnitude of the heart's electrical potential is then measured from twelve different angles (with the help of leads) and is recorded over a period of time. This gives the, the overall magnitude and direction of the heart's electrical depolarization and is captured at each moment throughout the cardiac cycle. The graph of voltage versus time produced by this non-invasive medical procedure is referred to as an electrocardiogram (ECG or EKG).

Fig. II 1 Three lead ECG profile of rat with Lab chart software

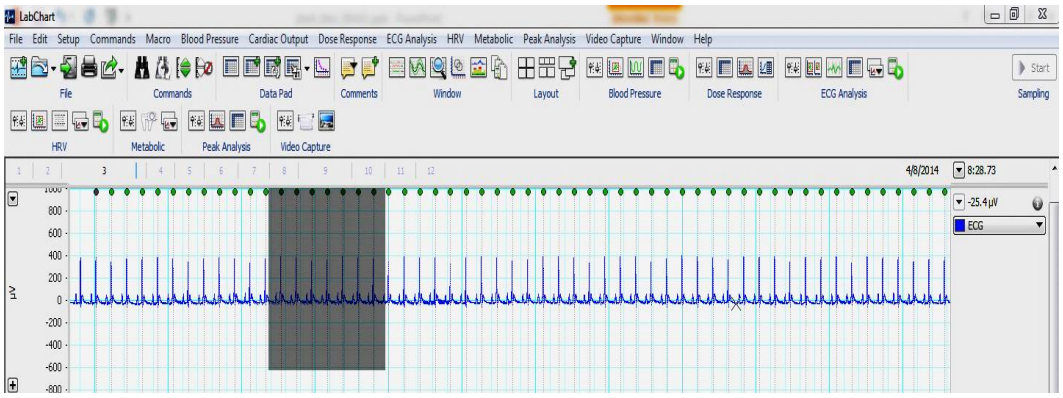

The three lead ECG profile screen grab taken with the lab chart software on a power lab system.

In humans usually a 12 lead ECG profile is recorded. The names and position of each electrode are as follows: RA is placed on the on the right arm, avoiding thick muscle. LA is placed on the same location where RA was placed, but on the left arm. RL is placed on the right leg, lateral to the calf muscle. LL is placed in the same location where RL was placed, but on the left leg. V_1, is placed in the fourth intercostal space (between ribs 4 and 5) just to the

right of the sternum (breastbone). V_2 is placed in the fourth intercostal space (between ribs 4 and 5) just to the left of the sternum. V_3 is placed between leads V_2 and V_4. V_4 is placed in the fifth intercostal space (between ribs 5 and 6) in the mid-clavicular line. V_5 is placed horizontally even with V_4, in the left anterior axillary line. V_6 is placed horizontally even with V_4 and V_5 in the mid axillary line. In rats, however, a 3 lead configuration is used, where the 2 electrodes serving as positive and negative are placed on both the fore limbs and an electrode serving as neutral placed on the hind limb. RA lead is usually placed on the surface or in the subcutaneous region of the right paw (with the needle electrode). LA lead is usually placed on the surface or in the subcutaneous region of the left paw. The LL electrode is placed on the surface or in the subcutaneous region of the left paw. The LL electrode serves as neutral. The combination of three leads gives the ECG profile in rats.

***II.2.2 Eco-cardiography (Echo)*:** With the development of very sensitive high frequency transducers with a small footprint and adequate computer software to measure indices of both systolic and diastolic function, Echo has become a very useful technique to study cardiac structures and functions. Moreover, with the use of M mode (motion mode) using Doppler effect (Reflected frequency of the sound wave sent towards an object depends upon its motion state) measurements of blood volumes, flow, velocity and direction are easily carried out, making echocardiography a very important tool in understanding and analyzing the cardiovascular effect of the new drugs under development.

The mammalian heart has 4 chambers: the left atrium, the left ventricle, the right atrium and the right ventricle. A cardiac cycle has two parts diastole and systole. Systole is the part when the ventricles contract and ejects the blood to the arteries and diastole is the part when the heart refills with blood. Following the systole (contraction), ventricular diastole is the period during which the ventricles are filling and relaxing, while atrial diastole is the period during which the atria are relaxing. When the smaller, upper atria chambers contract in late

diastole, they send blood down to the larger, lower ventricle chambers. When the lower chambers are filled and the valves to the atria are closed, the ventricles undergo isovolumetric contraction (contraction of the ventricles while all valves are closed), marking the first stage of systole. The second phase of systole sends blood from the left ventricle to the aorta and body extremities, and from the right ventricle to the lungs. Thus, the atria and ventricles contract in alternating sequence. The left and right atria feed blood, at the same time, into the ventricles. Then, the left and right ventricles contract simultaneously as well to complete a cardiac cycle. Echocardiography is used to measure the changes in the heart structure and functions during both the diastole and systole parts.

In our experiments anaesthetized rats lying in the dorsal recumbency position were used to get left parasternal and left apical echocardiographic images using the Hewlett Packard Sonos 5500 machine. The transducer used was a 12 MHz frequency transducer with a footprint of 10 x 13 mm. The transducer was used at an image depth of 2 cm to get the images to study the structural dimensions of the heart. The three-lead electrocardiogram (ECG) was recorded from the front limbs and the right hind limb.

Fig. II. 2 M-mode measurements of left ventricular dimensions

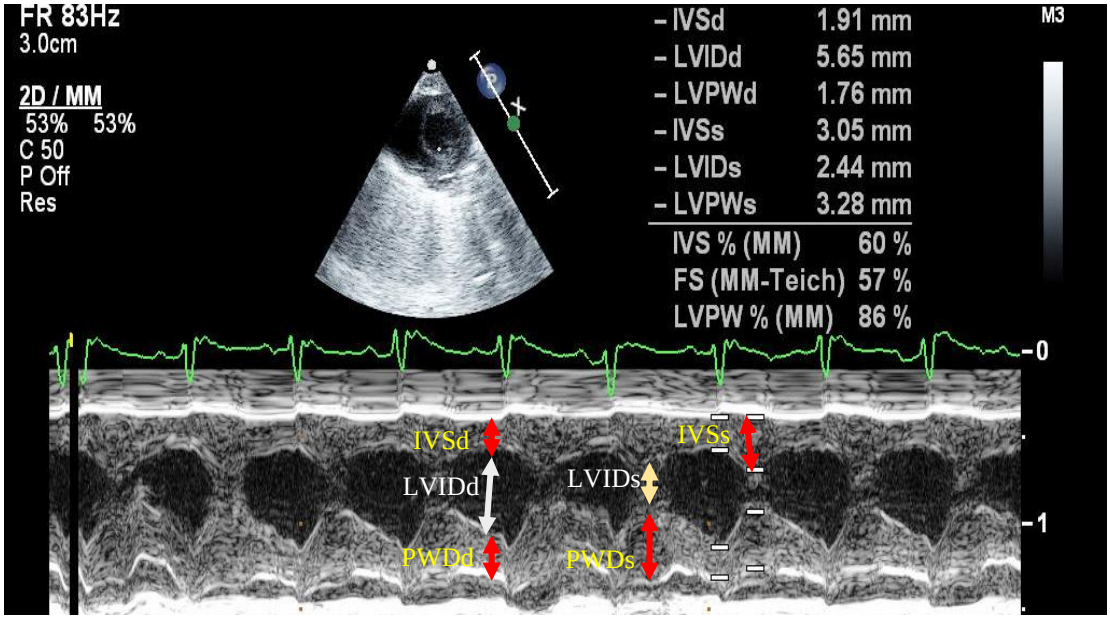

IVS- Interventricular septum, LVID- Left ventricular internal diameter, PW posterior wall d-diastole, s- systole

Left ventricle wall thicknesses and internal diameters at systole and diastole were defined using M-mode measurements at the level of the papillary muscles. The parameters were analyzed both in diastole and systole modes. The structural parameters studied were the following: (a) LV posterior wall thicknesses (LVPW), the thickness of the posterior walls of LV; (b) interventricular septum, the wall or septum dividing both the left and right ventricles. The corresponding end-systolic measurement is abbreviated as LVID which is the diameter of the lumen of the left ventricles which stores the blood to be pumped.

The Doppler tissue imaging was done from the apical view and for that four-chambers were viewed apically. The pulsed-wave Doppler probe was placed on the interventricular septum close to the mitral annulus. Suprastemal views with transmitral inflow and pulmonary venous profiles from the apical views were used to measure aortic arch diameter and pulsed-wave Doppler velocities of the ascending and descending aortic flows. This gives the aortic diameter and the blood velocities through them. Measurements of the peak velocity and

Fig. II. 3 Trans mitral Pulsed wave Doppler Echocardiography

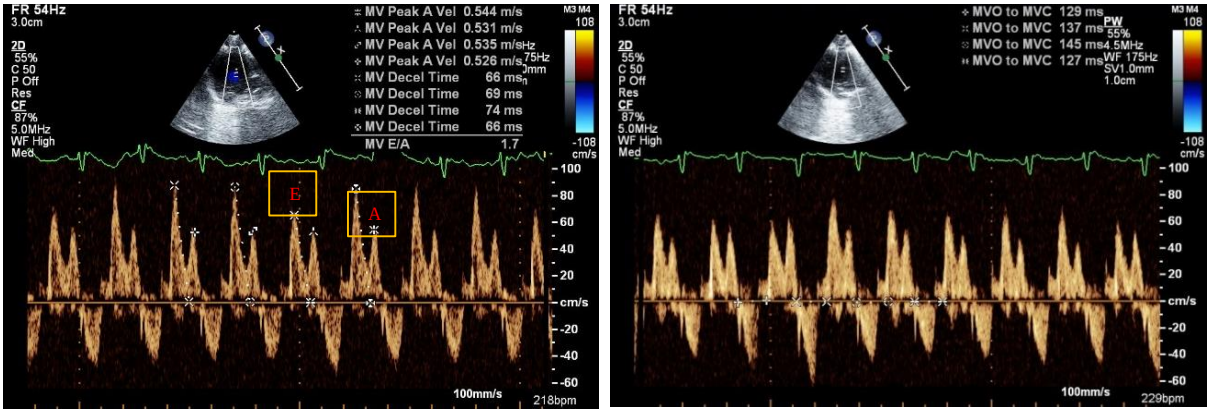

E=Early mitral inflow velocity;
A=Atrial mitral inflow velocity; MC-MO=Mitral valve closing to mitral valve opening time; DT=E-wave deceleration time.

ejection time were made from ascending aortic. Doppler profiles from the transmitral inflow trace were used to measure the different parameters such as, measurements of peak early diastolic velocity (E), peak velocity at atrial contraction (A), deceleration time and the period

between mitral valve closure and mitral valve opening (MC-MO). The left ventricular end-diastolic dimension was used as an index of systolic function. The transmitral Doppler profile was also used to assess left ventricular diastolic properties and various important parameters were derived from the resulting values by the software like LV mass, systolic and diastolic volumes, stroke volume and cardiac output.

II.3 Rats

Male Wistar rats (6-10 weeks, 300-330 g), bred at the BARC laboratory animal house facility, Mumbai, India, were procured after obtaining clearance from the BARC Animal Ethics Committee (BAEC/14/08 dated 05/09/2009). All the experiments were conducted with strict adherence to the ethical guidelines laid down by the European Convention for the Protection of Vertebrate Animals used for Experimental and Other Scientific Purposes. In addition, the ethical guidelines laid down by the Committee for the Purpose of Control and Supervision of Experiments on Animals, constituted by the Animal Welfare Division, Government of India, on the use of animals in scientific research were followed. The experiments were permitted by BAEC. The body weights, and food and water intakes of the rats were measured daily at 9.00 AM during the entire experimental period.

II.4 Drugs preparation

Stock solutions of different concentrations of mal C in DMSO were reconstituted in PEG to keep the final DMSO concentration <1%. A suitable stock solution of curcumin was also prepared in the same manner. Same volume (400 μl) of these solutions was administered to the rats to attain the required dose(s) of the test samples. The DOCA solution (24 mg/0.4 ml) was prepared in dimethyl formamide or DMSO.

II.5 Toxicity studies

For the chronic toxicity studies, mal C (100 mg/kg/day) was given to the rats every morning by oral gavage for one month. For the acute toxicity studies, a single bolus dose of

mal C (500 mg/kg) was given. Serum samples were pooled from the same group of rats after a month and the liver and kidney function tests were carried out. In addition, the effect of mal C (5, 10, 15, 20 and 100 mg/kg/day) on SBP of normal rats was also monitored. Each group contained 10 rats.

II.6 Plasma bioavailability of mal C

Rats were given mal C (10 mg/kg) and, were euthanized after 0, 1, 3, 6, 12 and 24 h, for plasma collection. Aqueous trichloroacetic acid (TCA, 7%) was added to an equal volume of plasma and centrifuged, at 12000 rpm for 10 min. The separated supernatant was treated with an equal volume of ethyl acetate (EA), the mixture vortexed for 10 min and the EA layer collected. This was purged with nitrogen gas and reconstituted with methanol. This methanol solution was analyzed by HPLC using a C-18 reverse phase column, 60:40 acetonitrile/water as the mobile phase at a flow rate of 1 ml/min and detecting the analyte at 354 nm. The concentration of mal C was determined from a standard curve, processed as above. The sample preparation was performed as reported earlier [184], while the HPLC conditions were standardized earlier by our group [180].

II.7 Development of DOCA-salt hypertensive rat model

This is a very well established rat model for studying cardiovascular modifications in rats. It is a physiological model of producing hypertension similar to humans. The model is established by decreasing the renal mass of rats by uninephrectomy (removal of one kidney) followed by administration of mineral corticoid DOCA (for retaining salts in the system) and 1% NaCl in drinking water. In this, HT along with pathological cardiovascular changes starts as early as 2nd day and statistically relevant number of surviving rats for analysis till the 28th day. In the present investigation, male Wistar rats were chosen for standardizing the model, as they are outbred and literatures show that the male rats develop higher HT than the female rats.

II.7.1 Anaesthesia standardization: For the surgical grade deep sedation of the rats, different

drug combinations at various doses are described in the literature [185]. Presently, the anaesthesia protocol was standardized using various combinations of drugs comprising of the following: ketamine (70-100 mg/kg), diazepam (2-5 mg/kg), xylazine (5-10 mg/kg), sodium thiopentone (30-70 mg/kg) and urethane (1-3 g/kg). The various drug combinations tested were ketamine + diazepam, ketamine + diazepam + xylazine, ketamine + xylazine, sodium thiopentone and urethane alone. These drugs or their combinations were administered to the rats via intraperitoneal (i. p.) route. The combinations were optimized so as to obtain deep surgical grade sedation for 4 h and light sedation (immobilization) for 1 h, and used for different assays as mentioned below. The important criteria considered for anesthetic were least cardiovascular depression, deep sleep, and complete recovery after sedation period, repeatability of sedation and minimum side effects. After several trials the drugs and their doses selected for our studies were as follows:

***II.7.1.1 For deep sedation*:** A mixture of ketamine 70 mg/kg (for its amnestic, anesthetic and dissociative property), diazepam 2 mg/kg (for its early sleep inducing and anti-anxiety property) and xylazine 5 mg/kg (for its anesthetic, muscle relaxant and pain killing properties) was administered in the rats by i. p. injection to obtain deep sedation. These rats were used for uninephrectomy surgery and also recording Echo.

***II.7.1.2 Light sedation for ECG, Echo-cardiography analyses*:** To achieve light sedation (immobilization) for 1 h, ketamine + diazepam was used. Ketamine 50 mg/kg was first injected followed by diazepam 2 mg/kg i.p. in the rats. In this case, the drugs were not mixed together. These rats were used for recording Echo and recording BP and ECG.

II.7.2 Preparation of uninephrectomized (UNX) rats: For uninephrectomy, male Wistar rats (6-10 weeks, 300-330 g), were used as older rats do not produce the same effects. The rats were anesthetized by i.p. injection of ketamine (70 mg/kg), diazepam (2 mg/kg) and xylazine (5 mg/kg). The left kidney was located by palpation and the lateral abdominal wall was shaved,

followed by a lateral abdominal incision above the left kidney to have access to the kidney and the left renal vessels. The ureter was ligated and the left kidney was removed and weighed. The body cavity wall was surgically sutured with sterile suture needles and the surface skin layer was surgically stapled with wound healing clips as a precautionary measure and to aid faster healing of the incision site.

In addition, DOCA 24 mg in 0.4 ml of DMF was injected subcutaneously every fourth day till 28th day from the surgery and ad libitum access to 1% sodium chloride (NaCl) in their drinking water for 4 weeks.

II.7.3 Experimental design: All the cardiological experiments were carried out with UNX rats. The rats were divided into several groups, each containing eight rats. The sham-treated UNX rats served as the control and received an oral dose of vehicle (1% DMSO in PEG, 0.4 ml) only. Except for the control, other rats were subcutaneously injected with DOCA solution every fourth day and given drinking water containing 1% NaCl for 28 days to develop the model. The model is developed by decreasing the renal mass of rats by uninephrectomy followed by administration of DOCA (for retaining salts in the system) and feeding with salt solution. All these factors are prerequisites of developing this model. Increasing the salt load in the system will increase the thirst, and hence more water intake by the rats. With only one kidney to work, the blood volumes of the system increases leading to volumetric stress followed by various pathological changes including hypertension, structural, electrical, physiological and biochemical modifications in the cardiovascular system.

For dose standardization, rats were given mal C (2.5, 5, 10, 15 and 20 mg/kg), curcumin (60 mg/kg) or the commercial drug, atenolol (10 mg/kg) by oral gavage every day at 10.00 AM during 15-28 days of the experiments. The doses of curcumin [173] and atenolol [185] were chosen based on the results of several previous studies using HT models. The anti-hypertensive effect of the respective treatments was assessed by measuring SBP of the control, DOCA-salt

and the treatment groups at the beginning (0 day, UNX rats without DOCA administration), 15th and 28th days of the experiments. For comparison, the SBPs of the normal as well as UNX rats given only 1% saline water were also measured. The SBPs of the rats orally given mal C (10 and 100 mg/kg) and curcumin (60 mg/kg) for 28 days were additionally measured.

II.8 Non-invasive Systolic blood pressure (SBP) measurements

The SBP was measured using non-invasive tail-cuff plethysmography. Rats were immobilized with an i.p. injection of ketamine (50 mg/kg) and diazepam (2 mg/kg). An inflatable cuff connected to a pressure transducer (MLT844 Physiological pressure transducer, AD Instruments, Sydney, Australia) was placed on the tail. The pulse transducer (MLT1010 Piezo-Electric Pulse Transducer, AD Instruments, Sydney, Australia) was then connected distal to the cuff. Both the transducers were connected to a non-invasive BP (NIBP) controller and PowerLab data acquisition unit on a computer, where the pulse and pressures were converted to an electrical signal and recorded. The tail cuff was inflated to inhibit the pulse signal and slowly released to enable the return of the pulse signal. The pressure where the pulse signal returned was recorded as the systolic pressure. The pressure was recorded 10 times per rat and the mean value recorded. The rats were kept under 60 W light bulb to keep them warm during sedation.

Fig. II. 4 Images of DOCA-salt rats during NIBP and Invasive BP measurements

A B

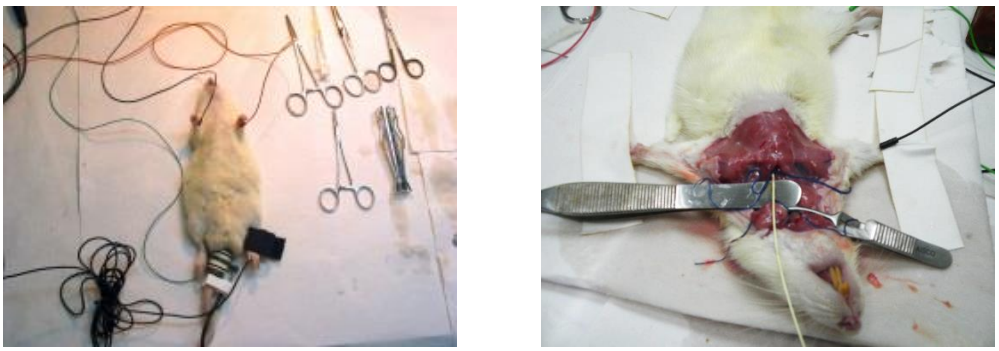

Rats were anaesthetized and noninvasive SBP (A) was measured using Piezo-Electric Pulse Transducer and a pressure cuff over the tail and the invasive blood pressure (B) was measured using Millar micro tip pressure sensitive transducer cannulated into the carotid artery.

II.9 Invasive blood pressure measurements

Invasive BP was measured by using Millar micro tip pressure sensitive transducer SPR 320. Closed-chest approach (right/left carotid artery (CA) catheter insertion) was used for measuring the pressures. Rats were immobilized with anesthesia (i.p. injection of ketamine (70 mg/kg), diazepam (2 mg/kg) and xylazine (5 mg/kg)). An inverted T-shaped middle-neck incision was made from mandible to the sternum. After carefully moving parotid glands to the side, the thin muscle layer around the throat was bluntly dissected with forceps to expose and isolate the right or left carotid artery. The vagus nerve was separated from carotid artery before catheter insertion. Suture were secured around the proximal end of the artery, gently pulled and taped to the table. Two additional sutures were placed beneath the carotid artery. A very loose knot was placed to the middle and distal suture (without securing it) and gently pulled with a needle holder. Left CA was blocked on both sides by bulldog clamps. Drops of physiological saline was put on the vessel area, and a small incision was made near the proximal end of the artery with a micro incision scissors and extended longitudinally for a short distance. Millar catheter tip was inserted into the vessel by pulling the arterial flaps, followed by gently securing the middle suture. Distal sutures were released simultaneously and pre-soaked catheter (for 30 min into physiological saline solution at 37 ^{o}C) was slid into the vessel. Arterial DBP and SBP were measured for 5 min. After measurements, the catheter was quickly advanced into the left ventricle (LV). After 5 min of measurements the catheter was pushed further inside until it reached the LV chamber to obtain the ventricular pressure (VP). VP trace can be identified with the absence of notch in the trace and only minimum and maximum pressure values were observed in the monitor. CA was sealed with the catheter inside. Pressure readings were taken with a powerlab machine connected to lab chart software (AD Instruments, Sydney, Australia). These measurements were carried out on the 28th day of experiment.

II.10 Biochemical and histological studies

Our dose standardization results revealed maximum SBP reduction of the DOCA-salt rats by mal C (10 mg/kg). Hence, we assessed the histopathological, and biochemical parameters using the same dose of mal C (10 mg/kg) and curcumin (60 mg/kg). The body weights and water intakes of the UNX, DOCA, and treatment (mal C and curcumin) groups were recorded every day throughout the experimental period. All other parameters were measured on the 28th day. For the plasma level assays, the rats were injected with heparin (200 IU in left femoral artery), blood from the abdominal vena cava collected in heparinized tubes, spun for 15 min at 2000 g, aliquoted and stored at -70 ^{o}C till further use. For analyzing the tissue samples, the rats were euthanized with a high dose of sodium thiopentone (100 mg/kg, i.p.), different organs removed immediately and the respective parameters evaluated (*vide infra*). To carry out the experiments in a blinded fashion, the rats were identified by typical notches in the ear and limbs and randomized. All the experiments were performed three times, each with eight rats per group. The data of the DOCA-salt group was compared to that of the UNX group, while those of the treatment groups were compared to that of the DOCA-salt group, throughout the manuscript.

II.11 Organ weights

The RV, LV, kidney, adrenal and spleen of the rats were removed following euthanasia with sodium thiopentone (100 mg/kg i.p.), washed with cold saline, blotted dry and weighed. The organ weights were normalized relative to the body weight of each rat.

II.12 Histology

Rats were anaesthetized with sodium thiopentone (100 mg/kg, i.p.), the heart and thoracic aorta were removed and the transverse sections of LV and thoracic aorta (2-3 cm long) were used for histological analyses. Tissues were fixed in 10% formol buffered saline solution for 7 days and transferred to a modified Bouin's solution (85 ml saturated picric acid, 5 ml

glacial acetic acid and 10 ml 37-40% formaldehyde), kept for two days followed by three changes in 70% ethanol over three days. Tissue samples were dehydrated overnight with solutions of 90% and with 100% (two changes, two h followed by one h) ethanol, cleared in toluene for two 20-min changes. For embedding, samples were placed into liquid paraffin wax for four 40-min changes followed by embedding in paraffin wax moulded into a wax block suitable to be cut with a rotary microtome. Sections of 15 μm or 10 μm thickness were cut with a microtome and floated onto a heated water bath (47 ^{o}C). Sections were placed onto glass slides coated with Mayer's albumin solution (1 g powdered egg albumin, 50 ml glycerol and 50 ml distilled water) where albumin acts as a protein glue. Sections were placed on racks to dry at room temperature for 24 h. Before staining, the slides were placed in an oven (56 ^{o}C) for one h. For deparaffinization, sections were immersed in xylene (three 15-min changes) and then hydrated with 100% (twice), 90% and 70% ethanol (3 min each), followed by brief immersion in 20% lithium carbonate in distilled water for one min to remove the excess picric acid from the Bouin's solution. Sections were then transferred to distilled water for a brief wash, bathed in phosphomolybdic acid (0.2% in distilled water) for 5 min to inhibit background autofluorescence and non-specific staining. After another brief rinse in distilled water, sections were placed in the collagen-selective stain picrosirius red (0.1% sirius Red F3BA in saturated picric acid) for 90 min. The sections were washed with 0.01 M HCl for 2 min, followed by dehydration with 70, 90 and 100% (three times) ethanol (30 secs each). Sections were cleared in xylene, mounted in Depex mounting medium and cover-slipped. The collagen depositions in LV and aorta were analyzed by laser confocal microscopy as described previously [186]. Image analysis was also performed via a blinded experimenter protocol using the software NIH-image (National Institute of Health, USA). The images were analyzed for saturated pixel intensity, which corresponded to collagen depositions.

For determination of the inflammatory infiltrations, tissue sections of LV and aorta were stained with haematoxylin and eosin (H&E). Sections of 10 µm thickness of LV and aorta were cut and floated onto glass slides for staining of inflammatory cells. After deparaffinization and hydration process as described above, sections were place in hematoxylin stain (1 g hematoxylin powder, 50 g aluminium potassium sulphate, 0.2 g sodium iodate, 1 g citric acid, 20 g choral hydrate and 1 lit. distilled water) for 6 min, and transferred to Scotts solution (4 g sodium bicarbonate, 20 g magnesium sulphate and 1 lit. distilled water) for 30 seconds to aid blue coloration of the nuclei. Sections were washed in a water bath for 5 min, immersed in 70% ethanol for approximately 1 min, followed by eosin stain (2 g eosin powder, 40 ml distilled water and 160 ml 95% ethanol; diluted 1:3 with 80% ethanol) for 11 min. The sections were rinsed in 95% ethanol, followed by dehydration and mounting as above.

For detecting O_2^- generation, the aorta was allowed to equilibrate for 30 min in an organ bath and set to a passive tension of 2 g in Krebs-Henseleit buffer of the following composition in (mM) (NaCl 118, KCl 4.7, $MgSO_4$ 1.2, KH_2PO_4 1.2, $CaCl_2$ 2.3, $NaHCO_3$ 25.0, glucose 11.0). The rings were incubated with DHE (10 µM) at 37 ^oC for 30 min, washed with Krebs buffer and flash frozen in liquid nitrogen. Tissue sections (10 µm) were cut with a cryostat and thaw-mounted on slides. The fluorescence was assessed by confocal microscopy (λ_{ex}: 508 nm, λ_{em}: 615-nm emission, 20X). For detecting infarct, the whole heart was snap frozen, tissue sections (10 µm) were cut, stained with trypan blue for 5 min, mounted on the slides and photographed.

II.13 Biochemical parameters

The respective tissues of different organs (LV, RV, aorta and liver) were washed with phosphate buffered saline (PBS), blot dried, snap frozen in liquid nitrogen and stored at -70 ^oC till further use. The tissues were minced and homogenized in a lysis buffer (20 mM Tris–HCl, pH 7.6, 150 mM NaCl, 1% Triton X-100) containing aprotinin (2 µg/ml), leupeptin (2 µg/ml), PMSF (0.4 µM) and type II phosphatase inhibitor. After centrifugation at 14000 g for 20 min

at 4 °C, the supernatants were collected, aliquoted, and kept at -70 °C. The protein concentrations in the tissue samples were assayed using Bradford reagent. The plasma levels of total nitrates, TBARS, PGI2, AVP, big ET, ET-1 and TAS were assayed using commercially available kits according to manufacturer's protocols.

II.14 Plasma Na^+ and K^+ and Ca^{2+} concentration

Rats were anaesthetized with sodium thiopentone (100 mg/kg i.p.) and heparin (1000 IU) were injected into the right femoral vein. After allowing 2 min for the heparin to fully circulate, rats were cut open from the ventral side and abdominal vena cava accessed. Blood from the abdominal vena cava of the rats was collected in heparinized tubes, spun for 15 min at 2000 g to separate plasma and stored at -70 ^oC. The aliquoted plasma was thawed by immediately putting it into a 37 ^oC incubator, the Na^+, K^+ and Ca^{2+} levels were estimated by AAS and are expressed in mEq/l.

II.15 Immunoblots

The aortic tissue extracts of different rat groups were separated by 10-15% SDS-polyacrylamide gel electrophoresis, and electro-transferred to nitrocellulose membrane. The membranes were blocked for 1 h at room temperature in TBST buffer (20 mM Tris–HCl, pH 7.6, 137 mM NaCl, and 0.1% Tween-20) containing 5% (w/v) nonfat milk, and then incubated overnight at 4 ^oC with the eNOS and iNOS-specific primary antibodies. After several washes, suitable HRP-conjugated secondary antibodies were added, the membranes were incubated further for 2 h, and the blots of eNOS and iNOS were developed using a Lumi-Light^{PLUS} western blotting kit. The bands were detected using a Kodak Gel-doc software and the intensity ratios of immunoblots to that of normal control, taken as 1 (arbitrary unit) were quantified after normalizing with respect to the loading controls.

II.16 Plasma biochemistry

Various plasma parameters of all the rat groups were analyzed with a blood biochemical

auto analyzer (Rx Daytona, Randox, crumlin county, Antrim, UK).

II.17 Organ bath studies

These were carried out as described previously, with minor modifications [187]. Briefly, rats were euthanized by i.p. injection of sodium thiopentone (100 mg/kg). The thoracic aorta was quickly excised and the connective and adipose tissues were cleaned from the vessel. The thoracic aortic rings (approximately 4 mm long) were suspended in organ bath chambers with a resting tension of 10 mN and bathed in a modified tyrode solution [composition (mM): NaCl (136.9), KCl (5.4), $MgCl_2$ (1.05), $CaCl_2$ (1.8), $NaHCO_3$ (22.6), NaH_2PO_4 (0.42), glucose (5.5), ascorbic acid (0.28) and EDTA (0.1)], purged with carbogen gas (95% O_2 /5% CO_2) and the temperature was maintained at 37 °C. The aortic rings were allowed to equilibrate for 60 min with regular washing every 15 min. After reaching equilibrium, cumulative concentration-response curves were recorded for NA from 1×10^{-9} to 1×10^{-4} M to examine changes to the force of contraction. For response curves with ACh or SNP, aortic tissues were washed for 60 min (with regular washing every 15 min) and pre-contracted submaximally (approximately 70%) with NA (1×10^{-6} M). Once the contraction had stabilized, changes to the force of relaxation were examined by a cumulative concentration response curve to concentrations of ACh or SNP (10^{-9} to 10^{-4} M). The contraction force was measured isometrically with MLT0201/RAD force transducers, connected via amplifiers to a computer via a Labchart 8.1 system. Results were analyzed as the maximal increase or decrease in force of contraction, in mN, for each drug concentration.

II.18 ECG recording

The ECG and heart rate in rats were recorded at the beginning (0^{th} day) and end (28^{th} day) of the experiments, under light sedation following i.p. injection of ketamine (50 mg/kg) and diazepam (2 mg/kg). Throughout the readings the rats were kept warm by a heating bulb. A 3 lead configuration ECG was recorded and analyzed. After 10 min of sedation, rats were

put in supine position and needle electrodes were subcutaneously inserted in the right, left and hind paws and secured with tape. Surface ECG (lead II), was recorded by needle electrodes that were connected to the Animal Bio-amp FE136 (ADInstruments Australia) and the data acquired with a Power lab data acquisition system PL3508/P (ADInstruments, Sydney, Australia). The rat ECG module of the Lab Chart pro software 8.1 (ADInstruments, Sydney, Australia) was used to analyze the data. The noise and electrical interference were rejected in the final analysis. All readings were average of 20 min recording. The Bazzet method was used for QTc (QT corrected by heart rate) calculations. All readings were an average of 20 min recording.

***II.18.1 Heart rate variability (HRV)*:** For HRV measurements, 20 min ECG recordings in a 3 lead configuration were used as described above to detect and study beat-to-beat (RR wave) intervals. Rat HRV module of the Lab Chart pro software 8.1 (AD instruments Australia) was used to analyze the data and ectopic beats were excluded. Power spectrum method was used to study HRV. For this purpose, low-frequency (LF, 0.2 to 0.8 Hz) and the high-frequency (HF, 0.8 to 3 Hz) bands were selected and analyzed to study the sympatho-vagal balance.

Fig. III 5. HRV by power spectrum analysis of rats.

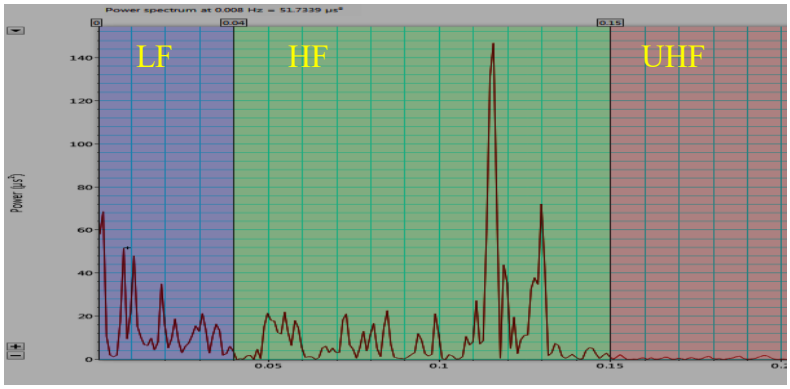

LF- low frequency, HF-high frequency, UHF- ultra low frequency

II.19 Isolated Langendorf Heart Preparation-

The LV function of the rats in all treatment groups was assessed using the non-recirculating isolated Langendorf heart setup. For this, terminal anesthesia was induced via

i.p. injection of thiopentone sodium (100 mg/kg) and heparin (1000 IU) into the right femoral vein. After allowing 2 min for the heparin to fully circulate, the heart was excised and placed in cooled (0 ^{o}C) modified Krebs-Henseleit bicarbonate buffer (KHB) containing [in mM]: NaCl 119.1; KCl 4.75; $MgSO_4$ 1.19; KH_2PO_4 1.19; $NaHCO_3$ 25.0; glucose 11.0 and $CaCl_2$ 2.16). The aorta was isolated and cleared of extraneous fat tissues and cannulated via the dorsal root.

The heart was attached to the cannula with the tip of the cannula positioned immediately above the coronary ostia of the aortic stump and perfused in a non-recirculating Langendorf fashion at 100 cm of hydrostatic pressure. Maintaining the temperature at 35 ^{o}C, the buffer was bubbled with carbogen gas (95% O_2/5% CO_2), giving a pH of 7.4. The apex of the heart was pierced to facilitate the besian drainage. A balloon catheter was inserted in the LV via the mitral orifce for measurement of left ventricular developed pressure. The catheter was connected via a three-way tap to a micrometer syringe and to a Capto SP844, MLT844 physiological pressure transducer and all connected to power lab system. The outer diameter of the catheter was similar to the mitral annulus to prevent ejection of the balloon during the systolic phase. After a 10 min stabilization period, steady-state left ventricular pressure was recorded from isovolumetrically beating hearts. Increments in balloon volume were applied to the heart until left ventricular end-diastolic pressure reached approximately 30 mm Hg. All LV end-diastolic pressures were measured by pacing the heart at 250 bpm using an electrical stimulator. End-diastolic pressures were obtained starting from 0 mm Hg up to 30 mm Hg. At the end of the experiment, the atria, RV and LV were separated and weighed. The diastolic stiffness constant (k, dimensionless) was calculated as reported previously (188), briefly to assess myocardial stiffness, stress (σ, dyne/cm2) and tangent elastic modulus (E, dyne/cm^2) for the mid-wall at the equator of the LV were calculated by assuming spherical geometry of the ventricle and considering the mid-wall equatorial region as representative of the remaining myocardium:

$$\sigma = \frac{VP}{W}\left(1 + \frac{4(V+W)}{[V^{1/3} + (V+W)^{1/3}]^3}\right)$$

$$E = 3\left\{\frac{VP}{W} - \sigma + \frac{\left(\frac{\sigma}{V} + \frac{(W\sigma - VP)}{W(V+W)} + \frac{\sigma.dP}{P.dV}\right) \times \left(V^{1/3} + (V+W)^{1/3}\right)}{\left(V^{-2/3} + (V+W)^{-2/3}\right)}\right\},$$

where V is chamber volume (ml), W is LV wall volume (0.943 ml/g ventricular weight), and P is end diastolic pressure (dyne/cm^2 = 7.5 X 10^{-4} mm Hg). Myocardial diastolic stiffness is calculated and defined as the diastolic stiffness constant (κ, dimensionless), which is the slope of the linear relation between the tangent elastic modulus (dyn/cm) and stress (dyn/cm^2), as used in previous studies (188).

II.20 Microelectrode studies on isolated LV papillary muscles

Rats were anesthetized by CO_2 inhalation and then euthanized by exsanguination. The thorax was opened quickly, and the heart was removed. The LV papillary muscles were quickly dissected in cold Tyrode physiological salt solution [composition (mM): NaCl (136.9), KCl (5.4), $MgCl_2.H_2O$ (1.0), $NaH_2PO_4.2H_2O$ (0.4), NaHCO (22.6), $CaCl_2.2H_2O$ (1.8), glucose (5.5), ascorbic acid (0.3), and Na EDTA (0.05) bubbled with carbogen gas (95% O_2/5% CO_2). A stainless steel hook was placed in one end of the papillary muscle. The muscle was placed in a 1.0 ml experimental chamber continuously perfused with gassed warm (35 ± 0.5°C) Tyrode solution at 3 ml/min and fixed at the other end with a small stainless steel pin embedded in a rubber base. The hook was attached to a modified sensor element (SensoNor AE801) connected to an amplifier (model TBM-4, World Precision Instruments). The muscle was slowly (over 1 min) stretched to optimal preload (5-10 mN). Contractions were induced by field stimulation (Grass SD-9) via electrodes on either side of the muscle (stimulation frequency = 1 Hz, pulse width = 0.5 ms, stimulus strength = 20% above threshold). After optimal preload was attained,

the muscle was allowed to equilibrate for a further 45 min before impalement with a filamented borosilicate glass microelectrode (1.5 mm OD; World Precision Instruments) with a tip resistance of 5–15 m Ω filled with 3 M KCl. The reference electrode was an Ag-AgCl electrode. An electrometer (Cyto 721, World Precision Instruments) was used to record bioelectrical activity. All signals were recorded via a PowerLab 4S data acquisition unit (AD Instruments, Sydney, Australia and Chart 5.5 software). All preparations with a stable resting potential more negative than -60 mV were accepted. Continual impalement throughout an experiment was not always possible; however, if displacement occurred, the results of a subsequent impalement were accepted, provided the data fitted the criteria described above. The action potential duration (APD) at 20% (ADP_{20}), 50% (ADP_{50}), and 90% (ADP_{90}) of repolarization and resting membrane potential were measured [187].

II.21 Echocardiography

For transthoracic echocardiographic assessment, rats were anaesthetized with i.p. injections of ketamine 50 mg/kg and diazepam 2 mg/kg to produce general anesthesia with minimal cardiovascular depression. Serial, echocardiographic images of different rat groups were recorded using the Hewlett Packard Sonos 5500 echocardiography machine (12 MHz neonatal transducer) with an image depth of 3 cm and using two focal zones. The front limbs and the right hind limb of the rats were shaved for the connection of three-lead ECG. In addition, the chest was shaved to provide an amenable surface for the ultrasound probe. LV M-mode measurements at the level of the papillary muscle were used to obtain the wall thicknesses. Suprasternal long axis views were used to obtain the internal diameters of the ascending aortic arch [189].

II.22 Survival studies

For the survival assay, a separate set of DOCA-salt rats were developed as described before, but continuing DOCA administration and salt water feeding up to 40 days. Different

concentrations of mal C (5, 10, 15, 20, 50 mg/kg), curcumin (60 mg/kg) and atenolol 10 (mg/kg) were given by oral gavage to these DOCA-salt rats every day from 15th to 40th day of the experiments. The survival of all the rats was monitored through the experimental period.

II.23 Statistical Analysis

All data are presented as mean ± S. E. M. of three independent experiments with similar results, carried out with 8 rats/group except for the toxicity and survival assays where 10 rats per group were used. The data were analyzed by paired t-test and one-way analysis of variance (ANOVA). A *p*-value of < 0.05 was considered statistically significant.

CHAPTER-III

RESULTS, DISCUSSION & CONCLUSIONS

III.1 Preamble

HT is an important public-health challenge and remains the primary cause of stroke, coronary artery disease and sudden cardiac mortality worldwide [190,191]. Its global burden is projected to increase enormously by 2025 [192]. HT management is perceived as the key in controlling CVD, since a reduction in BP by only 3 mm Hg may reduce the risk of death by 5% to 8% [193]. The many side effects of the conventional antihypertensive drugs have triggered research in finding alternative therapies to reduce high BP [194]. Ayurveda, one of the ancient Indian systems of medicine primarily targets ways to prevent and manage lifestyle disorders using herbs/plants and sometimes with some excipients [195,196]. The Ayurvedic medicines are effective, and affordable for common people [197]. Amongst the herbal/plant-derived compounds, anti-HT effect of the polyphenols has been demonstrated by many studies. The total dietary intake (approximately 1 g/day) of polyphenols is higher than other known dietary antioxidants. It is 10 times higher than dietary vitamin C and 100 times higher than vitamin E and carotenoid intakes. Polyphenol intake, assessed by total polyphenol excretion in urine, showed good correlation between polyphenol rich foods intake and reduced BP amongst the elderly Mediterranean population at high cardiovascular risk [198]. Polyphenols in cocoa extract [199], chokeberry juice [200] and purple passion fruit peel extract [201] showed impressive anti-hypertensive property, primarily by activating endothelial nitric oxide synthase (eNOS) to produce the vasodilatory NO. Given that CVD is feared to be reaching epidemic proportions in India [202], the present investigation was primarily aimed at evaluating the efficacy of mal C, a constituent of the exotic Indian spice, rampatri as an anti-hypertensive agent. However, besides HT [203], the CVD pathophysiology also involves multiple alterations in vascular reactivity and structure, interactions of the vessel wall with the circulating blood elements [204,205], OS in the endothelium of the vessel walls [206] as well as remodeling of the structural, electrophysical

and functional properties of heart. Hence all these aspects were also addressed to establish the true potential of mal C as an effective cardio-protective agent.

Understanding mechanisms leading to HT has been challenging even after several decades of research. Long-term regulation of arterial pressure is generally linked to the ability of the kidneys to maintain volume homeostasis by altering the renal excretion of salt and water in response to changes in arterial pressure (pressure-diuresis mechanism). But compelling evidence exists on the fact that modulation of sympathetic nerve activity via the central nervous system can play a role in long-term regulation of arterial pressure. Although mineralocorticoids are well-known to generate volume-dependent and renin-independent experimental hypertensive animal models, recent evidence points that they also cause sympathetic hyper-activity in HT. In this study, the DOCA-salt UNX rats were used as a model system to include both volume overload and sympathetic functions. DOCA, a precursor of aldosterone, acts in the kidneys to cause water and salt retention, suppression of renin release and low plasma angiotensin II levels. However, this non-genetic model has some deficiencies. It induces severe HT, with maximum arterial pressures in the range of 180-200 mm Hg, within a few weeks. Thus, the rate and magnitude of HT development are significantly greater than the slower developing and more modest increases in BP, observed in most hypertensive humans. It also may cause extensive end-organ damages. Nevertheless, it is an appropriate model for testing the effect of natural and synthetic compounds on CV remodeling to develop newer therapeutic agents, and is widely used [3]. One of the major impediments of any drug development is the toxicity and pharmacokinetics of the test sample. While the importance of non-toxicity is obvious, the pharmacokinetics of the drug that decides its absorption, bioavailability, distribution to tissues and metabolism is also crucial on its clinical use. Hence, prior to examining the pharmacodynamics of mal C, its toxicity to rats and bioavailability were first evaluated.

III.2 Toxicity and bioavailability of mal C

In the present investigations, both chronic and acute toxicities of mal C to rats after oral administration were evaluated from the behavioural changes, as well as plasma biochemistry of the mal C-fed rats. For the acute toxicity studies, the rats were given mal C (500 mg/kg, single dose) and observed for 1 month. The rats had normal food and water intake as well as stool during the experimental period. The comparative plasma biochemistry profiles and organ weight analyses of the normal rats and those treated with different oral doses of mal C are shown in **Figs. III.1A** and **III.1B** respectively. At none of the above doses mal C altered the wet weights of kidney, spleen and heart. However, it showed a minor hepatic toxicity at a very high dose of 500 mg/kg. This was evident from the fact that the SGPT and ALP levels of mal C (500 mg/kg)-treated rats rose to 68 ± 8 U/lit and 124 ± 11 U/lit respectively, compared to the corresponding values of 55 ± 5 U/lit and 104 ± 10 U/lit in the normal rats. The chronic toxicity studies, carried out by giving mal C (100 mg/kg/day) for one month to the mice revealed it to be non-toxic, as their behavioural features and biochemical parameters resembled to those of normal rats.

For assessing the bio-availability, rats were given mal C (10 mg/kg) and its plasma concentrations were analysed by HPLC at 0, 1, 3, 6, 12 and 24 h using a UV-Visible detector. The peak of mal C was detected at 354 nm and its retention time was found to be 7.7 min. The concentration of mal C in the plasma increased up to 3 h to reach the maximum value of 3.8 μg/ml. Thereafter, it reduced time-dependently and became negligible at 24 h (**Fig. III.1C**). Hence, for all subsequent experiments, mal C was supplemented every 24 h to have significant levels in plasma.

III.3 Mal C lowers both SBP and DBP of the DOCA-salt rats

In our studies, the SBPs were measured by the non-invasive method. The SBPs of the normal, UNX and UNX + saline groups of rats were similar. However, DOCA-salt

Fig. III. 1 (A) The comparative plasma biochemistry profiles, (B) Organ weight analyses of the normal rats and those treated with different oral doses of mal C. (C) Serum bioavailability of mal C after oral gavaging in rats.

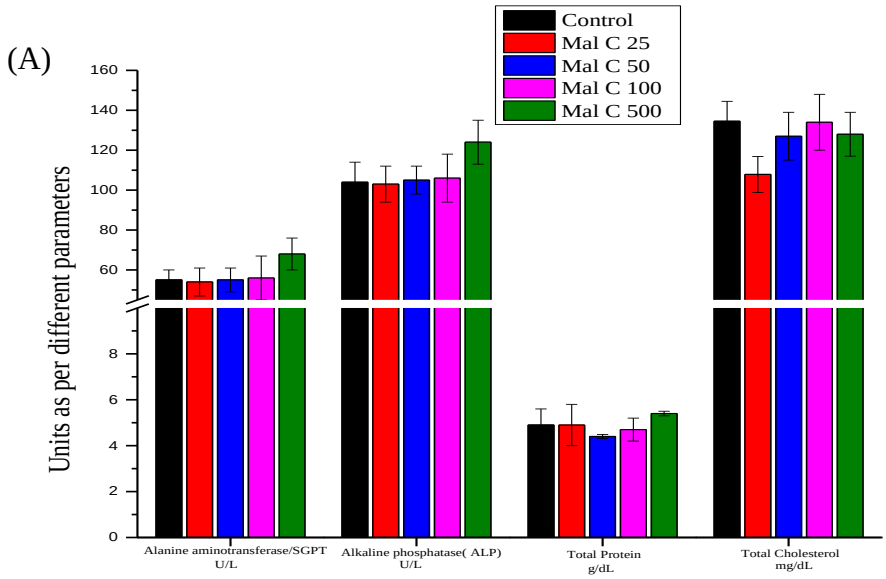

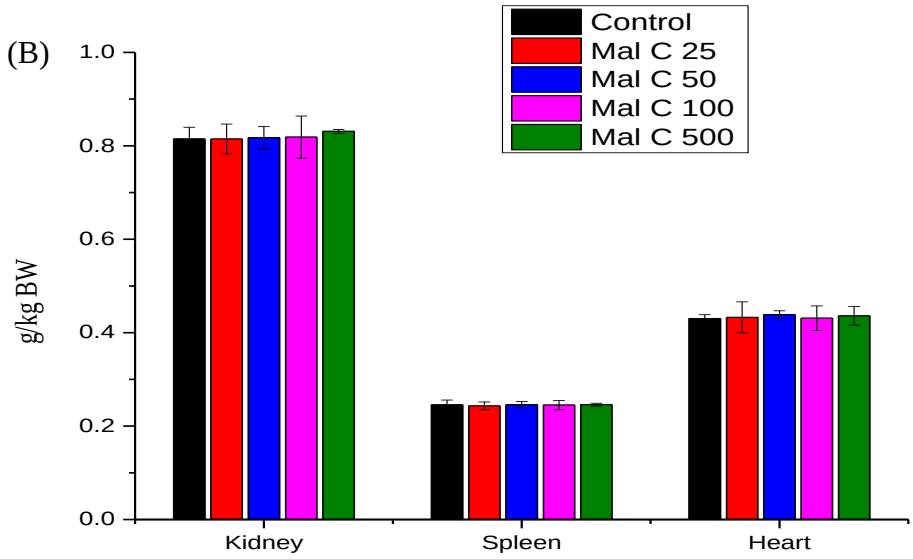

(C)

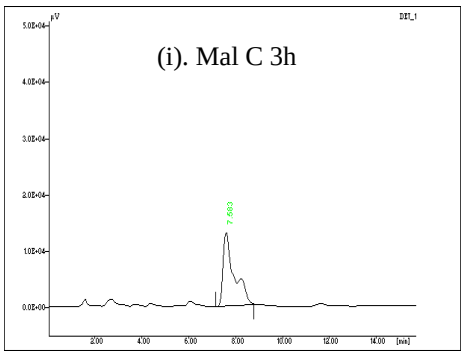

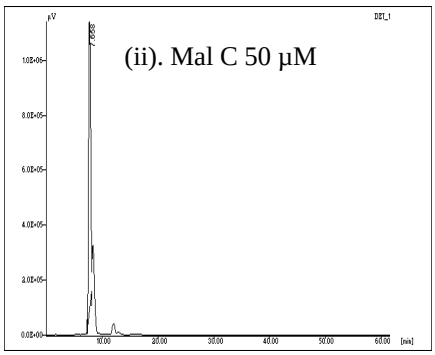

[a]The normal rats were daily given mal C (25, 50, 100, and 500 mg/kg) by oral gavage for one month. The rats were injected with heparin, and the plasma samples prepared. The biochemical parameters in the plasma were evaluated (A)

The rats were euthanized with sodium thiopentone, different organs removed and their wet weights measured (B). For serum bioavailability of mal C (C), after oral gavaging of mal C (10 mg/kg), rats were euthanized after 0, 1, 3, 6, 12 and 24 h, and the plasma collected. The concentration of mal C in serum was estimated by HPLC as discussed in chapter *II.6.* The experiments were repeated three times with similar results, and the values are mean ± S. E. M., each with 10 rats per group.

administration progressively elevated the SBP of the rats from 120±2 to 161±3 mm Hg on the 15th day, and thereafter, to 228±7 mm Hg on the 28th day Treatment with mal C (2.5, 5, 10, 15 and 20 mg/kg) dose-dependently reduced the SBP to 210±11, 195±7, 178±6, 178±6 and 175±5 mm Hg respectively on the 28th day (Fig. III.2A). In comparison, curcumin (60 mg/kg) and atenolol (10 mg/kg) reduced the SBP to 183±4 and 167±13 mm Hg respectively on the 28th day (Fig. III.2B). The doses of curcumin [173] and atenolol [186] were chosen based on the results of several previous studies using HT models. On their own, mal C (10 and 100 mg/kg) or curcumin (60 mg/kg) did not change the SBP of the UNX rats. The SBPs

Fig. III. 2 Dose-dependent anti-hypertensive effect of mal C in DOCA-salt rats[a].

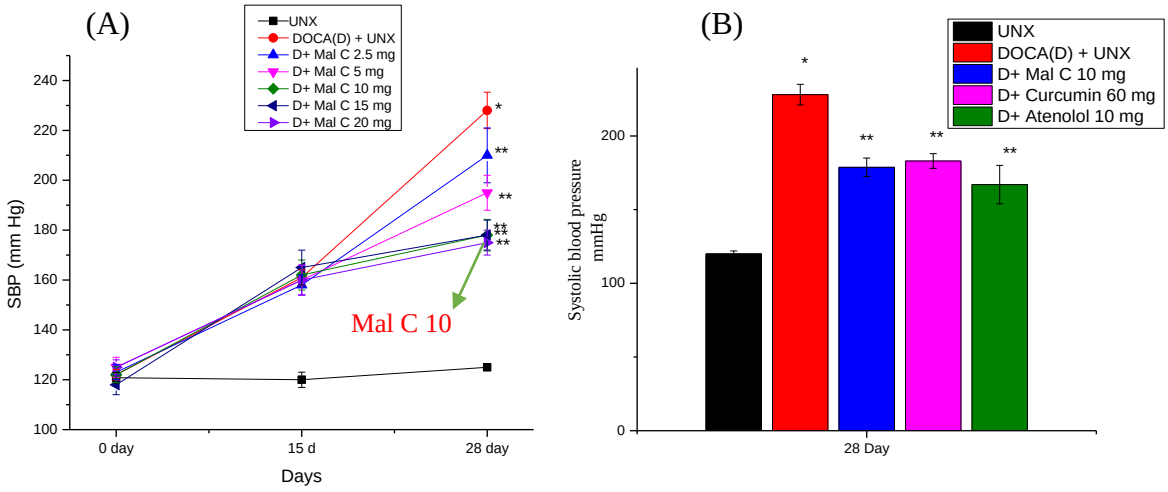

[a]Dose-dependent anti-hypertensive effect of mal C in DOCA-salt rats. **(A):** Dose optimization of mal C; **(B):** Comparative efficacies of mal C and the positive controls under the optimized treatment regime. The UNX rats were subcutaneously injected with DOCA solution every fourth day and given drinking water containing 1% NaCl for 28 days. The treatment groups were daily given different doses of mal C or a fixed dose of curcumin by oral gavage from 15-28th days. The SBP was non-invasively measured on 0, 15th and 28th day in the morning under light sedation. Similar experiments were also carried out with a fixed dose of atenolol, wherein the SBP was measured on the 28th day as above. The experiments were repeated three times with similar results, and the values are mean ± S. E. M., each with 8 rats per group. $^{*}P$<0.05 compared to UNX group; $^{**}P$<0.05 compared to the DOCA-salt group.

of the UNX, mal C (10 and 100 mg/kg)- and curcumin (60 mg/kg)-treated rats measured on 0^{th}, 15^{th} and 28^{th} days are shown in **Table III.1**. In these experiments, the UNX rats were not given DOCA-salt. Based on these results, a dose of 10 mg/kg of mal C was found to be optimum, and used for all subsequent studies.

Table III.1. Effect of mal C and curcumin on SBP (mm Hg) of the UNX rats[a]

Days	UNX	Mal C (100 mg/kg)	Mal C (100 mg/kg)	Curcumin (60 mg/kg)
0	119 ± 3	120 ± 4	120 ± 3	121 ± 5
15	121 ± 4	122 ± 3	122 ± 4	122 ± 6
28	122 ± 5	121 ± 4	124 ± 5	123 ± 5

[a]The UNX rats were daily given mal C (10 or 100 mg/kg) or curcumin (60 mg/kg) by oral gavage during 0-28^{th} days. The SBPs were non-invasively measured in the morning under light sedation. The experiments were repeated three times with similar results, and the values are mean ± S. E. M., each with 8 rats per group. These showed that neither mal C nor curcumin changed the SBP of the UNX rats.

Next the SBP of the rats was measured by the invasive method. In this case also, DOCA-salt administration elevated the SBP of the rats from 80±11 mm Hg on the 0^{th} day (UNX rats without DOCA-salt and/ or any drug administration) to 210±21 mm Hg on the 28^{th} day. Treatment with mal C (10 mg/kg) and curcumin (60 mg/kg) reduced the invasively measured SBP to 155±13 and 180±15 mm Hg respectively on the 28^{th} day **(Fig. III.2C).** Under the same conditions, the atenolol (10 mg/kg) and amlodipine (15 mg/kg)-treated DOCA-salt rats showed 150±17 and 145±12 mm Hg SBP respectively. The dose of amlodipine was chosen based on a previous report [186]. Overall, both invasive and non-invasive BP measurements revealed that atenolol (10 mg/kg), amlodipine (15 mg/kg) and mal C (10 mg/kg) had similar effects in reducing SBP. The DBP of the UNX rats was 65.3±7 mm Hg that was elevated to 148.6±9 mm Hg on the 28^{th} day in the DOCA-salt rats. There was no significant difference between the DBP of the UNX and normal rats. Treatment with mal C,

Fig. III. 2C Effect of DOCA-salt administration on the invasive SBP (mm Hg) of UNX rats and their modulation by mal C, curcumin, amlodipine and atenolol[a]

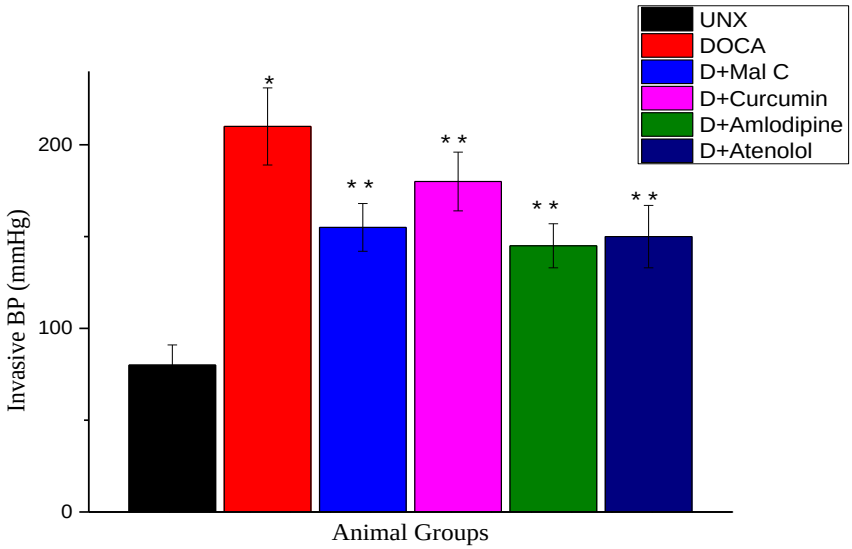

[a]The UNX rats were subcutaneously injected with DOCA solution every fourth day and given drinking water containing 1% NaCl for 28 days. The treatment groups were daily given mal C (10 mg/kg) or curcumin (60 mg/kg), amlodipine (15) or atenolol (10 mg/kg) by oral gavage during 15-28th days. Following anesthesia, the thorax was opened, the Millar catheter was inserted into the artery, and the SBP was measured. Blood pressure readings were taken with powerlab machine connected to it with the help of lab chart software (ADInstruments, Sydney, Australia). The experiment was repeated three times with similar results, and the values are mean ± S. E. M., each with 8 rats per group. $^{*}P<0.05$ compared to UNX group; $^{**}P<0.05$ compared to the DOCA-salt group.

curcumin and atenolol reduced the DBP of the DOCA-salt rats to 100±6, 120±7 and 105±4 mm Hg respectively on the 28th day. Likewise, the VP that was raised from 108±5 (UNX) to 188±7 in the DOCA-salt rats was reduced to 138±7, 159±6 and 144±6 mm Hg respectively on the 28th day by mal C, curcumin and atenolol.

In the present study, DOCA-salt treatment resulted in significant increase in the hemodynamic parameters like SBP, DBP and VP during 28 days of experiments. The increase in BP was significantly prevented by treatment with mal C at a dose of 10 mg/kg for 14 days. Amongst the various doses, the 10-mg dose of mal C remarkably reduced the SBP compared to even higher doses. Mal C (10 mg/kg) and atenolol (10 mg/kg) were almost equally effective in reducing the SBP of the rats, but both failed to restore it to the level of the control rats. Our results also confirmed that the increased HT in the DOCA-salt rats was

Table III.2. Effect of DOCA-salt administration on arterial DBP and VP of UNX rats and their modulation by mal C, curcumin, and atenolol[a]

Parameters	UNX	DOCA (D)	D + Mal C	D + Curcumin	D + Atenolol
DBP (mm Hg)	65 ±7	148 ± 9*	100 ± 6**	120 ± 7**	105 ± 4**
VP (mm Hg)	108 ± 5	188 ± 7*	138 ± 7**	159 ± 6**	144 ± 6**

[a]The UNX rats were subcutaneously injected with DOCA solution every fourth day and given drinking water containing 1% NaCl for 28 days. The treatment groups were daily given mal C (10 mg/kg) or curcumin (60 mg/kg) or atenolol (10 mg/kg) by oral gavage during 15-28th days. Following anaesthesia, the thorax was opened, the millar catheter was inserted into the artery, and the DBP was measured. After 10 min, the probe was pushed further into LV to obtain VP. The experiments were repeated three times with similar results, and the values are mean ± S. E. M., each with 8 rats per group. $^{*}P<0.05$ compared to UNX group; $^{**}P<0.05$ compared to the DOCA-salt group.

not due to salt stress, because the UNX and UNX + salt rats did not show significant changes in their SBP compared to the normal rats, during the experimental period. We measured SBP of the rats under anesthesia that is well-known to decrease BP. However, we used anesthesia to measure the SBPs of all groups of rats to nullify the effect of the anesthesia. Also, the non-invasive SBP measurement was carried after an induction of 10-min sedation to all the animals. This would minimize any variation due to anesthesia. We measured SBP both using both invasive and non-invasive routes, while DBP and VP were measured invasively. The SBP results of both types of measurements correlated well.

III.4 Mal C reduces water intake without changing the body weights of DOCA-salt rats

The UNX rats behaved like normal rats with proper food intakes and progressively increased body weights during the entire experimental period. This along with our SBP data signified that uninephrectomy is not responsible for any system malfunction including HT induction. The DOCA-salt rats had increased water intakes without any gain in body weights. The increased water intakes by DOCA-salt rats indicted a shift in the renal function curve, caused by sympathetic activity and/ or loss of renal mass that would result in water (and sodium)

curcumin decreased the water intakes of the DOCA-salt rats (**Fig. III.3A**). However, none of the test samples improved the body weights (**Fig. III.3B**).

Fig. III. 3 Effect of DOCA-salt administration on (A) water and (B) food consumption pattern of UNX rats and their modulation by mal C and curcumin[a]

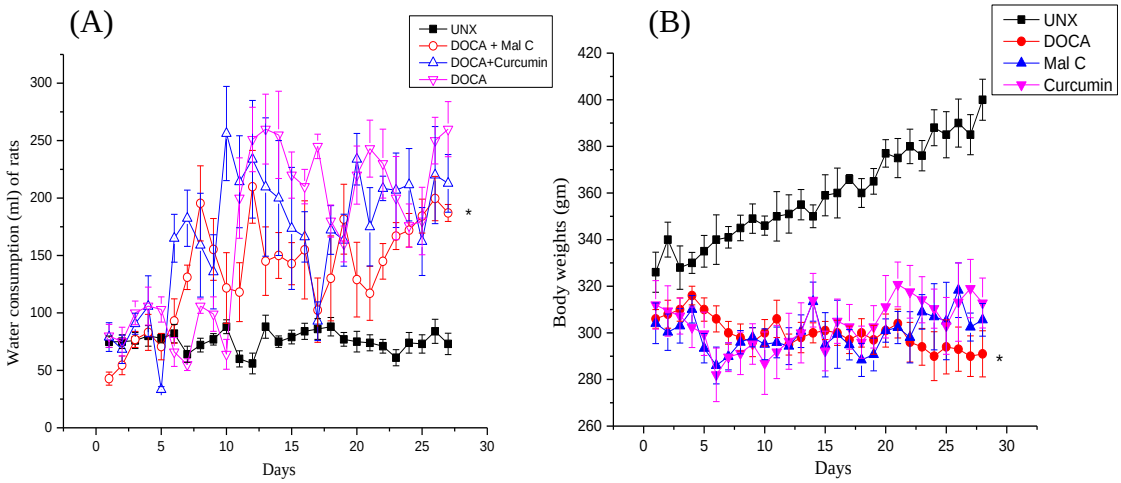

[a]Mal C reduces the water intakes, without helping in weight gains in the DOCA-salt rats. **(A):** Effect on body weight; **(B):** Water consumption. The UNX rats were subcutaneously injected with DOCA solution every fourth day and given drinking water containing 1% NaCl for 28 days. The treatment groups were daily given mal C (10 mg/kg) or curcumin (60 mg/kg) by oral gavage from 15-28th days. The body weights and water consumption were measured every morning till the 28th day. The experiments were repeated three times with similar results, and the values are mean ± S. E. M., each with 8 rats per group. $^{*}P<0.05$ compared to UNX group; $^{**}P<0.05$ compared to the DOCA-salt group.

III.5 Mal C reduces organ hypertrophy of DOCA-salt rats

Organ hypertrophy, in particular, of kidney and LV is almost ubiquitous in hypertensive humans and animals [208]. Since cardiac cells undergoes hypertrophy not hyperplasia, so an increase in the organ wet weight may indicate organ hypertrophy. Presently, DOCA-salt administration increased the wet weights of RV and LV as well as those of adrenal gland and kidney to 1.9, 1.8, 1.9 and 2.7 folds respectively. Thus, the DOCA-salt rats showed marked LV, RV, kidney, and adrenal glands hypertrophy. We included the adrenal glands weight also, as DOCA-salt rats show adrenal hypertrophy. LV hypertrophy may be implicated in the development of coronary insufficiency and arrhythmia that may lead to congestive heart failure [209].

Treatment with mal C attenuated such increases in RV, LV, adrenal gland and kidney wet weights by 38.7%, 11.6%, 40.1% and 17.4% respectively. This suggested that mal C could substantially decrease cardiac remodeling (or hypertrophy) of the DOCA-salt rats. This may reduce the cardiac load and improve cardiac and kidney functions to reduce SBP [210]. Its effects on the cardiac and kidney functions are presented later. The effects of curcumin for RV and LV were comparable to that of mal C, but it reduced the weights of adrenal gland and kidney by 59% and 35% respectively. The results are summarized in **Table III.3**. It is worth mentioning that the wet weights of the organs are presented after normalizing relative to the body weights of the rats to account for the variations due to different body weights of rats.

III.6 Mal C substantially reduces oxidative stress in DOCA-salt rats

Oxidative stress is believed to be primarily responsible for HT, vascular disease progression and endothelial dysfunction [211,212]. Oxidative damage to biomolecules, cells and hyper activation of ROS signalling pathways has been linked to the detrimental effects associated with HT. Due to the presence of unsaturation, membrane lipids are susceptible to peroxidation, producing various stable *viz*. malondialdehyde (MDA) and 4-hydroxynonenal (4-HNE) as well as unstable *viz*. lipid hydroperoxide (LOOH) and conjugated dienes (CD) as the bi-products. Measuring the lipid peroxidation (LPO) end products is one of the most reliable assays for OS. Under normal physiological conditions, the cellular concentration of free radicals is maintained by a system of enzymatic and non-enzymatic antioxidants and free radical scavengers. These antioxidants protect cells by maintaining ROS such as $O_2^{-\cdot}$ and H_2O_2 at low levels. The three major cellular enzymatic antioxidants are superoxide dismutase (SOD), glutathione peroxidase (GP_X) and catalase (CAT). SOD dismutates $O_2^{-\cdot}$ to H_2O_2 and is the first line of defence against the free radical attack. GP_X and CAT catalyze the reduction of H_2O_2 to water. Further, GP_X also removes other hydroperoxides, generated by free radical

Table III.3. Effect of DOCA-salt administration on organs weight of UNX rats and their modulation by mal C and curcumin[a]

Organ wet weights (mg/g × 100)	UNX	DOCA-salt	Mal C-treated	Curcumin-treated
Right ventricle	43.1 ± 4.7	80.2 ± 6.1*	49.1 ± 7.2**	50.4 ± 3.3**
Left ventricle	188.3 ± 6.7	338.1 ± 14.2*	297.8 ± 7.4**	303.6 ± 10.9**
Adrenal glands	17.4 ± 2.8	33.4 ± 3.9*	20.1 ± 3.1**	13.17 ± 2.6**
Kidney	247.4 ± 10.5	677.3 ± 30.6*	559.4 ± 60.1**	440.1± 81.4**

[a]The UNX rats were subcutaneously injected with DOCA solution every fourth day and given drinking water containing 1% NaCl for 28 days. The treatment groups were daily given mal C (10 mg/kg) or curcumin (60 mg/kg) by oral gavage during 15-28th days. The rats were euthanized with sodium thiopentone, different organs removed and their wet weights measured. The experiments were repeated three times with similar results, and the values are mean ± S. E. M., each with 8 rats per group. $^{*}P<0.05$ compared to UNX group; $^{**}P<0.05$ compared to the DOCA-salt group.

reactions. The non-enzymatic antioxidants include vitamins such as tocopherols, ascorbate and carotenes as well as other biological molecules including glutathione, uric acid and the metal-binding proteins [94]. Most of these non-enzymatic antioxidants neutralize or quench the reactive free radicals to dissipate OS [213]. However, rather than assaying the individual antioxidants, assessment of plasma total antioxidant status (TAS) provides a good measure of antioxidant defence including enzymatic and non-enzymatic systems [214].

In this investigation, OS in the DOCA-salt and the treated groups was first assessed by measuring (i) the TBARS levels in different tissue samples, and (ii) the plasma TAS of the UNX and other groups. The respective results on TBARS and plasma TAS are summarized in **Table III.4.** and **Fig. III.4A**. DOCA-salt treatment increased the TBARS levels in LV, aorta and liver to 4.4, 2.4 and 1.7 folds respectively, compared to the UNX rats. DOCA treatment also reduced the plasma TAS of the UNX rats by 54.2%. These results confirmed

significant OS in the DOCA-salt rats. Earlier several groups have shown reduced plasma TAS and high MDA levels in the LV and aorta in HT [215,216]. Mal C treatment reduced the TBARS levels in LV, aorta and liver by 60.6%, 53.7% and 31.1% respectively. In comparison, curcumin reduced these parameters by 45.1%, 20.9% and 21.9% only. Mal C and curcumin also prevented the loss of plasma TAS of DOCA-salt rats by 90.9% and 36.4% respectively. Thus, mal C treatment brought the plasma TAS nearly to that of the UNX groups, while reducing the MDA levels in different organs significantly more than by curcumin. This is consistent with our previous report, wherein mal C showed better in vitro antioxidant property than curcumin [179]. Both radical scavenging and metal chelating abilities were found to contribute to its antioxidant action.

Amongst the ROS contributing to OS, enhanced production of superoxide anion radicals ($O_2^{\cdot -}$) has been implicated in the pathogenesis of vascular hypertrophy and endothelial cell dysfunction [217]. Several cardiovascular medicines, such as the ACE inhibitor, captopril; the β-blocker, carvedilol etc. also possess antioxidant property [218,219]. NADH/NADPH oxidase contributes to $O_2^{\cdot -}$ production in all parts of the vasculature [220]. Likewise, chronic hypoxia can enhance XO activity and its release into the plasma, and these may be responsible for essential HT [221] and endothelial dysfunction in atherosclerotic humans [222]. In view of these, the level of $O_2^{\cdot -}$ in the aorta was detected by microscopy after staining with dihydroethidium (DHE). DHE is a cell-permeable compound that, upon entering the cells, reacts with $O_2^{\cdot -}$ to furnish oxyethidium (OE). On interaction with nucleic acids, OE produces a bright red stain that can be conveniently detected by fluorescent microscopy [223]. This protocol is very sensitive to detect even 1 pmol/mg protein of $O_2^{\cdot -}$; relatively specific with minimal interference from other ROS including H_2O_2, but not in the presence of excessive cytochrome C or other heme-containing proteins; and is generally reproducible [224]. Our microscopy results revealed extensive red stained aorta in the DOCA-salt rats, while this was negligible in case of the UNX rats. Treatment with mal C and

curcumin reduced it significantly, restoring to the level of the UNX rats (**Fig. III.4B**). The copious generation of XO in the DOCA-salt rats suggested possible activation of XO and NAD(P)H oxidase in these rats. The impaired endothelium-dependent vasorelaxation in DOCA-salt rats, controlled by the XO status may contribute to vascular endothelial dysfunction [225].

This implies that XO inhibition may be a potential strategy against HT as has been demonstrated in clinical studies also [226]. Increased XO activity may contribute to vascular dysfunction in HT including the low-renin ET-1-dependent HT [227]. Hence, the activities of XO and NAD(P)H oxidase in the DOCA-salt and treated groups were also monitored. Our results (**Table III.4.**) showed that the XO activities in the heart, aorta and plasma of the DOCA-salt rats were 4.5 fold, 3.6 fold and 5.1 fold respectively, compared to the UNX rats. Treatment with mal C reduced the above parameters of the DOCA-salt rats by ~67%, 49.3% and 51% respectively. The extents (29%, 26.8% and 19.6%) of reduction of these parameters by curcumin were much less. Studies have shown that NAD(P)H oxidase as another critical source of ROS production within the vascular wall, and its elevation in vascular cells and myocytes may play an important role in HT [102]. Moreover, NAD(P)H oxidase has been suggested to be the most important ROS source in the vascular walls of DOCA-salt rats [228]. Presently the NAD(P)H oxidase activity in the DOCA-salt rats was 4.0 fold, compared to the UNX rats. Mal C and curcumin treatment abrogated such an increase in the NAD(P)H oxidase activity by 50% and 25% respectively (**Fig. III.4C**). Although DOCA-salt rats have reduced circulating angiotensin II, its production in the vascular wall may stimulate $O_2^{\cdot -}$ production via NAD(P)H oxidase activation. In line with this, our histology also showed copious amount of O2.- in the aorta (Fig. III.4B). Earlier NAD(P)H oxidase inhibition by apocynin attenuated SBP, partly due to the increased NO bioavailability [228,229]. In our studies, mal C also elevated the NO level of DOCA-salt rats (vide infra). Moreover, NAD(P)H oxidase is a major cause of atherosclerosis, and its inhibitors may reverse

Fig. III. 4 Effect of DOCA-salt administration on some oxidative stress parameters and cardiac infarct of UNX rats and their modulation by mal C and curcumin[a]

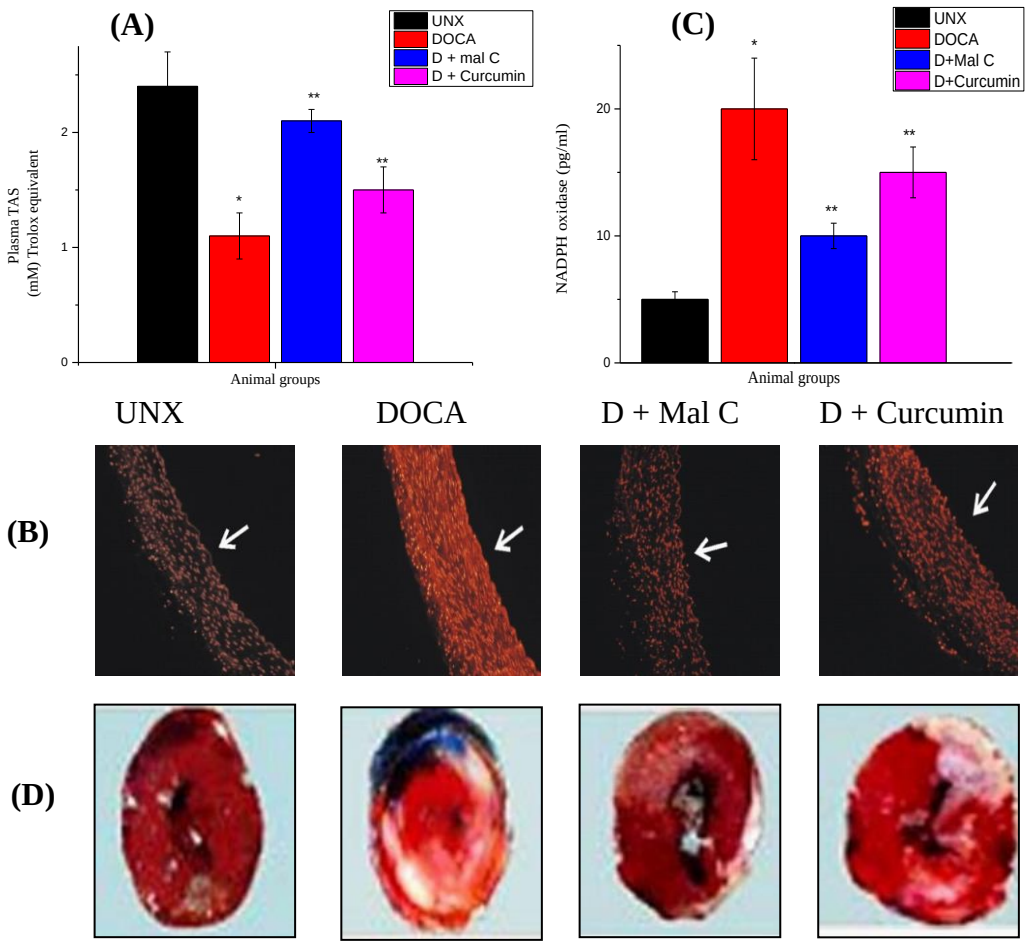

[a]The UNX rats were subcutaneously injected with DOCA solution every fourth day and given drinking water containing 1% NaCl for 28 days. The treatment groups were daily given mal C (10 mg/kg) or curcumin (60 mg/kg) by oral gavage during 15-28th days. The rats were injected with heparin, and the plasma samples prepared. The rats were euthanized with sodium thiopentone, different organs removed. The biochemical antioxidant parameters (A) Plasma TAS and (C) NADPH oxidases in the plasma were evaluated. The histological analysis of aortic $O_2^{\cdot-}$ (B) and heart infarct analysis (D) was observed by staining with DHE and trypan blue respectively as mentioned in the chapter *II.12.* The experiments were repeated three times with similar results, and the values are mean ± S. E. M., each with 8 rats per group. $^{*}P<0.05$ compared to UNX group; $^{**}P<0.05$ compared to the DOCA-salt group. The histological images are the representative images of the experiments repeated three times with similar results.

atherosclerosis [230]. From that perspective, mal C appears to be a potential cardio-protecting agent. Overall, the above evidences suggest that mal C may exert its anti-hypertensive action in the DOCA-salt rats through its antioxidant property. Previously mal C also accelerated healing of indomethacin-induced gastric ulceration in mice. The effect was

Table III.4. Effect of DOCA-salt administration on some oxidative stress parameters of UNX rats and their modulation by mal C and curcumin[a]

Parameter	UNX	DOCA-salt	Mal C-treated	Curcumin-treated
LV TBARS level (µmol MDA/l)	14.1 ± 3.2	61.7 ± 5.3*	24.3 ± 3.1**	33.9 ± 4.2**
Aorta TBARS level (µmol MDA/l)	10.3 ± 2.3	24.4 ± 1.5*	11.3 ± 1.2**	19.3 ± 1.2**
Liver TBARS level (µmol MDA/l)	19.4 ± 2.4	33.8 ± 3.3*	23.3 ± 2.4**	26.4 ± 1.8**
Heart XO activity (mU/ml)	15.1 ± 2.0	67.9 ± 7.1*	22.6 ± 3.2**	48.3 ± 5.1**
Aortic XO activity (mU/ml)	13.4 ± 3.2	47.6 ± 6.4*	24.1 ± 4.3**	34.8 ± 5.4**
Plasma XO activity (mU/ml)	17.5 ± 2.1	89.3 ± 8.5*	43.7 ± 5.2**	71.7 ± 6.4**

[a]The UNX rats were subcutaneously injected with DOCA solution every fourth day and given drinking water containing 1% NaCl for 28 days. The treatment groups were daily given mal C (10 mg/kg) or curcumin (60 mg/kg) by oral gavage during 15-28th days. The rats were injected with heparin, and the plasma samples prepared. The rats were euthanized with sodium thiopentone, different organs removed. The biochemical parameters in the organs/plasma were evaluated. The experiments were repeated three times with similar results, and the values are mean ± S. E. M., each with 8 rats per group. $^{*}P<0.05$ compared to UNX group; $^{**}P<0.05$ and compared to the DOCA-salt group.

partly through its antioxidative effect, since indomethacin produces copious amounts of ROS in animals [181].

III.7 Mal C reduces vasoconstriction in DOCA-salt rats

The endothelial cells play a major role in the control of vascular structure and function [231]. Under physiological conditions, there is a balance between the endothelial-derived vasodilators and vasoconstrictors [232]. Plasma AVP level is reported to increase 10-fold during the onset of malignant DOCA-salt HT [233], along with increased ET release. HT in vasopressin-deficient DOCA-salt rats is less compared to the vasopressin-synthesizing rats [234,235]. Since narrowing of blood vessels increases SBP, the status of the vasoconstrictors (AVP, big ET and ET-1) and a vital vasodilator (NO) levels in the different groups of rats were assessed. The plasma AVP and big ET levels of the DOCA-salt group were 2.9 and 5.0 folds respectively, compared to the corresponding values in the UNX rats. DOCA-salt administration to the UNX rats increased the ET-1 level in aorta to 4.4 folds. The excessive ET-1 may induce more ROS in the DOCA-salt rats partly via XO activation [236]. The results on AVP, Big ET-1 and ET-1 levels are summarized in **Table III.5**.

NO, produced by nitric oxide synthases (NOSs)-mediated catabolism of L-arginine is an important biological regulator in many physiological and pathological processes [236]. The NOSs exist as constitutive (eNOS), and inducible (iNOS) isoforms. The low concentration of NO produced by the constitutive eNOS increases blood flow. However, as a mediator of macrophage function, the enhanced generation of NO by iNOS may contribute to the pathogenesis of various inflammatory processes. The plasma nitrate level in the DOCA-salt group was reduced by 14.8%, compared to that in the UNX rats (**Fig. III. 5A**). The western blots of eNOS and iNOS expressions in the vascular tissues of the different groups of rats are shown in **Fig. III. 5B**. In vascular tissues of the UNX rats, the eNOS expression was detected, but iNOS was insignificant. DOCA-salt administration reduced the expression of eNOS while increasing that of iNOS. However, the contradictory results on NO level and iNOS expression in the DOCA-salt group could not be explained. It may be because of the fact that the expression of any enzyme does not necessarily reflect its activation. The

availability of the substrate and cofactors dictates the enzyme activity. The NOSs require five cofactors, and in particular, iNOS also requires binding with calmodulin. Besides NO, atrial natriuretic peptide (ANP), secreted by heart muscle cells is a hormonal vasodilator and helps in Na^+, K^+ and fat homeostasis to reduce BP [237], moreover it is a marker for hypertrophy Presently, DOCA-salt administration increased the ANP level of the rats by 4 folds, compared to the UNX rats. The increased levels of the vasoconstrictors (AVP, big ET, and ET-1) along with reduction of plasma NO levels in the DOCA-salt rats represent endothelial malfunction. This may arise due to OS and can lead to HT and other cardiac complications [238]. It is worth mentioning that the ET-1 and AVP systems can operate in an overlapping fashion to maintain the BP in the DOCA-salt rats.

The increased plasma AVP level of the DOCA-salt rats was reduced by mal C (68.3%) and curcumin (46.6%) respectively. Mal C and curcumin reduced the big ET level of the DOCA-salt rats by 45.2% and 37.5% respectively, and also the aortic ET-1 level by 56.8% and 42.3%. At the same time, mal C and curcumin reduced the ANP level of the DOCA-salt rats by 60.7% and 38.6 % respectively. Moreover, mal C restored the NO level of the DOCA-salt rats to that of the UNX group, while curcumin augmented the parameter even further. Our western blots showed that both mal C and curcumin reversed the adverse effect of DOCA-salt, increasing the eNOS expression and reducing the iNOS expression. Thus, both the test samples may be increasing NO via activating the beneficial eNOS expression. This is also reflected from the fact that the NO levels of the treated rats were near the normal value. The NO-releasing drugs are conceived important for management of HT and wound healing [239]. From that perspective, the ability of mal C to release sub-toxic dose of NO suggested it to be a potential anti-hypertensive agent.

ET plays an important role in the development and maintenance of HT in DOCA-salt model by increasing both peripheral resistance and venomotor tone [240,241]. The ET receptor antagonist, bosentan reduced arterial pressure in DOCA-salt HT and the effect was

Fig. III. 5 Effect of DOCA-salt administration on (A) plasma total nitrate levels and (B) aortic NOS expression levels of UNX rats and their modulation by mal C and curcumin[a].

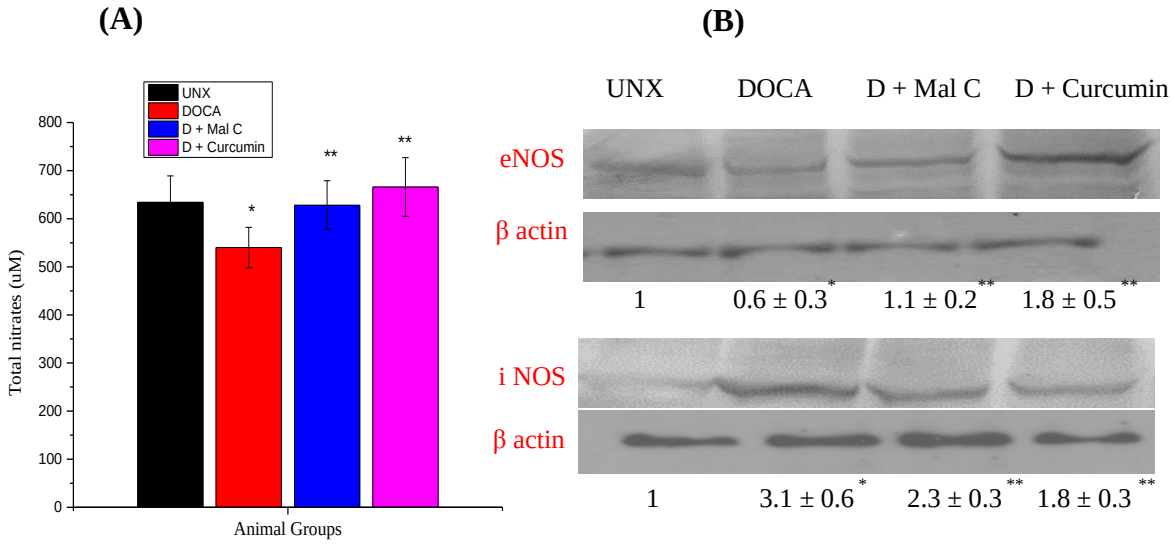

[a]The UNX rats were subcutaneously injected with DOCA solution every fourth day and given drinking water containing 1% NaCl for 28 days. The treatment groups were daily given mal C (10 mg/kg) or curcumin (60 mg/kg) by oral gavage during 15-28th days. The rats were injected with heparin euthanized with sodium thiopentone, plasma samples prepared and aorta removed. Total nitrate level (A) was measured in plasma and NOS expression level (B) was measured by immunoblotting of aortic tissue extracts. The experiments were repeated three times with similar results, and the values are mean ± S. E. M., each with 8 rats per group. $^{*}P<0.05$ compared to UNX group; $^{**}P<0.05$ compared to the DOCA-salt group.

further enhanced by administration of an AVP antagonist [92]. Moreover, AVP-deficiency attenuated HT and prevented the increase in extracellular fluid [242], while ET receptor antagonists reduced BP in the DOCA rats [243]. Thus, the ability of mal C to attenuate both AVP and ET-1 may contribute to its anti-hypertensive action in the DOCA rats. The observed increase of ET-1 level in the DOCA-salt rats may have link with the OS-dependent NF-κB activation [244]. Earlier, mal C suppressed ROS-mediated NF-κB activation in various inflammatory models [245]. It is possible that suppression of NF-κB activation via OS reduction may be responsible for the ability of mal C to reduce the ET-1 levels in DOCA-salt hypertensive rats. ET-1 can also induce OS by increasing vascular superoxide production via both NADPH oxidase-dependent and independent pathways in mineralocorticoid

hypertension [246]. This would reduce the plasma NO level in the DOCA-salts rats, as observed in the investigation [247]. Mal C may augment the NO level in these rats by suppressing ET-1. However, factors such as its effect on the arginine-metabolizing enzymes, other ROS/RNS levels etc. may also contribute to this.

Overall, mal C treatment reversed the detrimental effects of the DOCA-salt on vascular endothelial and smooth muscle function by reducing AVP, ANP, big ET and ET-1, and increasing the NO availability in plasma and/ or aorta. Reduced bioavailable NO is a major cause of endothelial dysfunction [248]. Because mal C attenuated OS substantially, it may increase NO availability to improve the endothelial function. This is disclosed later in terms of its effect on vascular smooth muscle proliferation and neutrophils infiltration.

III.8 Mal C reduces ventricular and vascular collagen depositions and inflammation in DOCA-salt rats

DOCA-salt rats show excessive collagen depositions, which is one of the causes as well as effects of HT. Earlier, DOCA-salt rats showed severe vascular hypertrophy and fibrosis in small and large arteries [249]. Presently, the DOCA-salt rats had significant collagen depositions in the interstitial (**Fig. III.6A.**) and perivascular (**Fig. III.6B.**) regions of the heart and in the aortic tissues (**Fig. III.6C.**), compared to the UNX rats. This may reduce the elasticity and contractibility of the endothelial layer in response to volumetric changes and hamper cardio-vascular function. Release of AVP and collagen-activated human platelets may release the arachidonic acid metabolites that are important mediators of inflammation in cardiovascular remodeling. Earlier, DOCA-salt rats were found to generate more vascular PGI2, possibly via activation of vascular PGI2 synthase (with a reduction in phospholipase C and A2 levels) [250].

Since the DOCA-salt rats showed significant vasoconstriction that can enhance PGI2 production, we assessed the effect of mal C and curcumin on PGI2 levels in the DOCA-salt rats. The PGI2 levels in the plasma, LV and aorta of the DOCA-salt group were 1.8, 1.5 and

Table III.5. Effect of DOCA-salt administration on some vasoactive and inflammatory parameters of UNX rats and their modulation by mal C and curcumin[a]

Parameter	UNX	DOCA-salt	Mal C-treated	Curcumin-treated
Plasma AVP level (pg/ml)	52.7 ± 3.7	153.4 ± 13.5*	66.2 ± 7.4**	88.5 ± 8.3**
Plasma Big Et level (pg/ml)	7.6 ± 0.9	38.2 ± 5.2*	12.1 ± 1.5**	20.0 ± 2.1**
Aorta Big Et level (pg/ml)	5.9 ± 0.8	26.1 ± 2.5*	14.3 ± 1.5**	16.3 ± 3.2**
Aorta Et-l level (pg/ml)	2.3 ± 0.6	15.6 ± 1.8*	9.4 ± 1.6**	13.3 ± 2.1**
ANP (pg/ml)	70.1 ± 5.1	280.3 ±13.2*	110.2 ± 13.1**	172.2 ± 11.2**
Plasma PGI2 level (pg/ml)	401.3 ± 16.5	718.3 ± 86.6*	622.0 ± 66.6**	642.1 ± 78.6**
LV PGI2 level (pg/ml)	306.7 ± 48.6	460.1 ± 68.6*	374.2 ± 25.8**	453.9 ± 55.3**
Aorta PGI2 level (pg/ml)	520.4 ± 67.6	1228.7 ± 153.8*	551.6 ± 74.6**	1051.2 ± 103.8**

[a]The UNX rats were subcutaneously injected with DOCA solution every fourth day and given drinking water containing 1% NaCl for 28 days. The treatment groups were daily given mal C (10 mg/kg) or curcumin (60 mg/kg) by oral gavage during 15-28th days. The rats were injected with heparin, and the plasma samples prepared. The rats were euthanized with sodium thiopentone, different organs removed. The biochemical parameters in the organs/plasma were evaluated. The experiments were repeated three times with similar results, and the values are mean ± S. E. M., each with 8 rats per group. $^{*}P<0.05$ compared to UNX group; $^{**}P<0.05$ compared to the DOCA-salt group.

2.4 folds respectively, compared to the UNX rats. Mal C treatment reduced such increases in these parameters by 13.4%, 18.7% and 55.1% respectively. Curcumin reduced the plasma and aorta PGI2 levels of the DOCA-salt group by 10.6% and 14.4% respectively, without

changing the PGI2 level in LV (**Table III.5.**). The observed increase in the plasma, LV and aortic PGI2 levels in the DOCA-salt rats may be due to the higher collagen depositions. PGI2 is a known inflammatory marker in many tissues. Hence its significant increase in the DOCA-salt rats reflected extensive inflammation. Consistent with this, the H&E staining revealed numerous monocyte infiltrations in their heart and fibrotic tissues of these rats (**Fig. III.6D**).

Mal C markedly attenuated the cardiac and vascular collagen depositions in the DOCA-salt rats. Moreover, scar tissue formation and inflammatory insults in the ventricle were also reduced in these rats, as revealed from the less extravasation of leukocytes into the ventricular tissues. Mal C also decreased the fibrotic tissues and thickening of the vascular media, which was increased in the DOCA-salt rats (**Fig. III.6E**). All these may reduce the LV wall thicknesses, cardiac dysfunction and ventricular arrhythmias of the DOCA-salt group. These were evidenced in our ECG and 2D-Echo results, presented latter. These would increase the blood flow to decrease SBP. The effect of curcumin was similar, but less than that of mal C. The Th1 cytokines promote collagen formation and fibrosis in both vascular and cardiac tissues, while the Th2 cytokines retard this. Earlier, mal C maintained Th1/Th2 cytokines balance in acute inflammation [245]. Taken together, the anti-inflammatory role of mal C may be responsible for its antifibrotic and PGI2 suppressing property leading to BP reduction.

III.9 Mal C improves vascular, endothelial and smooth muscle dysfunction of DOCA-salt rats

Vascular hypertrophy and fibrosis leads to smooth muscle and endothelial dysfunction, a key factor for HT [251,252]. Presently, the isolated thoracic rings of the DOCA-salt rats ***s***howed reduced maximal contraction force of the aortic tissues to NA and reduced relaxation responses to SNP and ACh. These may be due to dynamic volumetric load conditions, and implied smooth muscle and endothelial dysfunction. Generation of copious amounts of

Fig. III. 6 Effect of DOCA-salt administration on collagen deposition and inflammation in the heart and vessels of UNX rats and their modulation by mal C and curcumin[a]

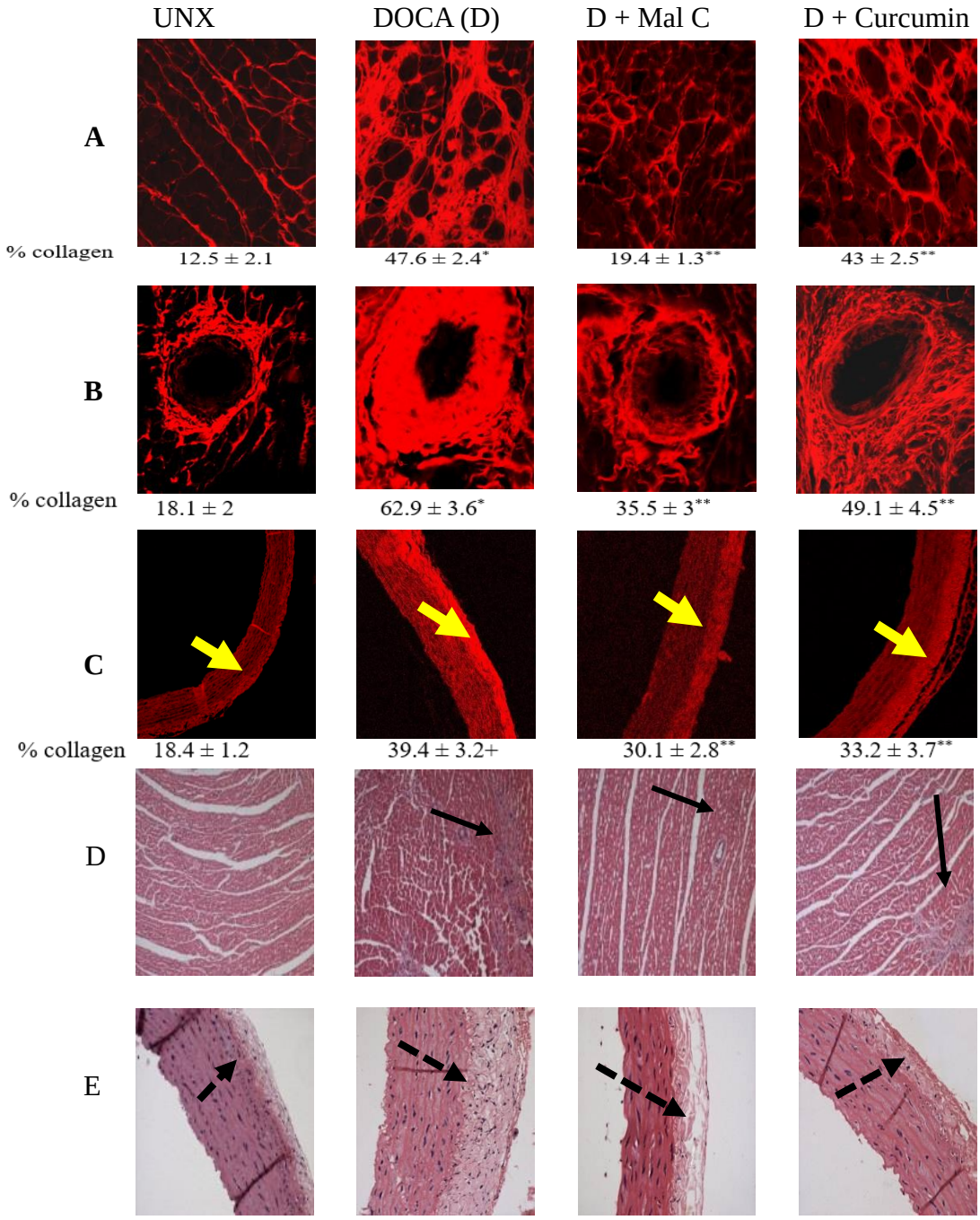

[a]Mal C reduces cardiac remodeling in the DOCA-salt rats. Collagen deposition in **(A)** cardiac interstitial and **(B)** perivascular regions and **(C)** thoracic aorta respectively; **(D)** inflammation and fibrosis in cardiac tissues and **(E)** thoracic aorta. The UNX rats were subcutaneously injected with DOCA solution every fourth day and given drinking water containing 1% NaCl for 28 days. The treatment groups were daily given mal C (10 mg/kg) or curcumin (60 mg/kg) by oral gavage from 15-28th days. The rats were euthanized with sodium thiopentone and different organs removed. The collagen deposition and monocyte infiltration in different tissues were analysed by histology after staining with picrosirrus red and H&E respectively. The experiments were repeated three times with similar results, and only representative images are shown. Bright red areas indicated by yellow arrows show stained collagen, monocyte infiltrations are shown with black arrows, while broken black arrows indicate thickening of the aortic media.

superoxide anions in these rats may explain the vascular endothelial dysfunction in them. Mal C and curcumin treatment increased the contraction response to NA and relaxation response to SNP and ACh (**Figs. III.7A-C**), suggesting improved smooth muscle and endothelial functions. ET-1 predominantly acts on smooth muscles in aorta and contracts them. The ability of mal C to reduce the aortic ET-1 level in the DOCA-salt rats might be responsible for the improved contraction and relaxations responses of the aorta of these rats.

III.10 Mal C modulates the electrochemical conduction pattern in DOCA-salt rats

Electrical remodeling that changes the electrogenic transport processes within the cardiac myocyte, is an important pathophysiological mechanism in CVD. Alterations in transmembrane ionic potential, governed by the Na^+, K^+ and Ca^{2+} fluxes control the electric conduction pattern of the heart. Changes in extracellular Na^+, K^+ and Ca^{2+} levels can alter the myocyte membrane potential gradients and alter the cardiac action potential (AP). There is a dynamic physiologic interrelationship to electrolyte homeostasis, and its changes can precipitate potentially life-threatening dysrhythmias [253]. Myocyte depolarization and repolarization depend on intra and extracellular shifts in the ion gradients. Hence the Na^+, K^+ and Ca^{2+} levels, AP and ECG of the UNX, DOCA-salt and treatment groups were studied to have an idea on the electrical remodeling.

III.10.1 Modulations of ions fluxes: During the AP of almost all cardiac muscle cells, depolarization is due to Na^+ influx. This is followed by a Ca^{2+} influx in the cardiac myocytes to maintain a prolonged depolarization plateau phase (lasting for several 10^{th} of seconds) that is essential to ensure a coordinated repolarization of the cardio myocytes. This is controlled by the slow acting L-type Ca^{2+} channels, predominantly expressed in the heart. In the present studies, the plasma Na^+ and Ca^{2+} levels were 1.6 and 1.5 folds respectively in the DOCA-salt rats, compared to the UNX group (**Table III.6.**). The increased Na^+ level in the DOCA-salt rats can affect the Na^+/ Ca^{2+} exchange mechanism to increase the amount of activator Ca^{2+} necessary for contraction of the smooth muscles [128]. Therefore, disturbances in such

mechanisms can produce contractile changes, which may be relevant for arterial BP homeostasis. Eventually a higher resting potential of the cardiomyocytes may result due to this anomaly. Mal C treatment reduced the Na^+ and Ca^{2+} levels in the DOCA-salt rats by 26.6% and 13.6% respectively. In comparison, curcumin reduced the above parameters by 23.2% and 34.1% respectively. DOCA-salt administration also reduced the plasma K^+ level by 23.8%, compared to the UNX rats. The hypokalemia could be a result of renal loss in the DOCA-salt rats. Substantial clinical and experimental evidence has established a negative impact of hypokalemia in contributing to the pathogenesis of HT, stroke, ventricular arrhythmias, and renal injury. Even mild potassium depletion can impair cardiac function and structure in humans leading to cardiac necrosis and fibrosis. Hence hypokalemia is considered as the clinical hallmark of mineralocorticoid excess [254]. Mal C and curcumin treatment raised the plasma K^+ level of the DOCA-salt rats by 22.0% and 19.07% respectively. This may lead to better conduction profile of the cardio myocytes, as observed in the QTc changes in ECG (*vide supra*).

***III.10.2 Modulation of AP cycle of cardiomyocytes*:** Heart consists of special excitatory and contractile muscles systems to execute specific roles. The APs of the muscles, present in different locations of heart have different conduction durations that allow the heart to function rhythmically. The cardiac AP results from a complex, but precisely regulated movement of ions across the sarcolemmal membrane. The movement of ions across cardiac cell membranes via the ion channels generates the electrical potentials to electrically activate the heart [115]. The cardiacmyocyte contraction mechanics are studied *in vitro* by examining the behavior of the isolated papillary muscle strip. The component fibers of the papillary muscles are arranged parallel to the longitudinal axis and hence, are used to study cardiac electrophysiology using single-cell microelectrode techniques [255]. These can detect and measure APs and other changes in membrane potentials at a single cell level. In case of paralysis of one of the papillary muscles, valve leaking can occur to induce severe or even

Figs. III. 7 Effect of DOCA-salt administration on cumulative concentration–response curves of thoracic aorta of UNX rats to vasoconstrictor and vasorelaxants, and their modulation by mal C and curcumin.[a]

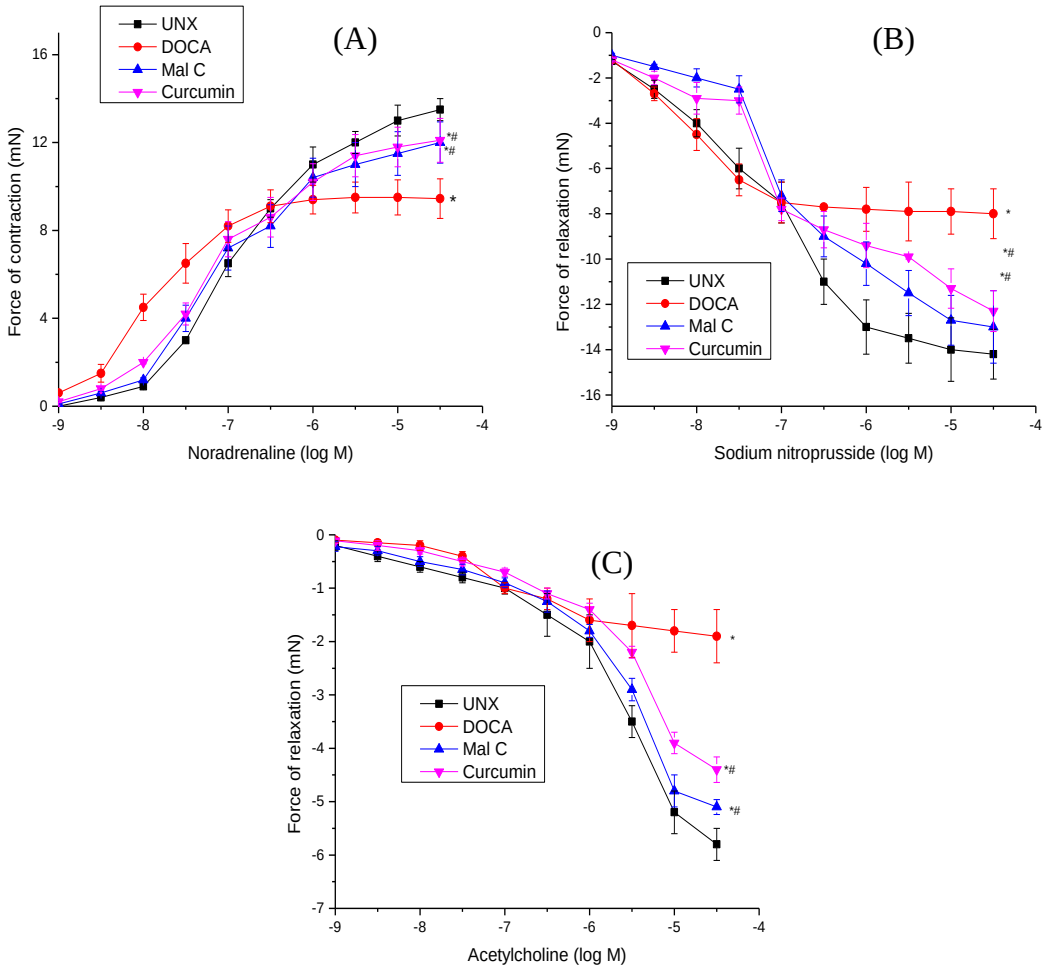

[a]Mal C improves vascular function by increasing endothelial and smooth muscle responses. Cumulative concentration–response curves for NA **(A)**, SNP **(B)** and ACh **(C)**. The thoracic aortic rings in a modified tyrode solution were suspended in an organ bath chamber with a resting tension of 10 mN. The cumulative concentration–response curves were recorded for NA, as well as separately with ACh and SNP in the presence of a submaximal contraction to NA. The experiments were repeated three times with similar results, and the values are mean ± S. E. M., each with 8 rats per group. $^{*}P<0.05$ compared to UNX group; $^{**}P<0.05$ compared to the DOCA-salt group.

lethal cardiac incapacity [128].

Presently, hearts of the DOCA-salt rats showed a markedly increased (12%) RMP, compared to the UNX rats. The RMP of cardio myocytes is controlled by the inward Na^+ and K^+ levels inside the cells. Absence of inward movement of Na^+ and outward movement of K^+

Table III.6. Effect of DOCA-salt administration on plasma ions concentration and electrical conduction pattern of isolated LV papillary muscle of UNX rats and their modulation by mal C and curcumin[a].

Parameters	UNX	DOCA	Mal C-treated	Curcumin-treated
Na^+ (mEq/l)	143.9 ± 7.8	232.2 ± 10.9*	170.5 ± 8.6**	178.3 ± 9.7**
K^+ (mEq/l)	5.37 ± 0.8	4.09 ± 0.6*	4.99 ± 0.9**	4.87 ± 0.6**
Ca^2 (mEq/l)	3.07 ± 0.3	4.48 ± 0.6*	3.87 ± 0.6**	2.95 ± 0.4**
ADP_{20} (ms)	7.1 ± 0.8	46.4 ± 4.1*	31.3 ± 5.8**	41.5 ± 4.7**
ADP_{50} (ms)	14.5 ± 1.3	59.3 ± 7.1*	38.6 ± 5.6**	49.4 ± 5.9**
ADP_{90} (ms)	32.8 ± 2.6	124.9 ± 15.6*	86.7 ± 9.1**	105.5 ± 9.8**
RMP (mv)	-71.1 ± 3.7	-79.5 ± 7.5*	-74.8 ± 2.4**	-76.8 ± 1.8**

[a]The UNX rats were subcutaneously injected with DOCA solution every fourth day and given drinking water containing 1% NaCl for 28 days. The treatment groups were daily given mal C (10 mg/kg) or curcumin (60 mg/kg) by oral gavage during 15-28th days. The rats were injected with heparin, the plasma samples prepared and ions concentration determined by AAS. For APD and RMP measurements, LV papillary muscle was quickly isolated and after optimum preload and equilibration, the microelectrode signals recorded. The experiments were repeated three times with similar results, and the values are mean ± S. E. M., each with 8 rats per group. $^{*}P<0.05$ compared to UNX group; $^{**}P<0.05$, compared to the DOCA-salt group.

keeps the potential negative, thus requiring higher stimulus for depolarization. Hence, the increased extracellular Na^+ and low K^+ in the DOCA-salt rats may account for the augmented RMP. Treatment with mal C and curcumin prevented the RMP rise of DOCA-salt rats by 6% and 3.4% respectively.

In the hypertrophied DOCA-salt hearts, after initial depolarization, the action potential duration (APD) is prolonged during repolarization. Measured at different stages (20%, 50% and 90%) of repolarization, APDs in the DOCA-salt rats were markedly

increased to 6.5 folds, 4.1 folds and 3.1 folds, compared to the respective values of the UNX rats. The increase in APD_{20} may be due to reduction in the early transient outward K^+ channel currents (I_{t0}) [119] as a result of down-regulation of K^+ channel expression [256]. On the other hand, APD_{50} increase is believed to be primarily owing to the increased L-type Ca^{2+} inward current (I_{Ca}) [117]. Consistent with these, we also observed increased extracellular Ca^{2+} level and reduced K^+ level in the plasma of the DOCA-salt rats. The hypokalemia of these rats may be a manifestation of the reduced K^+ channel numbers.

Mal C treatment reduced the ADP_{20} by 32.5%, which could be due to its ability to normalize the Na^+/K^+ ions imbalance. It also reduced the APD_{50} by 34.9% and prevented the ADP_{90} prolongation by 30.6%. The observed reduction in the extracellular Ca^{2+} level by mal C may be due to higher inward movement of the ions, which is possible if the L-type Ca^{2+} channels are increased. These would restrict the DOCA-salt induced prolongation of APD_{50}. Since mal C increased the extracellular K^+ level in the DOCA-salt rats, there will be an increase in the delayed rectifier K^+ current. Hence it could reduce the ADP_{90} prolongation also. In comparison, curcumin reduced APD_{20}, APD_{50} and APD_{90} by 10.6% 16.7% and 15.5% respectively. Thus, curcumin was less effective in reducing APD prolongation by DOCA-salt administration. The results correlated well with its ability to modulate the $Na^+/K^+/Ca^{2+}$ ions imbalance in the DOCA-salt rats. The reduction in APD and RMP by mal C would improve the depolarization and repolarization phases of the cardiac cycle. These changes help in better functioning of papillary muscles leading to superior valve functioning, and are also representative of improved electrical conduction pattern of the cardiomyocytes. The changes in the electrical conduction were also confirmed from the ECG profiles as discussed below. The results on the AP cycle modulation in different rat groups are shown in **Table III.6**.

***III.10.3 Modulations of ECG profile*:** To assess the cardiac electrical functions, the ECG profiles of the different groups of rats were categorized into three subsections. The HR and

RR interval (the interval between two successive R waves) were calculated to analyze the heart beat rhythms. The atrial contraction was assessed from the P and PR wave parameters, while the QRS, QTc and ST segments and the T wave parameters provided insights of the ventricular contractions. These are sequentially discussed below.

***III.10.4 Effect on the heart beat rhythms*:** The RR interval of the UNX rats was 213 ms that was reduced to 167 ms in the DOCA-salt rats. Given that RR interval bears an inverse relationship with HR, the DOCA salt rats showed an increased HR of 398 bpm *vis-à-vis* 285 bpm in the UNX rats. The influx of Na^+ and Ca^{2+} ions in the cardiac muscle cells and increased production of inflammatory molecules and ROS in the cardiovascular system of the DOCA-salt group may explain the results. The tachycardia would increase mechanical stress to the heart. There is a direct correlation between increased resting rate and higher cardiovascular risk [257]. Mal C treatment significantly improved heart rhythmicity of the DOCA-salt rats, as it increased the RR interval to 196 ms and reduced the HR to 320 bpm. In comparison, curcumin increased the RR to 201 ms and reduced the HR to 277 bpm. Possibly mal C treatment led to a slower conduction of potential and hence, contraction of the heart, by reducing the Na^+ and Ca^{2+} levels. The RR interval and HR results of different groups of rats are summarized in **Fig. III.8A**.

III.10.5 Effect on atrial conduction: The atrial conduction signal is generated in the SA node and progresses through atrial muscles to the AV node. The P wave of ECG provides information about the electrical conduction during atrial depolarization. Presently, DOCA-salt administration increased the P wave duration and amplitude from 16 ms and 60 µV respectively (of the UNX rats) to 19 ms and 102 µV. The increased P duration and its amplitude indicated that higher time and current are required for the depolarization of atria in the DOCA-salt rats than the UNX rats. In other words, it signifies left and right atrial hypertrophy. This may be because of the increased atrial myocyte mass and hypertrophy in the former group due to hemodynamic stress. Hypertrophied cardiomyocytes showed reduced

conduction through them [25]. The PR interval reflects the time taken by the electrical impulse to travel from the sinus node to the ventricles through the AV node. Longer PR interval indicates restriction to the conduction of impulse from atria to ventricle via the AV node and hence, first degree AV block. In our studies, DOCA-salt increased the PR interval from 61 ms of the UNX rats to 70 ms. Hypokalemia may prolong the PR interval to impair cardiomyocyte repolarization leading to a prolongation of APD and delayed depolarization [258]. It is possible that the observed hypokalemia in the DOCA-salt is partly responsible for the higher PR interval in their ECG. Moreover, since atrial repolarization precedes ventricular

Mal C reduced both P wave duration (16 ms) and amplitude (64 µV) indicating reduction in right and left atrial hypertrophy of the in DOCA-salt rats. However, curcumin increased the P wave duration to 21 ms, while reducing its amplitude to 79 µV. Nevertheless, both mal C and curcumin reduced the PR interval of the DOCA salt rats to 53 ms and 63 ms respectively that may reduce the first-degree AV block. The anti-hypertrophic effect of mal C, coupled with its ability to increase the K^+ level might be responsible for its cardio-protective activity. The better atrial electrical conduction and propagation of signals to ventricle in the mal C group would ensure proper blood flow from atria to ventricle and improve the valve functions to ensure better rhythmicity of the rat heart. The results on the P waves and PR intervals of different rat groups are summarized in **Fig. III.8B**.

***III.10.6 Effect on ventricular conduction*:** In a cardiac cycle, the impulse from atria proceeds to ventricles leading to their depolarization. The QRS complex reflects the depolarization of the RV and LV. In our studies, DOCA-salt increased the QRS duration to 20 ms from that (15 ms) of the UNX group. The increased QRS interval in DOCA-salt rats indicated ventricular hypertrophy. Due to increased muscle mass in them, the electrical signal took longer time to pass through the ventricles for the required depolarization. Moreover, the QRS wave of DOCA-salt rats occasionally showed ‘M’ pattern on the R wave indicating left bundle branch block. Mal C significantly reduced the QRS interval to 16 ms from that (20

ms) of the DOCA-salt rats, suggesting reduction in the ventricular hypertrophy. This also corroborated by our organ weight analysis and isolated heart preparations results, which also showed reduced ventricle hypertrophy in the mal C-treated DOCA-salt rats. This would lead to proper contraction of the ventricles to ensure better conduction of the bundle branches in both the ventricles of these rats. However, curcumin surprisingly increased the QRS interval to 23 ms.

The QT interval, measured from the beginning of the QRS complex to the end of the T wave varies with HR, and represents electrical depolarization and repolarization of LV and RV. For clinical relevance QTc, a heart rate adjusted QT is used. A prolonged QTc interval is a biomarker for ventricular tachyarrhythmia and a risk factor for sudden death. This also indicates ventricular hypertrophy along with altered conduction of myocytes, probably due to collagen depositions in the extracellular space and scar tissues in the cardio-myocytes. Hypokalemia is also known to increase QTc [258]. Presently, DOCA-salt administration increased the QTc interval of the rats to 205 ms from that (101 ms) of the UNX rats. In a previous section, it was shown that DOCA-salt increased fibrosis and scar tissues in the rat ventricles. These factors along with hypokalemia may explain the increase in QTc. Mal C treatment reduced the QTc interval of the DOCA-salt rats to 172 ms. This could be because of the antifibrotic and anti-hypertrophic properties of mal C, as evident in our histology and organ weight analyses, as well as the ventricular stiffness constants obtained with the isolated heart preparations (*vide infra* in section II.11). Besides, the reduced hypokalemic conditions of the mal C group may help in reducing ventricular tachyarrhythmia and lessen risk factor for sudden death of animals. In comparison, curcumin reduced the QTc interval to 189 ms only. The results on the QRS complex and QTc intervals of different rat groups are summarized in **Fig. III.8C**.

The DOCA-salt rats showed higher ST height (50 μV) compared to that (16 μV) of UNX rats, suggestive of infarction. Our histology data of heart, after trypan blue staining also

confirmed significant infarction in the DOCA-salt group (**Fig. III.4D**). Mal C treatment reduced ST height of the DOCA-salt rats appreciably to 33 µV. Consistent with this, mal C prevented the cardiac infarction in the DOCA-salt rats, as evident in the histology results. However, the preventive effect of curcumin was much less than that of mal C. The reduced inflammation, oxidative insult and fibrosis in the ventricles of the mal C group may account for the observed results. The T wave represents the repolarization (or recovery) of the ventricles. Its first half represents the absolute refractory period, while the last half signifies the relative refractory (vulnerable) period. The T peak to T end interval of the UNX rats was 12 ms. This was increased to 26 ms in that of the DOCA-salt rats. This may be due to the hypokalemic conditions and indicated improper and irregular repolarization of the ventricles. Under these conditions, the ventricles will not get rest for the next depolarization cycle and to receive blood from the atria. Mal C treatment substantially reduced the T wave duration of the DOCA-salt rats to 21 ms, but did not restore it to that of the UNX level. The results with mal C are consistent with its ability to increase the intracellular K^+ level and improve muscle conductions as shown by our single cell electrophysiology studies. Taken together, the above results revealed that mal C improved the cardiomyocytes conduction patterns, valve movements, blood flow and heart rthymicity, while reducing the AV blocks and ventricular tachyarrhythmia. Surprisingly, curcumin increased the ST height to 56 µV and the T wave duration to 34 ms. These along with the other features of the curcumin-treated DOCA-salt rats clearly showed its poorer cardio-protective effect than mal C. The results on this segment of ECG profiles of different rat groups are summarized in **Fig. III.8D**.

***III.10.7 Effect on heart rate variability (HRV)*:** Although cardiac automaticity is intrinsic to various pacemaker tissues, heart rate and rhythm are largely under the control of the autonomic nervous system [259]. There is a strong relationship between the autonomic nervous system and cardiovascular mortality including sudden cardiac death [129]. HRV that assesses fluctuations in the intervals among successive R waves in ECG represents one of the

most promising quantitative markers of autonomic activity [130]. It is also a strong and independent predictor of mortality after an acute myocardial infarction [124]. The frequency spectrum analysis of HRV has been shown to be effective in detecting disturbances in cardiac autonomic control in some experimental models of pathogenic conditions, such as myocardial infarction and diabetic neuropathy [125,126]. In the frequency spectrum analysis, the low frequency (LF) and high frequency (HF) power denote sympathetic and parasympathetic tones respectively, while the LF/HF ratio decides the predominant tone acting on the cardiovascular system.

In our studies, DOCA-salt administration raised the LF/HF ratio to 14.8 folds, compared to the UNX rats (**Fig. III.9A.**), implying more sympathetic activation. This would release the hormone, norepinephrine at the sympathetic nerve endings to increase the permeability of the fiber membrane to Na^{+} and Ca^{+2} ions. In the sinus node, an increase of Na^{+}-Ca^{+2} permeability causes a more positive resting potential and also increases rate of upward drift of the diastolic membrane potential toward the threshold level for self-excitation. Together, they accelerate self-excitation and therefore, increase HR. This along with the higher plasma Na^{+} and Ca^{2+} levels could be some of the reasons of tachycardia in the DOCA-salt rats. Mal C and curcumin reduced the LF/HF ratio by 50% and 63% respectively, signifying a shift towards parasympathetic mode by them. Stimulation of the parasympathetic nerves to the heart (the vagi) causes the hormone, ACh to be released at the vagal endings. This, in turn, can decrease the rhythmic rate of the sinus node, and the excitability of the AV junctional fibers between the atrial musculature and the AV node, slowing transmission of the cardiac impulse into the ventricles. Thus, mal C and curcumin would eventually slow down the HR to reduce tachycardia. Our results (**Fig. III.7B.**) with the isolated thoracic rings also showed increased relaxation response to ACh after mal C and curcumin treatments. The improved relaxation response is consistent with the HRV data and may be due to the reduced aortic ET-1 level in the mal C-treated DOCA-salt rats.

III.11 Mal C improves the cardiac function of the DOCA-salt HT rats

The primary function of heart is to ensure adequate perfusion of blood in different organs. This is achieved by contracting its muscular walls around a closed chamber so that sufficient pressure is generated to flow the blood from the LV to the aortic valve, and then into the aorta. A simultaneous contraction of the RV assists blood to flow through the pulmonic valve and artery to perfuse the lungs. Thus, any cardio-protective formulation needs to be tested for its ability to improve the cardiac function against HT. Amongst the techniques used for this, the Langendorf-perfused heart assay is a useful *in vitro* technique to observe myocardial function and study the responses to injury as well as to a drug. Essentially it allows measurement of the cardiac contractile strength and HR without using any animal [260].

In our studies, the diastolic stiffness constant (*k*) of the DOCA-salt rats increased to 30 from the value (20) of the UNX rats, indicating ventricular stiffness in diastole **(Fig. III.9B.**). The ventricular contractibility is adversely affected by the increased cardio-myocyte hypertrophy and fibrosis in the heart. Thus, our Langendorf-perfused heart assay results may be due to the hypertrophy and fibrosis, observed in the DOCA-salt rats. The ventricular stiffness can occur in both systolic and diastolic phases of the cardiac cycle, and often leads to diminished pump activity and increased resting DBP. We also observed high DBP with the DOCA-salt rats. Mal C treatment completely abrogated the ventricular diastolic stiffness bringing the *k*-value to that of the UNX level. This may be due to the reduced ventricular hypertrophy induced by mal C, as revealed by the ventricular organ wet analysis. The ECG traces of the mal C-treated rats also showed reduction in the DOCA-salt induced prolonging of QRS and QTc profiles, supporting our Langendorf-perfused heart assay results. Moreover, mal C also attenuated fibrotic tissues in the ventricle and collagen depositions in the interstitial region of the ventricles (**Fig. III.6**). Thus, it is expected to improve ventricular contractility, blood carrying capacity and pumping functions of the heart. In comparison, curcumin reduced the diastolic stiffness constant (*k*) to 23 that is consistent with its poorer

Fig. III.8. Effect of DOCA-salt administration on ECG profile of UNX rats and their modulation by mal C and curcumin.[a]

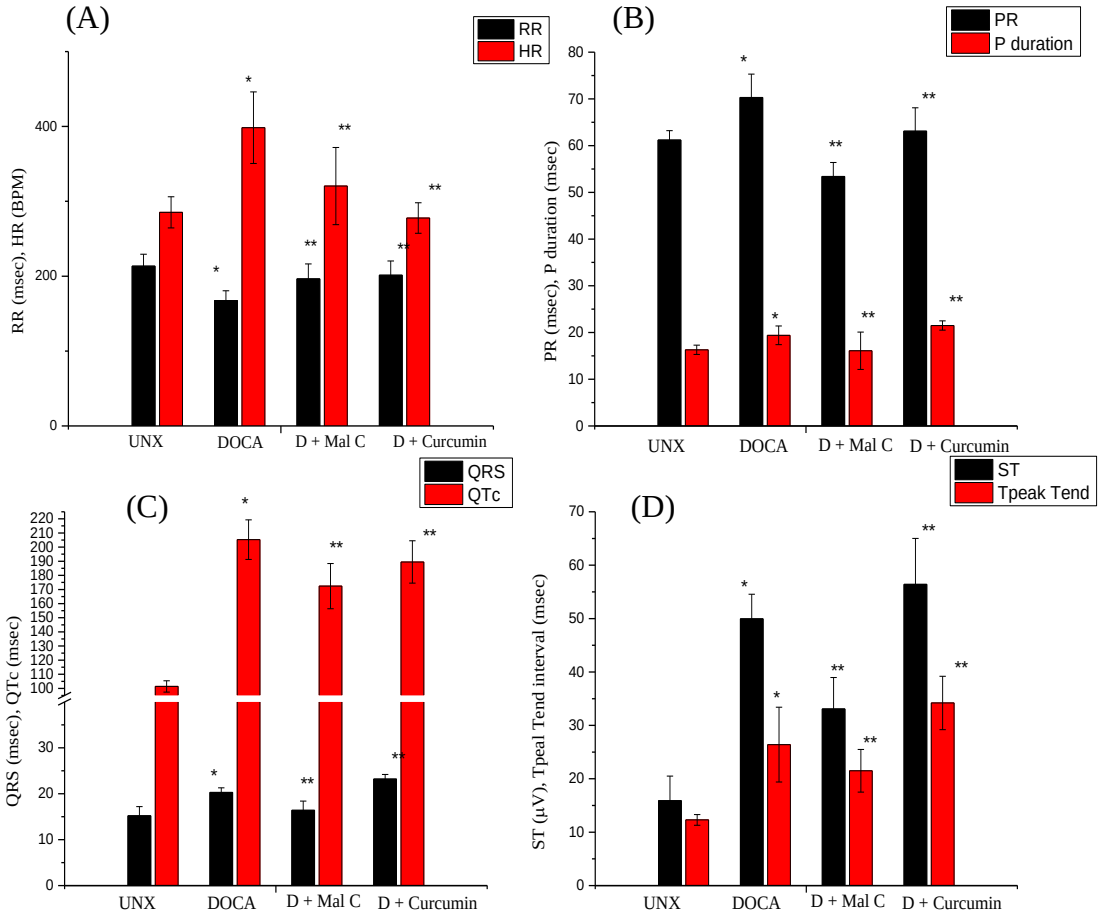

[a]Effect of mal C administration on DOCA- salt rats on the ECG profile. (A) RR interval and HR, (B) PR and P wave durations, (C) QRS and QTc durations and (D) ST and Tpeak to Tend interval. The UNX rats were subcutaneously injected with DOCA solution every fourth day and given drinking water containing 1% NaCl for 28 days. The treatment groups were daily given mal C (10 mg/kg) or curcumin (60 mg/kg) by oral gavage during 15-28th days. ECG and heart rate in rats were measured on 28th day under light sedation. After 10 min of sleep ECG was recorded for 30 min. with needle electrodes in a 3 lead configuration. Needle electrodes were inserted in the right, left and hind paw subcutaneously. The recording was done with Animal Bio-amp FE136 (AD instruments, Sydney, Australia) and data acquired with Power lab data acquisition system PL3508/P (AD instruments Australia). Lab Chart pro software 8.0 (AD instruments, Sydney, Australia) was used to analyze the data. QTc (QT corrected by heart rate) was calculated by Bazzet method. All the readings were average of 20 min recording. The experiments were repeated three times with similar results, and the values are mean ± S. E. M., each with 8 rats per group. $^{*}P<0.05$ compared to UNX group; $^{**}P<0.05$ compared to the DOCA-salt group.

cardio-protective property than mal C. Compared to the perfused heart assay, 2-dimensional echocardiography (2D-Echo) is the most popular technique for the *in vivo* assessment of size and shape of the heart, its pumping capacity and the location and extent of any damage to its

tissues. Hence it is considered as the gold standard in clinical cardiology. Since our results showed that mal C reduces hypertrophy, fibrosis and diastolic stiffness, and also improved electrical conduction of the muscles, the Echo studies were carried out to confirm these conclusively. For this, the interventricular septa (IVS) (the wall between both the ventricles) in both diastolic and systolic dimensions were analyzed by Echo. The mean thickness of IVS of the DOCA-salt rats in diastole and systole were increased by 28.2% and 28% respectively, compared to the UNX rats. The LV posterior wall thicknesses (LVPWs) in diastole and systole of the DOCA-salt rats were increased to by 29.5% and 26.9%, compared to the UNX group. These results indicated increased ventricular mass, and hence, diminished contractibility of the ventricles that would reduce the ventricular dilatation. Consistent with this, the LV internal diameters (LVIDs) in diastole and systole were also decreased by 14.9% and 16.1% respectively on DOCA-salt administration to the UNX rats.

Furthermore, both the ascending and descending aortic blood flow velocities were increased (to 1.7 and 1.9 folds respectively) along with increased descending aorta diameter by 17.4% in the DOCA-salt group. Our histology results with H&E staining also revealed more vascular media wall thickness in these rats that would reduce the lumen size. This and the increased aortic blood flow velocities would result in HT. The systolic and diastolic volumes were reduced by 40.9% and 36.2% in the DOCA-salt group. These would impair the blood transport.

Mal C treatment reduced the ventricular mass by reducing the both systole and diastole IVS (by 6.3% and 15.3% respectively) and the LVPWs by 8.8% (systole) and 18.4% (diastole). The reduced masses could be due to/ and also indicative of reduced cardiomyocytes hypertrophy and ventricular fibrosis. The Echo results were well supported by those obtained from the ECG, histology, organ weight and Langendorf analyses of the mal C group. Consistent with its ability to reduce the ventricular mass and diameter, mal C also increased LVIDs in diastole and systole by 23% and 37.7% respectively. This would increase

Fig. III.9. Effect of DOCA-salt administration on (A) HRV and (B) diastolic stiffness constant of UNX rats and their modulation by mal C and curcumin.[a]

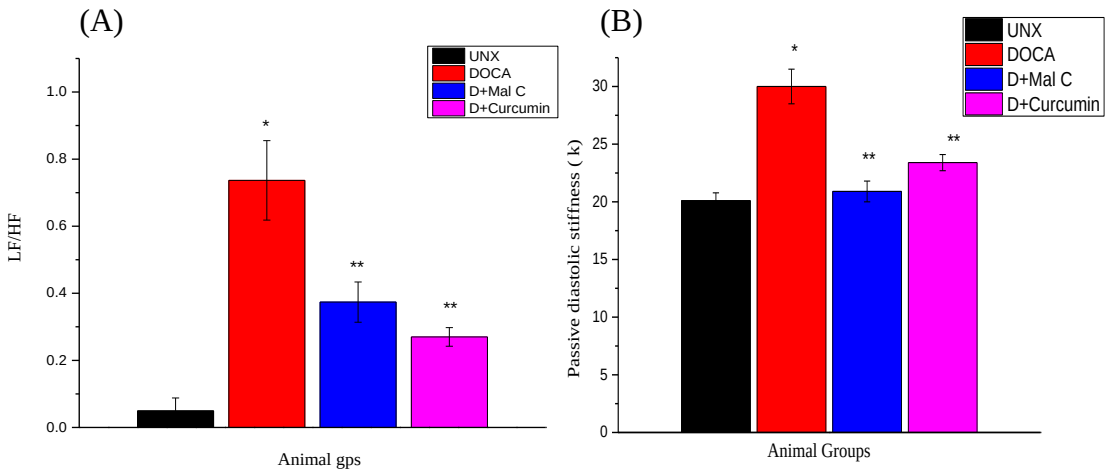

[a]The UNX rats were subcutaneously injected with DOCA solution every fourth day and given drinking water containing 1% NaCl for 28 days. The treatment groups were daily given mal C (10 mg/kg) or curcumin (60 mg/kg) by oral gavage during 15-28th days. **(A)** HRV by power spectral analysis method (LF/HF) was measured and analyzed on the 28th day from the ECG traces with the help of CHART 8.1 software (AD instruments, Sydney, Australia) as described before in chapter ***II.18.1***. For the diastolic stiffness constant, after euthanasia heart was excised out and mounted on a langendorf system and the constant (*k*) is calculated as described in the chapter ***II.19.*** The experiments were repeated three times with similar results, and the values are mean ± S. E. M., each with 8 rats per group. $^{*}P<0.05$ compared to UNX group; $^{**}P<0.05$ compared to the DOCA-salt group.

ventricular dilatation and cavity space during diastole, resulting in improved contractibility and increased space for carrying and pumping blood. In comparison, the effect of curcumin was significantly less, as it reduced the IVS by 3.5% (systolic) and 9.8% (diastolic), and LVPWs by 3.5% (systolic) and 6.6% (diastolic).

Besides reducing the media thickness of the aortic wall (as seen by histology, **Fig. III 6. C.**), mal C also prevented the increase in ascending and descending aortic blood flow velocities by 8% and 20.4% respectively. It also reduced the aortic diameters of DOCA-salt rats by 7.4% (ascending) and 14.8% (descending). The systolic and diastolic volumes were increased to 2.2 and 1.8 folds respectively in the mal C group, compared to the DOCA-salt rats. Overall, mal C prevented the DOCA-salt-induced increase in fluid pressure, and thus, the BP. However, compared to the DOCA-salt group, curcumin reduced the aortic blood flow

velocities by 20.8% (ascending) and 31.5% (descending) and descending aorta diameters by 7.4. Taken together the results showed improvement in cardiac flow dynamics by mal C as well as curcumin. The 2D-Echo results showing the structural and functional changes of heart are presented in **Tables III.7** and **III.8** respectively.

The pulsed-wave Doppler analyses of the UNX rats showed early mitral inflow velocity (E, 0.8 m/sec), atrial mitral inflow velocity (A, 0.4 m/sec) and the E/A ratio of ~1.9. DOCA-salt administration reduced E by 47.7% and A by 16.7%. This amounted to a reduction of E/A ratio [261], a marker of the LV function by 37.8%. The abnormalities in the E/A ratio suggested that the LV (which pumps blood into the circulation) can't fill with blood properly, indicating diastolic dysfunction as an eventual symptoms of heart failure. The increased P wave amplitude as well as P and PR wave prolongation, observed in the ECG also suggested atrial hypertrophy and mitral and tricuspid stenosis. These would stiffen the valves to impair the electrical conduction and may lead to atrial fibrillation and restrictive filling of the atria. Mal C treatment increased the values of E (80.5%), A (37.1%) and E/A ratio (31.7%) of the DOCA-salt rats. This would improve the diastolic filling pattern of ventricles and increase mitral flows of the rats, resulting in better atrial conduction and mitral function. This was also supported by the fact that mal C reduced both P wave duration and amplitude, indicating reduction in the right and left atrial hypertrophies along with mitral and tricuspid stenosis in the DOCA-salt rats. In comparison, curcumin increased the values of E (34.1%), A (17.1%) and E/A ratio (12%) of the DOCA-salt rats. Compared to the UNX rats, DOCA-salt increased the time of mitral valve closing and opening (MC-MO value) by 30.8%, and the E wave deceleration time by 30.9%, signifying restricted blood flow through the valves. Mal C treatment reduced the above two parameters by 16.0% and 32.8% respectively to allow improved blood flow through the valves. Curcumin reduced these parameters less, by 8.4% and 8.1% respectively. Finally, the stroke volume and cardiac output in the DOCA-salt rats were reduced by 37.1% and 30.5% respectively, compared to

Table III.7. Effect of DOCA-salt administration on structural modifications in the UNX rats heart and their modulation by mal C and curcumin[a].

Parameters	UNX	DOCA	Mal C-treated	Curcumin-treated
IVSd (mm)	1.74 ± 0.08	2.23 ± 0.13*	1.89 ± 0.08**	2.01± 0.09**
IVSs (mm)	2.86 ± 0.12	3.48 ± 0.13*	3.26 ± 0.12**	3.4 ± 0 .14**
LVIDd (mm)	5.71 ± 0.07	4.86 ± 0.39*	5.98 ± 0.19**	5.11 ± 0.21**
LVIDs (mm)	2.43 ± 0.07	2.04 ± 0.31*	2.81 ± 0.22**	2.2 ± 0.09**
LVPWd (mm)	1.76 ± 0.12	2.28 ± 0.22*	1.86 ± 0.1**	2.13 ± 0.23**
LVPWs (mm)	2.68 ± 0.03	3.4 ± 0.28*	3.10 ± 0.06**	3.28 ± 0.07**
Fractional shortening (%)	54.33 ± 1.15	58.33 ± 3.17*	52.71 ± 2.64**	56.31 ± 3.4**
Aortic Arch Diameter (cm)	0.25 ± 0.02	0.27 ± 0.01*	0.25 ± 0.01**	0.28 ± 0.01
Descending Aorta Diameter (cm)	0.23 ± 0.01	0.27 ± 0.02*	0.23 ± 0.01**	0.25 ± 0.01**

[a]The UNX rats were subcutaneously injected with DOCA solution every fourth day and given drinking water containing 1% NaCl for 28 days. The treatment groups were daily given mal C (10 mg/kg) or curcumin (60 mg/kg) by oral gavage during 15-28th days. After anaesthesia, the serial *in vivo* echocardiographic images were recorded with an image depth of 3 cm using two focal zones. The experiments were repeated three times with similar results, and the values are mean ± S. E. M., each with 8 rats per group. $^{*}P<0.05$ compared to UNX group; $^{**}P<0.05$, compared to the DOCA-salt group.

the UNX rats. This indicated reduced blood ejection per beat as well as reduced volume ejected per min by the ventricles. In other words, the pumping efficiency and cardiac function were reduced in the DOCA-salt rats. Mal C treatment increased the stroke volume and

cardiac output of the DOCA-salt rats by 56% and by 30.8% respectively. Likewise, curcumin increased the stroke volume by 33.2% and cardiac output by 13.4%. The improved stroke volume and cardiac output in the treated groups indicated overall better cardiac functioning and performance.

III.12 Mal C improves renal and hepatic function of DOCA-salt rats

There is a strong association between HT and disruption of liver tissue architecture and vacuolation as well as impaired renal functions. Disruption of liver tissue architecture under HT is an indication of hepatocellular injury. Clinical diagnosis of disease and damage to the structural integrity of the liver is commonly assessed by monitoring the status of serum AST, ALP and ALT activities, which are sensitive serological indicators of liver toxicity. Increased AST and ALT release from the damaged tissues has become a definitive diagnostic and prognostic criterion for various diseases and disorders. Likewise, kidney plays a central role in regulating the balance of salt and water in the body. Disordered regulation of renal functions is responsible for the pathophysiological states including some experimental HT models [262].

ALP and gamma-glutamyl transpeptidase (GGT) are the membrane bound enzymes and their elevation indicates membrane disruption in the organ. In our studies, the plasma ALT, ALP, proteins and creatinine levels of the DOCA-salt group were 1.8, 1.3, 3.7 and 1.4 folds respectively, compared to the corresponding values in the UNX rats. The increased activities of ALT and ALP in serum might be mainly due to the leakage of these enzymes from the liver cells into the blood stream [263], which indicated the hepatotoxic effect of DOCA-salt. The reduced TAS in this group of rats might be involved in the hepatic injury, because reactive free radicals are implicated as the potential mediators of tissue injury. The LPO products disperse from the site of tissue damage and therefore, can be measured in plasma [264]. Nevertheless, in this investigation, the LPO products were measured at various tissues in terms of MDA. These also confirmed damages at heart (LV and aorta) as well as liver.

Creatinine, a transformed product of creatine is made by the body to supply energy to muscles and is removed from the body entirely by the kidneys. Hence, its increased level in blood reflects less clearance through urine, implying kidney malfunction and detrimental glomerular filtration. Our results showed a considerable increase in plasma creatinine level in the DOCA-salt rats, indicating that the HT in DOCA-salt rats may be due to kidney damage, propelled by OS. Renal damage in both human and experimental salt-sensitive HT is well-known, and may result due to the increased superoxide formation. Presently, the DOCA-salt rats had excessive superoxide generation via the activation of XO (**Table III.4.**) and NAD(P)H oxidase **(Fig. III.4C)**. About one-half of essential hypertensives have a salt-sensitive HT type, and the amount of renal damage that occurs in salt-sensitive hypertensives greatly exceeds that of non-salt-sensitive hypertensives.

Oral administration of mal C reduced the augmented ALT, proteins, ALP and creatinine levels of the DOCA-salt group by 73.4%, 17.6%, 31.3% and 18.7% respectively. In comparison, curcumin reduced the designated parameters by 59.7%, 10.8%, 21.1% and 17.0% respectively. These suggested that both the test samples, especially mal C brought about remarkable recovery in liver and the remnant kidney in the DOCA-salt hypertensive rats. Moreover, the relative effects correlated with their respective antioxidant property. The malfunctioning of liver may lead to severe metabolic disorders, complicating the cases of HT.

Previously hyperlipidemia in the DOCA-salt hypertensive rats was found to be due to metabolic changes, and not because of high food intake [265]. Presently, despite not showing higher food consumption, the DOCA-salt had higher serum cholesterol level, compared to that of the UNX rats. Treatment with mal C and curcumin reduced serum cholesterol level of the DOCA-salt rats by 6.9% and 2.3% respectively. Thus, both mal C and curcumin significantly corrected metabolic disorders. The impaired renal functions would change the balance of salt and water, and may also be a causative factor for the observed HT in the DOCA-salt group [266]. The ability of mal C against oxidative damage to liver and kidney of

Table III.8. Effect of DOCA-salt administration on functional modifications in the UNX rats heart and their modulation by mal C and curcumin[a].

Parameters	UNX	DOCA	Mal C-treated	Curcumin-treated
Ascending aorta (m/sec)	0.75 ± 0.15	1.25 ± 0.07*	1.15 ± 0.09**	0.99 ± 0.03**
Descending aorta (m/sec)	0.56 ± 0.11	1.08 ± 0.02*	0.86 ± 0.09**	0.74 ± 0.05**
E velocity (m/sec)	0.79 ± 0.03	0.41 ± 0.03*	0.74 ± 0.03**	0.55 ± 0.02**
A velocity (m/sec)	0.42 ± 0.11	0.35 ± 0.06*	0.48 ± 0.03**	0.41 ± 0.04**
E/A ratio	1.88 ± 0.48	1.17 ± 0.31*	1.54 ± 0.08**	1.31 ± 0.09**
decel time (msec)	82.5 ± 20.5	108.0 ± 27.12*	72.57 ± 3.9**	99.3 ± 8.1**
MC-MO (msec)	117.2 ± 21	153.2 ± 17.4*	128.71 ± 3.4**	140.3 ± 6.4**
		Derived	**Calculations**	
Systolic Volume (µl/l)	17.18 ± 1.5	10.16 ± 1.9*	22.07 ± 2.4**	19.4 ± 2.5**
Diastolic Volume (µl/l)	195.79 ± 7.4	124.86 ± 27.3*	229.01 ± 15.8**	200.1 ± 18.5**
Stroke Volume (µl)	182.6 ± 7.1	114.7 ± 23.7*	178.9 ± 26.4**	152.8 ± 21.6**
LV Mass (g)	0.67 ± 0.04	1.24 ± 0.5*	0.75 ± 0.06**	0.85 ± 0.03**
Ejection fraction (%)	84.3 ± 7.1	92.6 ± 7.3*	89.2 ± 9.1**	92.9 ± 6.3
Cardiac output (ml/min)	75.3 ± 4.1	52.3 ± 4.2*	68.4 ± 5.4**	59.3 ± 4.2**

[a]The UNX rats were subcutaneously injected with DOCA solution every fourth day and given drinking water containing 1% NaCl for 28 days. The treatment groups were daily given mal C (10 mg/kg) or curcumin (60 mg/kg) by oral gavage during 15-28th days. After anesthesia, echocardiographic images were recorded with an image depth of 3 cm using two focal zones. The experiments were repeated three times with similar results, and the values are mean ± S. E. M., each with 8 rats per group. *P<0.05 compared to UNX group; **P<0.05, compared to the DOCA-salt group.

the DOCA-salt rats, along with the reduced daily water intake by the mal C group (**Fig. III.3A**) would decrease hemodynamic load on the remnant kidney of the UNX rats. These may be beneficial in controlling the SBP, as observed in this study. The comparative plasma biochemistry results of different groups of rats are shown in **Fig. III.10 A-E**.

III.13 Mal C improves survival of DOCA-salt rats

For examining the cardio-protective effect of mal C, the experiments on the DOCA-salt hypertensive rats were carried out for 28-day. However, the ultimate utility of any drug can only be established in terms of increased the survival of the subjects. Hence, the survival of the DOCA-salt rats as such, and after drug administration was observed till 40 days. To this end, DOCA-salt administration was continued up to 40 days, and treatments with various doses (5-50 mg/kg) of mal C as well as the positive controls curcumin (60 mg/kg) and atenolol (10 mg/kg) were carried out during 15-40 days of the experiments. The drugs at the designated doses were given to the rats by oral gavage only once every day. The UNX rats showed 100% survival during the experimental period (up to 40 day). The DOCA-salt and treated groups also had >90% survival on the 28^{th} day. Thereafter, survival of the DOCA-salt rats was drastically reduced to 38% and 12% respectively on the 35^{th} and 40^{th} days. Mal C treatment improved the survival of DOCA-salt rats in a concentration dependent manner up to 10 mg/kg. Beyond this concentration, mal C did not significantly change the survival of the DOCA-salt rats. For example, the survival percentages on the 35^{th} and 40^{th} days of the mal C groups were: 5 mg/kg: 62% and 50%; 10, 15, and 20 mg/kg: 80% and 75%; 50 mg/kg 82% and 75%. In comparison, the survival percentages on 35^{th} and 40^{th} days of the curcumin group were 70% and 66%, and that for atenolol group were 72% and 68% respectively.

III.14 Comparative anti-hypertensive and cardio-protective properties of mal C

Given that the major aim of the present investigation was to assess the cardio-protective potential of mal C, it was of prime importance to compare its effect on several pertinent and critical parameters in DOCA-salt hypertensive rats *vis-à-vis* some clinical anti-

hypertensive drugs and another spice-derived phenolic, curcumin. It is well-known that drugs that target different mechanistic pathways might improve the clinical outcomes in CVD. Hence, we included several biochemical, electro-physical and functional parameters of heart to establish the drug efficacy. To this end, the antihypertensive effect of mal C was compared with two clinically used anti-hypertensive drugs, atenolol and amlodipine. Extensive studies have demonstrated that the antihypertensive property of atenolol follows a different mechanism without involving any antioxidant effect [265,266]. While besides reducing BP, the beneficial cardiovascular effects of the calcium channel blockers such as amlodipine is also due to protection of cardiac remodeling by preventing kidney damage and excessive renin production [269]. Hence, we included these drugs to measure the BP only, but not for studying the biochemical effects on the DOCA-salt rats. Our BP data, measured both by non-invasive and invasive methods clearly demonstrated similar anti-hypertensive effect of mal C (10 mg/kg), atenolol (10 mg/kg) and amlodipine (15 mg/kg). In view of the crucial role of OS in HT and CVD, the well-known natural phenolic antioxidant, curcumin was also included in the studies. The modulatory properties of mal C on the biochemical, histological, electrophysiological and functional parameters of the DOCA-salt rats were compared with that of curcumin. The effects of curcumin on all the studied biochemical parameters of the DOCA-salt rats were similar to that of mal C. However, its effect on most of these parameters were less than that of mal C. This was also reflected from their relative anti-parameters were less than that of mal C. This was also reflected from their relative anti-hypertensive properties.

III.15 Conclusions

There are several salient features of the present study. In this study, it was found for the first time that chronic oral administration of the spice-derived phenolic, mal C can reduce blood pressure (BP) and attenuate cardio-vascular remodeling in DOCA-salt hypertensive rats. Mal C (10 mg/kg) showed almost same anti-hypertensive potency as that of atenolol

Fig. III.10 Effect of DOCA-salt administration on the plasma biochemistry profile of the UNX rats heart and their modulation by mal C and curcumin[a]

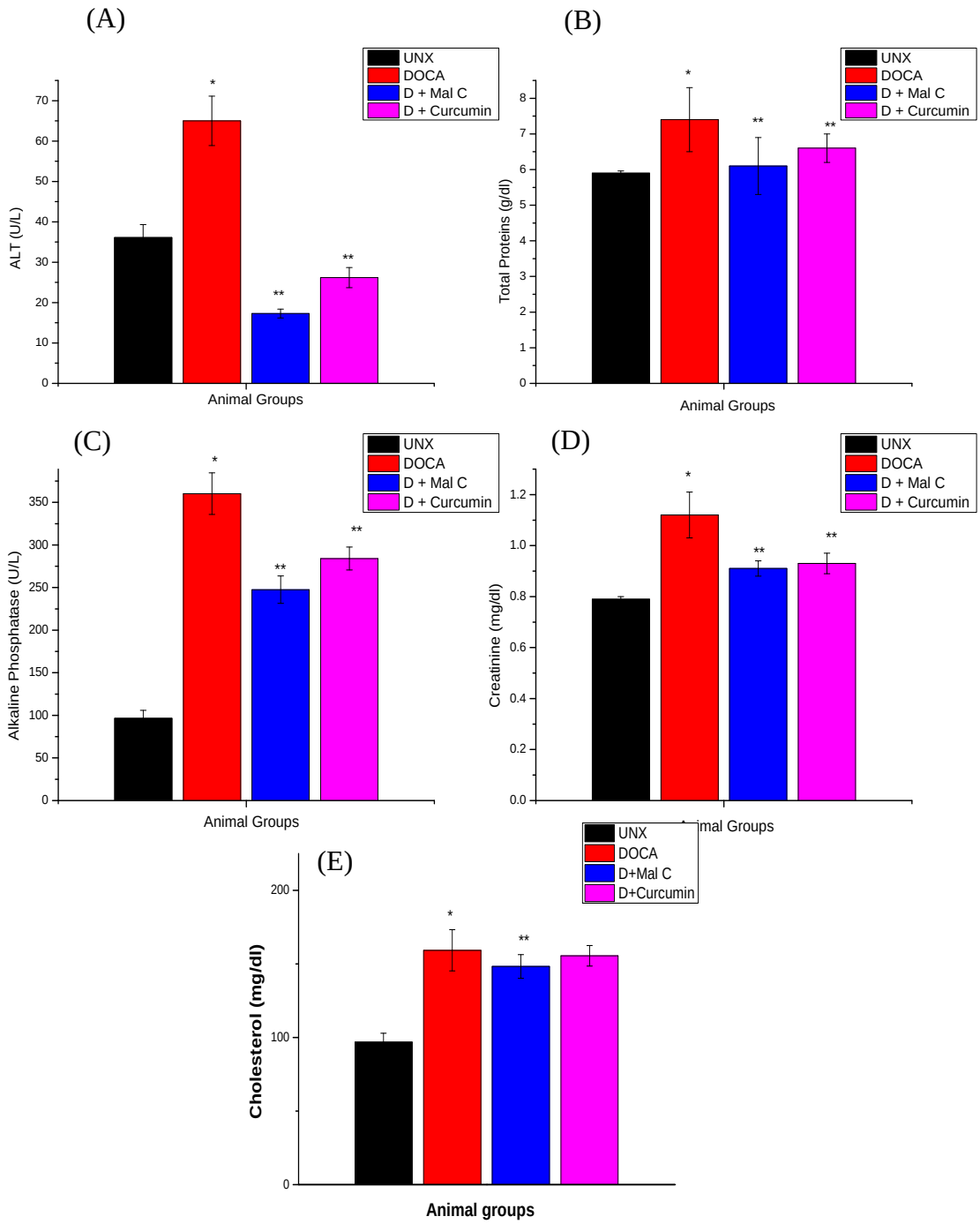

[a]Modulation of plasma biochemistry of DOCA-salt rats by mal C. (A) ALT, (B) Total proteins, (C) ALP, (D) Creatinine, (E) Total cholesterol. UNX rats were subcutaneously injected with DOCA solution every fourth day and given drinking water containing 1% NaCl for 28 days. The treatment groups were daily given mal C (10 mg/kg) or curcumin (60 mg/kg) by oral gavage during 15-28th days. The rats were injected with heparin, the plasma samples were prepared, and the parameters evaluated. The experiments were repeated three times with similar results, and the values are mean ± S. E. M., each with 8 rats per group. $^{*}P<0.05$ compared to UNX group; $^{**}P<0.05$ compared to the DOCA-salt group.

(10 mg/kg) and amlodipine (15 mg/kg), as revealed from the BP measurements. Mal C exerted cardioprotective effect to DOCA-salt rats, as evidenced by (i) reduction of ventricular hypertrophy, structural remodeling of vessel walls, and inflammation in ventricles and aorta; (ii) reduction of the ischemia-reperfusion-mediated increase in ventricular dysfunction and

Fig. III 11. Effect of DOCA-salt administration on the survival of UNX rats and their modulation by mal C and curcumin[a].

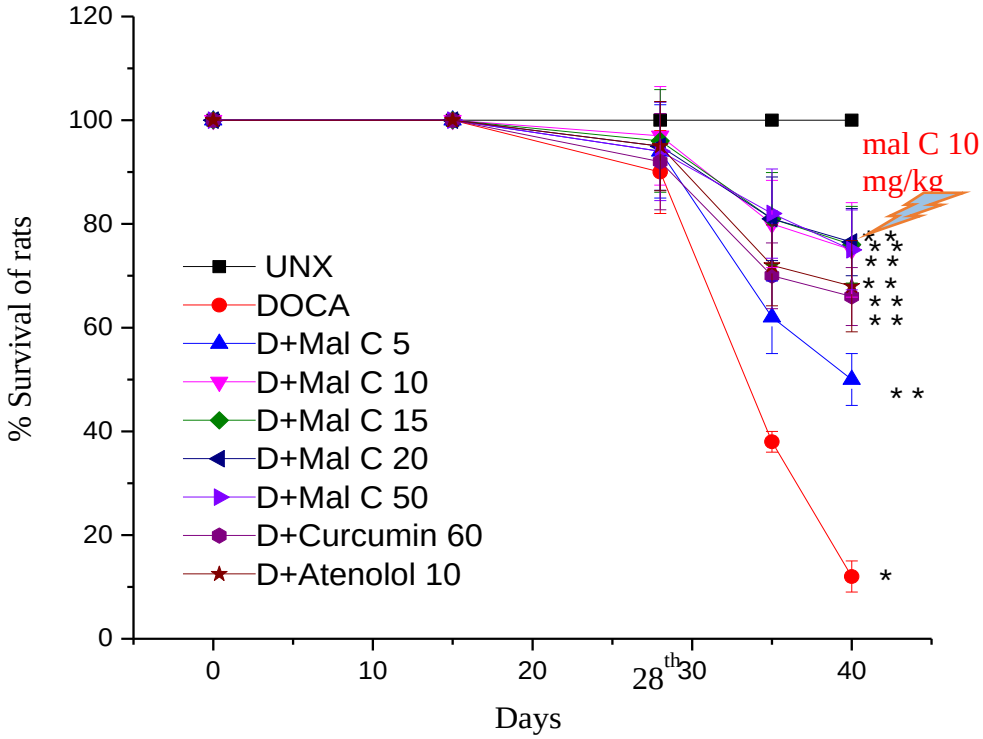

[a]40-day survival experiment. Survival of rats was observed till 40 days. Drugs were started on 15th day and given till 40th day. On 28th day statistically relevant numbers of animals are alive, hence all other experiments are carried out on 28th day. Mal C shows concentration dependent increases in survival till 10 mg/kg. Mal C 50 mg/kg does not show any significant change in survival than mal C. Atenolol 10 mg/kg and curcumin 60 mg/kg has similar effect. The experiments were repeated three times with similar results, and the values are mean ± S. E. M., each with 10 rats per group. $^{*}P<0.05$ compared to UNX group; $^{**}P<0.05$ compared to the DOCA-salt group.

arrhythmias, and (iii) improving the vascular endothelial and smooth muscle as well as liver and kidney functions. Many of the cardiac and vascular changes including structural and functional abnormalities caused by the DOCA-salt treatment were prevented or attenuated by the treatment with mal C resulting in improved functioning of the cardiovascular system of

mal C treated animals. Thus, mal C could positively influence multiple targets that can induce HT and CVD. It is tempting to propose that its antioxidant action may be the primary mechanism accounting for the cardioprotective property. These results are promising to promote mal C as a potential anti-hypertensive agent, especially in view of its appreciable natural abundance and non-toxicity to animals. Further studies on its role in improving cardiac functions in other hypertensive models would establish its efficacy against CVD.

CHAPTER - IV

BIBLIOGRAPHY

1. Gaziano, T.; Reddy, K. S.; Paccaud, F.; Horton, S.; Chaturvedi, V. (2006). Cardiovascular disease. In: Disease Control Priorities in the Developing World; Jamison, D. T.; Mosley, W. H. eds; *Oxford: Oxford University Press* p. 645–662.
2. WHO (2012). World health statistics report. http://www.who.int/gho/publications/ world _ health_statistics/2012/en/.
3. Iyer, A.; Chan, V.; Brown, L. (2010). The DOCA-salt hypertensive rat as a model of cardiovascular oxidative and inflammatory stress. *Curr. Cardiol. Rev*. 6:291–297.
4. Cambien, F.; Tiret, L. (2007). Genetics of cardiovascular diseases from single mutations to the whole genome. *Circulation*, 116:1714–1724.
5. The Indian Heart Watch (IHW) study (2012). Deedwania, P. Univ. Calif., San Francisco, USA. (http://www.world-heart-federation.org/press/releases/detail/article reasons-for-indias-growing-cardiovascular-disease-epidemic-pinpointed-in-largest ever-risk-factor/).
6. Bohr, D. F.; Dominiczak, A. F.; Webb, R. C. (1991). Pathophysiology of the vasculature in hypertension. *Hypertens*. 18:S69–S75.
7. Rodgers, A.; Lawes, C.; MacMahon, S. (2000). Reducing the global burden of blood pressure related cardiovascular disease. *J. Hypertens*. 18 (Suppl 1):S3–S6.
8. Law, M.; Wald, N. J; Morris, J. K (2003). Lowering blood pressure to prevent myocardial infarction and stroke: a new preventive strategy. *Health Technol Assess* 7:1–94. doi:10.3310/hta7310. PMID 14604498.
9. Cohn, J. N.; Ferrari, R.; Sharpe, N. (2000). Cardiac remodeling concepts and clinical implications. A consensus paper from an international forum on cardiac remodeling. *J. Am. Coll. Cardiol*. 35:569–582.
10. Millar, J. T.; O'Rourke, R. A.; Crawford, M. H. (1988). Left atrial enlargement: an early sign of hypertensive heart disease. *Am. Heart J*. 116:1048–1051.

11. Vaziri, S. M.; Larson, M. G.; Lauer, M. S.; Benjamin, E. J.; Levy, D. (1995). Influence of blood pressure on left atrial size the Framingham Heart study. *Hypertens*. 25:1155–1160.
12. Barbier, P.; Alioto, G.; Guazzi, M. D. (1994). Left atrial function and ventricular filling in hypertensive patients with paroxysmal atrial fibrillation. *J. Am. Coll. Cardiol*. 24:165–170.
13. Madu, E. C.; Baugh, D. S.; Gbadebo, T. D.; Dhala, A.; Cardoso, S. (2001). Effect of ethnicity and hypertension on atrial conduction: evaluation with high-resolution P-wave signal averaging. *Clin. Cardiol*. 24:597–602.
14. Ravelli, F.; Allessie, M. (1997). Effects of atrial dialation on refractory period and vunerability to atrial fibrillation in the isolated langendorf perfused rabbit heart. *Circulation* 96 :1686–1695.
15. Shapiro, L. M.; Sugden, P. H. (1996). Left ventricular hypertrophy. In: Julian, D. G.; Camm, A. J.; Fox, K. M.; Hall, R. T. C.; Poole-Wilson, P. A. (eds.); *Diseases of the Heart, 2nd Ed.*; London, England: c v Saunders.
16. Frohlich, E. D.; Apstein, C.; Chobanian, A.V.; Devereux, R. B.; Dustan, H. P.; Dzau, V.; Fauad- Tarazi, F. et al. (1992). The heart in hypertension. *New Eng. J. Med*. 327:998–1008.
17. Hunter, J. J.; Chien, K. R. (1999). Signaling pathways for cardiac hypertrophy and failure. *New Eng. J. Med*. 341:1276–1283.
18. Moalic, J. M.; Charlemagne, D.; Mansier, P.; Chevalier, B.; Swynghedauw, B. (1993). Cardiac hypertrophy and failure-a disease of adaptation. Modifications in membrane proteins provide a molecular basis for arrhythmogenicity. *Circulation* 87(5 Suppl) : IV21–26.
19. Swynghedauw, B. (1999). Molecular mechanisms of myocardial remodeling. *Physiol.*

Rev. 79:216–262.

20. Devereux, R.B.; de Simone, G.; Ganau, A.; Koren, M. J.; Roman, M. J. (1993). Left ventricular hypertrophy associated with hypertension and its relevance as a risk factor for complications. *J. Cardiovasc. Pharmacol*. 21: S38–S44.
21. Benjamin, E. J.; Levy, D. (1999). Why is left ventricular hypertrophy so predictive of morbidity and mortality? *Am. J. Med. Sci*. 317:168–175.
22. Marcus, M. L.; Harrison, D. G., Chilian, W. M. (1987). Alterations in the coronary circulation in hypertrophied ventricles. *Circulation* 75:I19–I25.
23. Mueller, T. M.; Marcus, M. L.; Kerber, R. E.; Young, J. A.; Barnes, R. W.; Abboud, F. M. (1978). Effect of renal hypertension and left ventricular hypertrophy on the coronary circulation in dogs. *Circ. Res*. 42:543–549.
24. Fouad, F. M.; Slominski, J. M.; Tarazi, R. C. (1984). Left ventricular diastolic function in hypertension: relation to left ventricular mass and systolic function. *J. Am. Coll. Cardiol*. 3:1500–1506.
25. McLenacham, J. M.; Henderson, E.; Morris, K. I.; Dargie, H. J. (1987). Ventricular arrhythmias in patients with hypertensive ventricular hypertrophy. *New Eng. J. Med*. 317:787–792.
26. Chapman, D.; Weber, K. T.; Eghbali, M. (1990). Regulation of fibrillar collagen types I and III and basement membrane type IV collagen gene expression in pressure overloaded rat myocardium. *Circ. Res*. 67:787–794.
27. Yamamoto, K.; Masuyama, T.; Sakata, Y.; Nishikawa, N.; Mano, T.; Yoshida, J.; Miwa, T.; Sugawara, M.; Yamaguchi, Y.; Ookawara, T.; Suzuki, K.; Hori, M. (2002). Myocardial stiffness is determined by ventricular fibrosis, but not by compensatory or excessive hypertrophy in hypertensive heart. *Cardiovas. Res*. 55:76–82.
28. Foster, K. A.; Hock, C. E.; Reibel, D. K. (1991) Altered responsiveness of

hypertrophied rat hearts to alpha- and beta-adrenergic stimulation. *J. Mol. Cell. Cardiol*. 23: 91–101

29. Houser, S. R.; Piacentino III, V.; Weisser, J. (2000). Abnormalities of calcium cycling in the hypertrophied and failing heart. *J. Mol. Cell. Cardiol*. 32:1595–1607.
30. Norton, G. R.; Woodiwiss, A. J.; Gaasch, W. H.; Mela, T.; Chung, E. S.; Aurigemma, G. P.; Meyer, T. E. (2002). Heart failure in pressure overload hypertrophy. The relative roles of ventricular remodeling and myocardial dysfunction. *J. Am. Col. Cardiol*. 39:664–671.
31. Colucci, W. S. (1997). Molecular and cellular mechanisms of myocardial failure. *J. Am. Col. Cardiol*. 80:15L–25L.
32. Dzau, V. J.; Gibbons, G. H. (1993). Vascular remodeling: Mechanisms and implications. *J. Cardiovas. Pharmacol*. 21:S1–S5.
33. Leonetti, G.; Cuspidi, C. (1995). The heart and vascular changes in hypertension. *J. Hypertens*. 13:S29–S34.
34. Mulvany, M. J.; Baumbach, G. L.; Aalkjaer, C.; Heagerty, A. M.; Korsgaard, N.; Schiffrin, E. L.; Heistad, D. D. (1996). Vascular remodeling. *Hypertension* 28:505–506.
35. Schiffrin, E.L., Deng, L.Y. and Larochelle, P. (1993). Morphology of resistance arteries and comparison of effects of vasoconstrictors in mild essential hypertensive patients. *Clinical and Investigative Medicine*, 16:177-186.
36. Cuspidi, C.; Boselli, L.; Bragato, R.; Lonati, L.; Sampieri, L.; Bocciolone, M.; Leonetti, G.; Zanchetti, A. (1992). Echocardiographic and ultra-sonographic evaluation of cardiac and vascular hypertrophy in patients with essential hypertension. *Cardiol.* 80:305–311.
37. Ichiki, T.; Usui, M.; Kato, M.; Funakoshi, Y.; Ito, K.; Egashira, K.; Takeshita, A.

(1998). Downregulation of angiotensin II type 1 receptor gene transcription by nitric oxide. *Hypertens* 31:342–348.

38. Strauer, B. E. (1988). Coronary hemodynamics in hypertensive heart disease. Basic concepts, clinical consequences, and experimental analysis of regression of hypertensive microangiopathy. *Am. J. Med*. 84:45–54.
39. Weber, K. T. (1989). Cardiac interstitium in health and disease: The fibrillar collagen network. *J. Am. Coll. Cardiol*. 13:1637–1652.
40. Corda, S.; Samuel, J.; Rappaport, L. (2000). Extracellular matrix and growth factors during heart growth. *Heart Failure Rev*. 5:119–130.
41. Weber, K.T.; Sun, Y.; Tyagi, S. C.; Cleutjens, P. M. (1994). Collagen network of the myocardium: function, structural remodeling and regulatory mechanisms. *J. Mol. Cell. Cardiol*. 26:279–292.
42. Eghbali, M.; Weber, K. T. (1990). Collagen and the myocardium: fibrillar structure, biosynthesis and degradation in relation to hypertrophy and its regression. *Mol. Cell. Biochem*. 96:1–14.
43. Yang, C. M.; Kandaswamy, V.; Young, D.; Sen, S. (1997). Changes in collagen phenotypes during progression and regression of cardiac hypertrophy. *Cardiovas. Res*. 36:236–245.
44. Norton, G. R.; Tsotetsi, J.; Trifunovic, B.; Hartford, C.; Candy, G. P.; Woodiwiss, A. J. (1997). Myocardial stiffness is attributed to alterations in cross-linked collagen rather than total collagen or phenotypes in spontaneously hypertensive rats. *Circulation* 96 :1991–1998.
45. Conrad, C. H.; Brooks, W. W.; Hayes, J. A.; Sen, S.; Robinson, K. G.; Bing, O. H. L. (1995). Myocardial fibrosis and stiffness with hypertrophy and heart failure in the spontaneously hypertensive rat. *Circulation* 91:161–170.

46. Díez, J.; Querejeta, R.; López, B.; González, A.; Larman, M.; Martínez Ubago, J. L. (2002). Losartan-dependent regression of myocardial fibrosis is associated with reduction of left ventricular chamber stiffness in hypertensive patients. *Circulation* 105:2512–2517.
47. Weber, K.T.; Brilla, C.G.; Janicki J.S. (1993). Myocardial fibrosis: functional significance and regulatory factors. *Cardiovas. Res*. 27:341-348.
48. Kuwahara, F.; Kai, H.; Tokuda, K.; Takeya, M.; Takeshita, A.; Egashira, K.; Imaizumi, T. (2004). Hypertensive myocardial fibrosis and diastolic dysfunction. Another model of inflammation? *Hypertens* 43:739–745.
49. Assayag, P.; Carré, F.; Chevalier, B.; Delcayre, C.; Mansier, P.; Swynghedauw, B. (1997). Compensated cardiac hypertrophy: arrhythmogenicity and the new myocardial phenotype. I. *Fibrosis. Cardiovasc. Res*. 34:439–444.
50. Brilla, C. G.; Maisch, B.; Weber, K. T. (1992). Myocardial collagen matrix remodelling in arterial hypertension. *Eur. Heart J*. 13(Suppl. D):24–32.
51. Boluyt, M. O.; Bing, O. H. L. (1995). The lonely failing heart: a case for ECM genes. *Cardiovas. Res*. 30:835–840.
52. Mujumdar, V. S.; Tyagi, S. C. (1999). Temporal regulation of extracellular matrix components in transition from compensatory hypertrophy to decompensatory heart failure. *J. Hypertens*. 17:261–270.
53. Brown, L.; Duce, B.; Miric, G.; Sernia, C. (1999). Reversal of cardiac fibrosis in deoxycorticosterone acetate-salt hypertensive rats by inhibition of the renin-angiotensin system. *J. Am. Soc. Nephrol*. 10:S143–S148.
54. Dolber, P. C.; Spach, M. S. (1993). Conventional and confocal fluorescence microscopy of collagen fibers in the heart. *J. Histochem. Cytochem*. 41:465–469.
55. Delorme, R.; Benchaib, M.; Bryon, P. A.; Souchier, C. (1998). Measurement accuracy

in confocal microscopy. *J. Microscopy* 192:151–162.

56. Young, A. A.; Legrice, I. J.; Young, M. A.; Smaill, B. H. (1998). Extended confocal microscopy of myocardial laminae and collagen network. *J. Microscopy* 192:139–150.
57. Pickering, J. G.; Boughner, D. R. (1990). Fibrosis in the transplanted heart and its relation to donor ischaemic time: assessment with polarized light microscopy and digital image analysis. *Circulation* 81:949–958.
58. Bishop, J. E.; Laurent, G. J. (1995). Collagen turnover and its regulation in the normal and hypertrophying heart. *Eur. Heart J*. 16(Suppl. C):38–44.
59. Brilla, C. G.; Maisch, B.; Zhou, G.; Weber, K. T. (1995). Hormonal regulation of cardiac fibroblast function. *Eur. Heart J*. 16(Suppl. C):45–50.
60. Weber, K. T. (1997). Extracellular matrix remodeling in heart failure. A role for de novo angiotensin II generation. *Circulation* 96:4065-4082.
61. Villarreal, F. J.; Dillmann, W. H. (1992). Cardiac hypertrophy-induced changes in mRNA levels for TGF-β1, fibronectin, and collagen. *Am. J. Physiol*. 262:H1861–H1866.
62. Engelmyer, E.; van Goor, H.; Edwards, D. R.; Diamond, J. R. (1995). Differential mRNA expression of renal cortical tissue inhibitor of metalloproteinase-1, -2 and -3 in experimental hydronephrosis. *J. Am. Soc. Nephrol*. 5:1675–1683.
63. Kim, N. N.; Villegas, S.; Summerour, S. R.; Villarreal, F. J. (1999). Regulation of cardiac fibroblast extracellular matrix production by bradykinin and nitric oxide. *J. Mol. Cell. Cardiol*. 31:457–466.
64. Kolpakov, V.; Gordon, D.; Kulik, T. J. (1995). Nitric oxide-generating compounds inhibit total protein and collagen synthesis in cultured vascular smooth muscle cells. *Circulation Res*. 76:305–309.
65. Booz, G. W.; Baker, K. M. (1995). Molecular signalling mechanisms controlling

growth and function of cardiac fibroblasts. *Cardiovas. Res*. 30:537–543.

66. Hinglais, N.; Heudes, D.; Nicoletti, A. ; Mandet, C ; Laurent, M.; Bariéty, J.; Michel, J. (1994). Colocalization of myocardial fibrosis and inflammatory cells in rats. *Lab. Invest*. 70:286–294.
67. Nicoletti, A.; Heudes, D.; Mandet, C.; Hinglais, N.; Bariety, J.; Michel, J. (1996). Inflammatory cells and myocardial fibrosis: spatial and temporal distribution in renovascular hypertensive rats. *Cardiovas. Res*. 32:1096–1107.
68. Luft, F. C.; Mervaala, E.; Muller, D. N.; Gross, V.; Schmidt, F.; Park, J. K.; Schmitz, C (1999). Hypertension-induced end-organ damage: A new transgenic approach to an old problem. *Hypertens* 33:212–218.
69. Li, Y. Y.; McTiernan, C. F.; Feldman, A. M. (2000). Interplay of matrix metalloproteinases, tissure inhibitors of metalloproteinases and their regulators in cardiac matrix remodeling. *Cardiovas. Res*. 46:214–224.
70. Dollery, C. M.; McEwan, J. R.; Henney, A. M. (1995). Matrix metalloproteinases and cardiovascular disease. *Circulation Res*. 77: 863–868.
71. Tyagi, S. C. (1997). Proteinases and myocardial extracellular matrix turnover. *Mol. Cell. Biochem*. 168:1–12.
72. Spinale, F. G. (2002). Matrix metalloproteinases. Regulation and dysregulation in the failing heart. *Circulation Res*. 90:520–530.
73. Nishikawa, N.; Yamamoto, K.; Sakata, Y.; Mano, T.; Yoshida, J.; Miwa, T.; Takeda, H. (2003). Differential activation of matrix metalloproteinases in heart failure with and without ventricular dilatation. *Cardiovas. Res*. 57:766–774.
74. Boulanger, C. M. (1999). Secondary endothelial dysfunction: Hypertension and heart failure. *J. Mol. Cell. Cardiol*. 31:39–49.
75. Griendling, K. K.; Alexander, R. W. (1996). Endothelial control of the cardiovascular

system: recent advances. *FASEB J*. 10:283–292.

76. Inagami, T.; Naruse, M.; Hoover, R. (1995). Endothelium as an endocrine organ. *Annu. Rev. Physiol*. 57: 71–189.
77. Ferro, C. J.; Webb, D. J. (1997). Endothelial dysfunction and hypertension. *Drugs* 53(Suppl. 1):30–41.
78. Spieker, L. E.; Noll, G.; Ruschitzka, F. T.; Maier, W.; Lüscher, T. F. (2000). Working under pressure: the vascular endothelium in arterial hypertension. *J. Human Hypertens*. 14:617–630.
79. Konishi, M.; Su, C. (1983). Role of endothelium in dilator responses of spontaneously hypertensive rat arteries. *Hypertens.* 5:881–886.
80. Lockette, W. E.; Otsuka, Y.; Carretero, O. A. (1986). The loss of endothelium-dependent vascular relaxation in hypertension. *Hypertens*. 8(Suppl. II):II61–II66.
81. Lüscher, T. F.; Raij, L.; Vanhoutte, P. M. (1987). Endothelium-dependent vascular responses in normotensive and hypertensive Dahl rats. *Hypertens*. 9:157–163.
82. Hirata, Y.; Hayakawa, H.; Suzuki, E.; Kimura, K.; Kikuchi, K.; Nagano, T.; Hirobe, M. (1995). Direct measurements of endothelium-derived nitric oxide release by stimulation of endothelin receptors in rat kidney and its alteration in salt-induced hypertension. *Circulation* 91:1229–1235.
83. Linder L., Kiowski W., Buhler F.R.; Luscher T.F. (1990). Indirect evidence for release of endothelium derived relaxing factor in human forearm circulation *in vivo*: blunted response in essential hypertension. *Circulation*. 81:1762-1767.
84. Panza, J.A.; Casino, P. R.; Kilcoyne, C. M.; Quyyumi, A. A. (1993). Role of endothelium-derived nitric oxide in the abnormal endothelium-dependent vascular relaxation of patients with essential hypertension. *Circulation* 87:1468–1474.
85. Winquist, R. J.; Bunting, P. B.; Baskin, E. P.; Wallace, A. A. (1984). Decreased

endothelium-dependent relaxation in New Zealand genetic hypertensive rats. *J. Hypertens*. 2:541–545.

86. Wu, X.; Mäkynen, H.; Kähönen, M.; Arvola, P.; Porsti, I. (1996). Mesenteric arterial function in vitro in three models of experimental hypertension. *J. Hypertens*. 14:365–372.
87. Haynes, W. G.; Ferro, C. J.; O'Kane, K. P. J.; Somerville, D.; Lomax, C. C.; Webb, D. J. (1996). Systemic endothelin receptor blockade decreases peripheral vascular resistance and blood pressure in man. *Circulation*, 93:1860–1870.
88. Schiffrin, E.L. (1999). Role of endothelin-1 in hypertension. Hypertension, 34:876-881.
89. Haynes, W. G.; Hand, M. F.; Johnstone, H.; Padfield, P. L.; Webb, D. J. (1994). Direct and sympathetically mediated venoconstriction in essential hypertension. *J. Clin. Invest*. 94:1359–1364.
90. Yoshida, M.; Nonoguchi, H.; Owada, A.; Ishiyama, S.; Maeda, Y.; Ando, K.; Iwamoto, H.; Shiigai, T.; Marumo, F.; Tomita, K. (1994). Three cases of malignant hypertension: the roles of endothelin-1 and the renin-angiotensin-aldosterone system. *Clinical Nephrol*. 42: 295–299.
91. Nava, E.; Lüscher, T. F. (1995). Endothelium-derived vasoactive factors in hypertension: nitric oxide and endothelin. *J. Hypertens*. 13:S39–S48.
92. Yu, M.; Gopalakrishnan, V.; Wilson, T. W.; McNeill, J. R. (2001). Endothelin antagonist reduces hemodynamic responses to vasopressin in DOCA-salt hypertension. *Am. J. Physiol. Heart Circ. Physiol*. 281:H2511–H2517.
93. Singal, P. K.; Khaper, N.; Palace, V.; Kumar, D. (1998). The role of oxidative stress in the genesis of heart disease. *Cardiovas. Res*. 40:426-432.
94. Singal, P. K.; Khaper, N.; Palace, V.; Kumar, D. (1999). Oxidative stress in heart

failure: current understanding and prospective. *Heart Failure Rev*. 4:111–120.

95. Kaul, N.; Siveski-Iliskovic, N.; Hill, M.; Slezak, J.; Singal, P. K. (1993). Free radicals and the heart. *J. Pharmacol. Toxicol. Meth*. 30:55–67.
96. Singh, N.; Dhalla, A. K.; Seneviratne, C. K.; Singal, P. K. (1995). Oxidative stress and heart failure. *Mol. Cell. Biochem*. 147:77–81.
97. Li, J.; Gall, N. P.; Grieve, D. J.; Chen, M.; Shah, A. M. (2002). Activation of NADPH oxidase during progression of cardiac hypertrophy to failure. *Hypertens*. 40:477-484.
98. Sawyer, D. B.; Siwik, D. A.; Xiao, L.; Pimentel, D. R.; Singh, K.; Colucci, W. S. (2002). Role of oxidative stress in myocardial hypertrophy and failure. *J. Mol. Cell. Cardiol*. 34:379–388.
99. Ames, B. N.; Shigenaga, M. K.; Hagen, T. M. (1993). Oxidants, antioxidants, and the degenerative diseases of aging. *Proc. Nat. Acad. Sci. USA* 90:7915–7922.
100. Lee, S. H.; Blair, I. A. (2001). Oxidative DNA damage and cardiovascular disease. *Trends Cardiovas. Med*. 11:148–155.
101. Marnett, L. J. (2000). Oxyradicals and DNA damage. *Carcinogenesis* 21:361–370.
102. Griendling, K. K.; Sorescu, D.; Ushio-Fukai, M. (2000). NAD(P)H oxidase: role in cardiovascular biology and disease. *Circulation Res*. 86:494–501.
103. Heymes, C.; Habib, A.; Yang, D.; Mathieu, E.; Marotte, F.; Samuel, J.; Boulanger, C. M. (2000). Cyclo-oxygenase-1 and 2 contribution to endothelial dysfunction in ageing. *Br. J. Pharmacol*. 131:804–810.
104. Takimoto, E.; Kass, D. A. (2007). Role of oxidative stress in cardiac hypertrophy and remodeling. *Hypertension* 49:241–248.
105. Dhalla, A. K.; Singal, P. K. (1994). Antioxidant changes in hypertrophied and failing guinea pig hearts. *Am. J. Physiol*. 266:H1280–H1285.
106. Nakamura, K.; Fushimi, K.; Kouchi, H.; Mihara, K.; Miyazaki, M.; Ohe, T.; Namba,

M. (1998). Inhibitory effects of antioxidants on neonatal rat cardiac myocyte hypertrophy induced by tumor necrosis factor-alpha and angiotensin II. *Circulation* 98 :794–799.

107. Cheng, T. H.; Shih, N. L.; Chen, S. Y.; Wang, D. L.; Chen, J. J. (1999). Reactive oxygen species modulate Endothelin-I-induced c-fos gene expression in cardiomyocytes. *Cardiovas. Res*. 41:654–662.
108. Amin, J. K.; Xiao, L.; Pimentel, D. R.; Pagano, P. J.; Singh, K.; Sawyer, D. B.; Colucci, W. S. (2001). Reactive oxygen species mediate alpha-adrenergic receptor-stimulated hypertrophy in adult rat ventricular myocytes. *J. Mol. Cell. Cardiol*. 33:131–139.
109. Farré, A. L.; Casado, S. (2001). Heart failure, redox alterations, and endothelial dysfunction. *Hypertens*. 38:1400–1405.
110. Keith, M.; Geranmayegan, A.; Sole, M. J.; Kurian, R.; Robinson, A.; Omran, A. S.; Jeejeebhoy, K. N. (1998). Increased oxidative stress in patients with congestive heart failure. *J. Am. Coll. Cardiol*. 31:1352–1356.
111. Siwik, D. A.; Pagano, P. J.; Colucci, W. S. (2001) Oxidative stress regulates collagen synthesis and matrix metalloproteinase activity in cardiac fibroblasts. *Am. J. Physiol. Cell Physiol*. 280:C53–C60.
112. Li, P.; Dietz, R.; von Harsdorf, R. (1999). Superoxide induces apoptosis in cardiomyocytes, but proliferation and expression of transforming growth factor-β1 in cardiac fibroblasts. *FEBS Lett*. 448:206–210.
113. Kojda, G.; Harrison, D. (1999). Interactions between NO and reactive oxygen species: pathophysiological importance in atherosclerosis, hypertension, diabetes and heart failure. *Cardiovas. Res*. 43:562–571.
114. Katz, A. M. (1993). Cardiac ion channels. *New Eng. J. Med*. 328:1244–1251.

115. Deal, K. K.; England, S. K.; Tamkun, M. M. (1996). Molecular physiology of cardiac potassium channels. *Physiol. Rev*. 76:49–67.

116. Reddy, H. K.; Wasson, S.; Koshy, S. K. G.; Komatireddy, R. (2003). Structural correlates of electrical remodeling in ventricular hypertrophy. *Cardiovas. Res*. 58: 495–497.

117. Hart, G. (1994). Cellular electrophysiology in cardiac hypertrophy and failure. *Cardiovasc. Res*. 28:933–946.

118. Boyden, P. A.; Jeck, C. D. (1995). Ion channel function in disease. *Cardiovas. Res*. 29:312-318.

119. Momtaz, A.; Coulombe, A.; Richer, P.; Mercadier, J.; Coraboeuf, E. (1996). Action potential and plateau ionic currents in moderately and severely DOCA-salt hypertrophied rat hearts. *J. Mol. Cel. Cardiol*. 28:2511–2522.

120. Li, Q.; Keung, E. C. (1994). Effects of myocardial hypertrophy on transient outward current. *Am. J. Physiol*. 266:H1738–H1745.

121. Acharya, R.; Kannathal, U. N.; Hua, L. M.; Yi, L. M. (2005). Study of heart rate variability signals at sittingand lying postures. *J. Bodywork Movement Therap*. 9:134–141.

122. Akselrod, S. G.; Ubelf, S.; Bergeracan, C. (1981). Power spectrum analysis of heart-rate fluctuation – A quantitative probe of beat to-beat Ccardiovascular control. *Science* 213:220–222.

123. Taskforce of the European Society of Cardiology and the North American Society of Pacing and Electrophysiology (1996). Heart rate variability. Standards of measurement, physiological interpretation, and clinical use. *Circulation* 93:1043–1065.

124. Bigger, J. T.; Fleiss, J. L.; Steinman, R. C.; Rolnitzky, L. M.; Kleiger, R. E.; Rottman, J. N. (1992). Frequency domain measures of heart period variability and mortality after

myocardial infarction. *Circulation*. 85:164–171.

125. Krüger, C.; LAnderer, V.; Zugck, C.; Ehmke, H.; Kübler, W.; Haass, M. (2000). The bradycardic agent zatebradine enhances baroreflex sensitivity and heart rate variability in rats early after myocardial infarction. *Cardiovasc. Res*. 45:900–912.
126. Sanyal, S. N.; Arita, M.; Ono, K. (2002). Inhomogeneous derangement of cardiac autonomic nerve control in diabetic rats. *Circ. J*. 66:283–288.
127. Jalife, J.; Michaels, D. C. (1994). Neural control of sinoatrial pacemaker activity. In: Levy MN, Schwartz PJ, eds. Vagal Control of the Heart: Experimental Basis and Clinical Implications. Armonk, NY: Futura :173–205.
128. Hall, J. E. (2010). Guyton and Hall Textbook of Medical Physiology. 12th ed.; Saunders, Elsevier, Philadelphia: USA, USA.
129. Lown, B.; Verrier, R. L. (1976). Neural activity and ventricular fibrillation. *New Engl. J. Med*. 294:1165–1170.
130. Dreifus, L. S. Agarwal, J. B.; Botvinick, E. H.; Ferdinand, K. C.; Fisch, C.; Fisher, J. D.; Kennedy, J. W.; Kerber, R. E.; Lambert, C. R.; Okike, O. N.; Prystowsky, E. N.; Saksena, S. V.; Schroeder, J. S.; Williams, D. O. (1993). Heart rate variability for risk stratification of life-threatening arrhythmias. *J. Am. Coll. Cardiol*. 22:948–950.
131. Pereira-Junior, P. P.; Marocolo, M.; Rodrigues, F. P.; Medei, E.; Nascimento, J. H. M. (2010). Noninvasive method for electrocardiogram recording in conscious rats: feasibility for heart rate variability analysis. *Anals Acad. Brasil Ciências* 82:431–437.
132. Koley, K. M.; Lal, J. (1994). Pharmacological effects of azadirachta indica (neem) leaf extract on the ecg and blood pressure of rat. *Indian J. Physiol. Pharmacol* 38:223–225.
133. Obiefuna, I.; Young, R. (2005). Concurrent administration of aqueous *Azadirachta indica* (Neem) leaf extract with DOCA-salt prevents the development of hypertension

and accompanying electrocardiogram changes in the rat. *Phytother. Res*. 19:792–795.

134. Akita, M.; Kuwahara, M.; Tsubone, H.; Sugano, S. (1998). Electrocardiographic changes during furosemide-induced hypo-kalemia in the rat. *J. Electrocar-diology* 31:45–49.

135. Anderson, B. (2000). Echocardiography: The normal examination and echocardiographic measurements. Brisbane, Australia: MGA Graphics.

136. Ommen, S. R.; Nishimura, R. A.; Appleton, C. P.; Miller, F. A.; Oh, J. K.; Redfield, M. M.; Tajik, A. J. (2000). Clinical utility of Doppler echocardiography and tissue Doppler imaging in the estimation of left ventricular filling pressures: A comparative simultaneous Doppler-catheterization study. *Circulation* 102:1788–1794.

137. Bjornerheim, R.; Grogaard, H. K.; Kjekshus, H., Attramadal, H.; Smiseth, O. A. (2001). High frame rate Doppler echocardiography in the rat: an evaluation of the method. *Eur. J. Echocardio*. 2:78–87.

138. de Simone, G.; Wallerson, D. C.; Volpe, M.; Devereux, R. B. (1990). Echocardiographic measurement of left ventricular mass and volume in normotensive and hypertensive rats. Necropsy validation. *Am. J. Hypertens*. 3:688–696.

139. Litwin, S. E.; Katz, S. E.; Morgan, J. P.; Douglas, P. S. (1994). Serial echocardiographic assessment of left ventricular geometry and function after large myocardial infarction in the rat. *Circulation* 89:345–354.

140. Brown, L.; Fenning, A.; Chan, V.; Loch, D.; Wilson, K.; Anderson, B.; Burstow, D. (2002). Echocardiographic assessment of cardiac structure and function in rats. *Heart, Lung Circ*. 11:167–173.

141. Doggrell, S. A.; Brown, L. (1998). Rat models of hypertension, cardiac hypertrophy and failure. *Cardiovas. Res*. 39:89–105.

142. Pinto, Y. M.; Paul, M.; Ganten, D. (1998). Lessons from rat models of hypertension:

from Goldblatt to genetic engineering. *Cardiovasc*. *Res*. 39:77–88.

143. Crofton, J. T.; Share, L. (1997). Gonadal hormones modulate deoxycorticosterone-salt hypertension in male and female rats. *Hypertens* 29:494–499.
144. de Champlain, J., Farley, L.; Cousineau, D.; van Ameringen, M. R. (1976). Circulating catecholamine levels in human and experimental hypertension. *Circ. Res*. 38:109–114.
145. Inada, Y.; Wada, T.; Shibouta, Y. (1994). Antihypertensive effects of a highly potent and long-acting angiotensin II subtype-1 receptor antagonist, (±)-1-(cyclohexyloxycarbonyloxy)ethyl-2-ethoxy-1-[[2'-(1H-tetrazol-5-yl)biphenyl-4-yl] methyl]-1H-benzimidazole-7-carboxylate (TCV-116), in various hypertensive rats. *J. Pharmacol. Exp. Therap*. 268:1540–1547.
146. Fernandes, S.; Bruneval, P.; Hagege, A.; Heudes, D.; Ghostine, S.; Bouby, N. (2002). Chronic V2 vasopressin receptor stimulation increases basal blood pressure and exacerbates deoxycorticosterone acetate-salt hypertension. *Endocrinol*. 143:2759–2766.
147. Larivière, R.; Day, R.; Schiffrin, E. L. (1993). Increased expression of endothelin-1 gene in blood vessels of deoxycorticosterone acetate-salt hypertensive rats. *Hypertens* 21:916–920.
148. Matsumura, Y.; Hashimoto, N.; Taira, S.; Kuro, T.; Kitano, R.; Ohkita, M.; Opgenorth, T. J. et al. (1999). Different contributions of endothelin-A and endothelin-B receptors in the pathogenesis of deoxycorticosterone acetate-salt-induced hypertension in rats. *Hypertens* 33:759–765.
149. Schenk, J.; McNeill, J. H. (1992). The pathogenesis of DOCA-salt hypertension. *J. Pharmacol. Toxicolo. Meth*. 27:161–170.
150. Bouvier, M.; de Champlain, J. (1986). Increased sympathoadrenal tone and adrenal

medulla reactivity in DOCA-salt hypertensive rats. *J. Hypert*. 4:157–163.

151. Wright, J. M.; Musini, V. M. (2009). First-line drugs for hypertension. Cochrane Database of Systematic Reviews 8 (3): doi: 10.1002/14651858.CD001841.
152. Zillich, A. J.; Garg, J.; Basu, S.; Bakris, G. L.; Carter, B. L. (2006). Thiazide diretics, potassium and the development of diabetes: a quantitative review. *Hypertens.*48:19–224.
153. Lindholm, L. H.; Carlberg, B.; Samuelsson, O. (2005). Should beta blockers remain first choice in the treatment of primary hypertension? A meta-analysis. *Lancet* 366(9496):1545–1553.
154. Wu, H. Y.; Huang, J. W.; Lin, H. J.; Liao, W. C.; Peng, Y. S.; Hung, K. Y.; Wu, K. D.; Tu, Y. K.; Chien, K. L. (2013). Comparative effectiveness of renin-angiotensin system blockers and other antihypertensive drugs in patients with diabetes: systematic review and Bayesian network meta-analysis. *BMJ* 347:f6008. doi:10.1136/bmj.f6008.
155. ALLHAT Officers and Coordinators for the ALLHAT Collaborative Research Group (2003). Diuretic versus alpha-blocker as first-step antihypertensive therapy. *Hypertens* 42:239–246. doi:10.1161/01. HYP.0000086521.95630.5A.
156. Granger, C. B.; McMurray, J. J.; Yusuf, S. et al. (2003). Effects of candesartan in patients with chronic heart failure and reduced left-ventricular systolic function intolerant to angiotensin-converting-enzyme inhibitors: the CHARM-Alternative trial. *Lancet* 362(9386):772–776.
157. Julius, S.; Kjeldsen, S. E.; Weber, M. et al. (2004). Outcomes in hypertensive patients at high cardiovascular risk treated with regimens based on valsartan or amlodipine: the VALUE randomised trial. *Lancet* 363(9426):2022–2031.
158. Wright, Jr., J.T. (2002). Effect of blood pressure lowering and antihypertensive drug class on progression of hypertensive kidney disease: Results from the AASK trial.

JAMA 288(19):2421.

159. Leenen, F. H. H.; Nwachuku, C. E.; Black, H. R.; Cushman, W. C.; Davis, B. R.; Simpson, L. M.; Alderman, M. H.; Atlas, S. A.; Basile, J. N.; Cuyjet, A. B.; Dart, R.; Felicetta, J. V.; Grimm, R. H.; Haywood, L. J.; Jafri, S. Z.A.; Proschan, M. A.; Thadani, U.; Whelton, P. K.; Wright, J. T. (2006). Clinical events in high-risk hypertensive patients randomly assigned to calcium channel blocker versus angiotensin-converting enzyme inhibitor in the antihypertensive and lipid-lowering treatment to prevent heart attack trial. *Hypertens* 48:374–384.
160. ALLHAT Officers and Coordinators for the ALLHAT Collaborative Research Group. (2002). Major outcomes in high-risk hypertensive patients randomized to angiotensin-converting enzyme inhibitor or calcium channel blocker vs diuretic: The antihypertensive and lipid-lowering treatment to prevent heart attack trial (ALLHAT). *JAMA* 288(23):2981–2997.
161. Russell, R. P. (1988). Side effects of calcium channel blockers. *Hypertens* 11:II42-44.
162. Appel, L. J.; Moore, T. J.; Obarzanek, E.; Vollmer, W. M.; Svetkey, L. P.; Sacks, F. M.; Bray, G. A.; Vogt, T. M.; Cutler, J. A.; Windhauser, M. M.; Lin, P. H.; Karanja, N. (1997). A clinical trial of the effects of dietary patterns on blood pressure, *N. Engl. J. Med*. 33:1117–1124.
163. Margetts, B. M.; Beilin, L. J.; Vandongen, R.; Armstrong, B. K. (1986). Vegetarian diet in mild hypertension: a randomised controlled trial. *BMJ* 293:1468–1471.
164. He, F. J.; Nowson, C. A.; MacGregor, G. A. (2006). Fruit and vegetable consumption and stroke: meta-analysis of cohort studies. *Lancet* 367:320–326.
165. Mlakar, P.; Salobir, B.; Čobo, N.; Janja Strašek, N.; Prezelj, M.; Debevc, A.; Jug, B.; Terčelj, M.; Šabovič, M. (2015). The effect of cardioprotective diet rich with naturalantioxidants on chronic inflammation and oxidized LDL during cardiac

rehabilitation on in patients after acute myocardial infarction. *IJC Heart & Vasculature* 7:40–48.

166. Bravo, L. (1998). Polyphenols: Chemistry, dietary sources, metabolism, and nutritional significance. *Nutr. Rev*. 56:317–333.
167. Manach, C.; Scalbert, A.; Morand, C.; Remesy, C.; Jimenez, L. (2004). Polyphenols: food sources and bioavailability. *Am. J. Clin. Nutr*. 79:727–747.
168. Frankel, E. N.; Waterhouse, A. L.; Kinsella, J. E. (1993). Inhibition of human LDL oxidation by resveratrol. *Lancet* 341:1103–1104.
169. Hertog, M. G.; Feskens, E. J.; Hollman, P. C.; Katan, M. B.; Kromhout, D. (1993). Dietary antioxidant flavonoids and risk of coronary heart disease: The Zutphen elderly study. *Lancet* 342:1007–1011.
170. Williamson, G.; Manach, C. (2005). Bioavailability and bioefficacy of polyphenols in humans. II. Review of 93 intervention studies. *Am. J. Clin. Nutr*. 81:243–255.
171. Wongcharoen, W.; Phrommintikul, A. (2009). The protective role of curcumin in cardiovascular diseases. *Int. J. Cardiol.* 133:145–151.
172. Alappat, L.; Awad, A. B. (2010). Curcumin and obesity: evidence and mechanisms. *Nutr. Rev*. 68:729–738.
173. Hlavačková, L.; Janegová, A.; Uličná, O.; Janega, P.; Černá, A.; Babál, P. (2011). Spice up the hypertension diet curcumin and piperine prevent remodeling of aorta in experimental L-NAME induced hypertension. *Nutr. Metab. (Lond.)* 8:72 (doi: 10.1186/1743-7075-8-72).
174. Morimoto, T.; Sunagawa, Y.; Kawamura, T.; Takaya, T.; Wada, H.; Nagasawa, A.; Komeda, M.; Fujita, M.; Shimatsu, A.; Kita, T.; Hasegawa, K. (2008). The dietary compound curcumin inhibits p300 histone acetyltransferase activity and prevents heart failure in rats. *J. Clin. Invest*. 118:868–878.

175. Cheng, A. L.; Hsu, C. H.; Lin, J. K.; Hsu, M. M.; Ho, Y. F.; Shen, T. S.; Ko, J. Y.; Lin, J. T.; Lin, B. R.; Ming-Shiang, W.; Yu, H. S.; Jee, S. H.; Chen, G. S.; Chen, T. M.; Chen, C. A.; Lai, M. K.; Pu, Y. S.; Pan, M. H.; Wang, Y. J.; Tsai, C. C.; Hsieh, C. Y. (2001). Phase I clinical trial of curcumin, a chemopreventive agent, in patients with high-risk or pre-malignant lesions. *Anticancer Res*. 21:2895–2900.

176. Soni, K. B.; Kuttan, R. (1992). Effect of oral curcumin administration on serum peroxides and cholesterol levels in human volunteers. *Indian J. Physiol. Pharmacol.* 36:273–275.

177. Ramírez-Boscá, A.; Soler, A.; Carrión, M. A.; Díaz-Alperi, J.; Bernd, A.; Quintanilla, C.; Almagro, Q. E.; Miquel, J. (2000). Ahydroalcoholic extract of curcuma longa lowers the apo B/apoA ratio. Implications for atherogenesis prevention. *Mech. Ageing Dev*. 119:41–47.

178. Palani, V.; Senthilkumaran, R. K.; Govindasamy, S. (1999). Biochemical evaluation of antitumor effect of Muthu Marunthu (a herbal formulation) on experimental fibrosarcoma in rats. *J. Ethnopharmacol*. 65:257–265.

179. Patro, B. S.; Bauri, A. K.; Mishra, S.; Chattopadhyay, S. (2005). Antioxidant activity of *Myristica malabarica* extracts and their constituents. *J. Agric. Food Chem.* 53:6912–6918.

180. Banerjee, D.; Maity, B.; Bauri, A. K.; Bandyopadhyay, S. K.; Chattopadhyay, S. (2007). Gastroprotective properties of *Myristica malabarica* against indomethacin-induced stomach ulceration: a mechanistic exploration. *J. Pharm. Pharmacol*. 59:1555–1565.

181. Banerjee, D.; Bauri, A. K.; Guha, R. K.; Bandyopadhyay, S. K.; Chattopadhyay, S. (2008). Healing properties of malabaricone B and malabaricone C against

indomethacin-induced gastric ulceration and mechanism of action. *Eur. J. Pharmacol.* 578:300–312.

182. Tyagi, M.; Bhattacharyya, R.; Bauri, A. K.; Patro, B. S.; Chattopadhyay, S. (2014). DNA damage dependent activation of CHK1 and MAPK-p38 are required in malabaricone C-induced mitochondrial cell death. *Biochim. Biophys. Acta (General)* 1840:1014–1027.
183. Tyagi, M.; Patro, B. S.; Chattopadhyay, S. (2014). Mechanism of the malabaricone C-induced toxicity to the MCF-7 cell line. *Free Radic. Res*. 48:466–477.
184. Heath, D. D.; Pruitt, M. A.; Brenner, D. E.; Rock, C. L. (2003). Curcumin in plasma and urine: quantitation by high-performance liquid chromatography. *J. Chrom. B*, 783:287–295.
185. Alves, H.N.C; Aura Silva, L.M.D; Olsson, I.A.S; Orden, J.M.L; Antunes, L.M. (2010). Anesthesia with Intraperitoneal Propofol, Medetomidine, and Fentanyl in Rats. *J Am Assoc Lab Anim Sci.* 49(4):454–459.
186. Han, P.; Shen, F. M.; Xie, H. H.; Chen, Y. Y.; Miao, C. Y.; Mehta, J. L.; Sassard, J.; Feng Su, D. (2009). The combination of atenolol and amlodipine is better than their monotherapy for preventing end-organ damage in different types of hypertension in rats. *J. Cell. Mol. Med*. 13:726–734.
187. Fenning, A.; Harrison, G.; Rose'meyer, R.; Hoey, A.; Brown, L. (2005). L-Arginine attenuates cardiovascular impairment in DOCA-salt hypertensive rats. *Am. J. Physiol. Heart Circ. Physiol*. 289:H1408–1416.
188. Mirkovic, S.; Seymour, A.M.L; Fenning, A; Strachan, A; Margolin, S.B; Taylor, S.M; Brown, L. (2002). Attenuation of cardiac fibrosis by pirfenidone and amiloride in DOCA-salt hypertensive rats. *Br J Pharmacol* 135:961–968.
189. Chan, V.; Hoey, A.; Brown, L. (2006). Improved cardiovascular function with

aminoguanidine in DOCA-salt hypertensive rats. *Br. J. Pharmacol.* 148:902–908.

190. Lawes, C. M. M.; Bennett, D. A.; Feigin, V. L.; Rodgers, A. (2004). Blood pressure and stroke: an overview of published reviews. *Stroke* 35:1024–1033.
191. Moser, M.; Roccella, E. J. (2013). The treatment of hypertension: a remarkable success story. *J. Clin. Hypertens. (Greenwich)* 15:88–91.
192. Whelton, P. K. (2005). Global burden of hypertension: an analysis of worldwide data. *Lancet* 365 (9455): 217–223.
193. Padwal, R.; Campbell, N.; Touyz, R. M. (2005). Applying the 2005 Canadian Hypertension Education Program recommendations: 3. Lifestyle modifications to prevent and treat hypertension. *Can. Med. Assoc. J*. 173:749–751.
194. Sruthy, P. N.; Anoop, K. R. (2013). Healing Hypertension: A focus on alternative systems of medicine. *Int. J. Pharm. Sci. Rev. Res*. 21:264–273.
195. Balachandran, P. (2005). Cancer- an ayurvedic perspective. *Pharmacol. Res*. 51:19–30.
196. Chandola, H. M. (2012). Lifestyle disorders: Ayurveda with lots of potential for prevention. *Ayu*, 33:327. doi:10.4103/0974-8520.108814.
197. World Health Organization (2002). The World Health Report: Reducing Risk, Promoting Healthy Life. Geneva, Switzerland: *World Health Organization.*
198. Medina-Remón, A.; Zamora-Ros, R.; Rotchés-Ribalta, M.; Andres-Lacueva, C.; Martnez-González, M. A. et al, (2011). Total polyphenol excretion and blood pressure in subjects at high cardiovascular risk. *Nutr. Metabol. Cardiovas. Dis*. 21:323–331.
199. Taubert, D.; Roesen, R.; Schomig, E. (2007). Effect of cocoa and tea intake on blood pressure. *Arch. Internal Med*. 167:626–634.
200. Hellström, J. K.; Shikov, A. N.; Makarova, M. N.; Pihlanto, A. M.; Pozharitskaya, O. N.; Ryhänen, E.; Kivijärvi, P.; Makarov, V. G.; Mattila, P. H. (2010). Blood pressure-

lowering properties of chokeberry (*Aronia mitchurinii*, var. Viking). *J. Funct. Foods* 2:163–169.

201. Zibadi, S.; Farid, R.; Moriguchi, S.; Lu, Y.; Foo, L. Y.; Tehrani, P. M.; Ulreich, J. B.; Watson, R. R. (2007). Oral administration of purple passion fruit peel extract attenuates blood pressure in female spontaneously hypertensive rats and humans. *Nutr. Res*. 27:408–416.
202. World Health Organization (2004). Mortality and burden of disease estimates for WHO member states in 2004, Geneva: *WHO*.
203. D'Agostino Sr., R. B.; Vasan, R. S.; Pencina, M. J.; Wolf, P. A.; Cobain, M.; Massaro, J. M.; Kannel, W. B. (2008). General cardiovascular risk profile for use in primary care: The Framingham heart study. *Circulation* 117:743–753.
204. Lüscher, T. F. (1994). The endothelium and cardiovascular disease-a complex relation. *New Engl. J. Med*. 330:1081–1083.
205. Libby, P. (2001). Current concepts of the pathogenesis of the acute coronary syndromes. *Circulation* 104:365–372.
206. Hamilton, C. A.; Miller, W. H.; Al-Benna, S.; Brosnan, M. J.; Drummond, R. D.; McBride, M. W.; Dominiczak, A. F. (2004). Strategies to reduce oxidative stress in cardiovascular disease. *Clin Sci*. 106:219–234.
207. Guyton, A. C. (1989). Dominant role of the kidneys and accessory role of whole-body autoregulation in the pathogenesis of hypertension. *Am. J. Hypertens*. 2:575–585.
208. Folkow, B. (1982). Physiological aspects of primary hypertension. *Physiol. Rev*. 62:347–354.
209. Levy, D.; Larson, M. G.; Vasan, R.; Kannel, W. B.; Ho, K. K. L. (1996). The progression from hypertension to congestive heart failure. *JAMA* 275:1557–1562.
210. Karam, H.; Heudes, D.; Gonzales, M. F.; Loffler, B. M.; Clozel, M.; Clozel, J. P.

(1996). Respective role of humoral factors and blood pressure in aortic remodeling of DOCA hypertensive rats. *Am. J. Hypertens*. 9:991–998.

211. Pepine, C. J.; Handberg, E. M. (2001). The vascular biology of hypertension and atherosclerosis and intervention with calcium antagonists and angiotensin-converting enzyme inhibitors. *Clin. Cardiol*. 24:V 1–5.
212. Zhu, Z. (2009). Window period for oxidative stress attenuating intervention (WPOS Theory). *Am. J. Biomed. Sci*. 1:250–259.
213. Aruoma, A. (1991). The radical cation of N, N-Diethyl-para-phenilendiamine: a possible indicator of oxidative stress in biological samples. *Res. Chem. Intermed*. 26:253–267.
214. Rice-Evans, C., Miller, N. J. (1994). Total antioxidant status in plasma and body fluids. *Method Enzymol*. 234:279–293.
215. Manning, R. D.; Tian, N.; Meng, S. (2005). Oxidative stress and antioxidant treatment in hypertension and the associated renal damage. *Am. J. Nephrol*. 25:311–317.
216. McEniery, C. M. (2006). Novel therapeutic strategies for reducing arterial stiffness. *Br. J. Pharmacol*. 148:881–883.
217. Griendling, K. K., Minieri, C. A., Ollerenshaw, J. D., & Alexander, R. W. (1994). Angiotensin II stimulates NADH and NADPH oxidase activity in cultured vascular smooth muscle cells. *Circ. Res*. 74:1141–1148.
218. Mittra, S.; Singh, M. (1998). Possible mechanism of captopril induced endothelium-dependent relaxation in isolated rabbit aorta. *Mol. Cell Biochem*. 183:63–67.
219. Feuerstein, G., Yue, T. L., Ma, X., & Ruffolo, R. R. (1998). Novel mechanism in the treatment of heart failure: inhibition of oxygen radicals and apoptosis by carvedilol. *Prog. Cardiovasc. Dis*. 41:17–24.
220. Di Wang, H., Hope, S., Du, Y., Quinn, M. T., Cayatte, A., Pagano, P. J., & Cohen, R.

A. (1999). Paracrine role of adventitial superoxide anion in mediating spontaneous tone of the isolated rat aorta in angiotensin II induced hypertension. *Hypertens* 33:1225–1232.

221. Suzuki, H., DeLano, F. A., Parks, D. A., Jamshidi, N., Granger, D. N., Ishii, H., Suematsu, M., Zweifach, B. W., & Schmid-Schonbein, G. W. (1998). Xanthine oxidase activity associated with arterial blood pressure in spontaneously hypertensive rats. *Proc. Natl. Acad. Sci. USA* 95:4754–4759.
222. Houston, M., Estevez, A., Chumley, P., Aslan, M., Marklund, S., Parks, D. A., & Freeman, B. A. (1999). Binding of xanthine oxidase to vascular nitric oxide-dependent signaling. *J. Biol. Chem*. 274:4985–4994.
223. Tarpey, M. M.; Wink, D. A.; Grisham, M. B. (2004). Methods for detection of reactive metabolites of oxygen and nitrogen: in vitro and in vivo considerations. *Am. J. Physiol. Regul. Integr. Comp. Physiol*. 286:R431–R444.
224. Benov, L.; Sztejnberg, L.; Fridovich, I. (1998). Critical evaluation of the use of hydroethidine as a measure of superoxide anion radical. *Free Radic. Biol. Med.* 25:826–831.
225. Berry, C. E.; Hare, J. M. (2004). Xanthine oxidoreductase and cardiovascular disease: molecular mechanisms and pathophysiological implications. *J Physiol*. 555:589–606.
226. Doehner, W.; Schoene, N.; Rauchhaus, M.; Leyva-Leon, F.; Pavitt, D. V.; Reaveley, D. A.; Schuler, G.; Coats, A. J. S.; Anker, S. D.; Hambrecht, R. (2002). Effects of xanthine oxidase inhibition with allopurinol on endothelial function and peripheral blood flow in hyperuricemic patients with chronic heart failure. *Circulation* 105:2619–2624.
227. Viel, E. C.; Benkirane, K.; Javeshghani, D.; Touyz, R. M.; Schiffrin, E. L. (2008). Xanthine oxidase and mitochondria contribute to vascular superoxide anion generation

in DOCA-salt hypertensive rats. *Am. J. Physiol. Heart and Circ. Physiol*. 295:H281–H288.

228. Beswick, R. A.; Dorrance, A. M.; Leite, R.; Webb, R. C. (2001). NADH/NADPH oxidase and enhanced superoxide production in the mineralocorticoid hypertensive rat. *Hypertens* 38:1107–1111.
229. Unger, B. S.; Patil, B. M. (2009). Apocynin improves endothelial function and prevents the development of hypertension in fructose fed rat. *Indian J. Pharmacol*. 41:208–212.
230. Curtiss, L. K. (2009). Clinical implications of basic research: Reversing atherosclerosis? *New Engl. J. Med*. 360:1114–1116.
231. Vane, J. R.; Anggard, E. E.; Botting, R. M. (1990). Regulatory functions of the vascular endothelium. *New Engl. J. Med*. 323:27–36.
232. Moncada, S.; Vane, J. R. (1978). Pharmacology and endogenous roles of prostaglandin endoperoxides, thromboxane A2, and prostacyclin. *Pharmacol. Rev*. 30:293–331.
233. Mohring, J.; Mohring, B.; Petri, M.; Haack, D. (1977). Vasopressor role of ADH in the pathogenesis of malignant DOC hypertension. *Am. J. Physiol.* 232: F260–269.
234. Kunes, J.; Nedvidek, J.; Zicha, J. (1989). Vasopressin and water distribution in rats with DOCA-salt hypertension. *J. Hypertens. Suppl*. 7: S204–205.
235. Zicha, J.; Kunes, J.; Lebl, M.; Pohlova, I.; Slaninova, J.; Jelinek, J. (1989). Antidiuretic and pressor actions of vasopressin in age-dependent DOCA-salt hypertension. *Am. J. Physiol*. 256: R138–145.
236. Bogdan, C. (2001). Nitric oxide and the immune response. *Nat. Immunol*. 2:907–916.
237. Potter, L. R.; Yoder, A. R.; Flora, D. R.; Antos, L. K.; Dickey, D. M. (2009). Natriuretic peptides: their structures, receptors, physiologic functions and therapeutic

applications. *Handbook Exp. Pharmacol*. 191:341–366.

238. Hughes, A. K.; Stricklett, P.; Padilla, E.; Kohan, D. E. (1996) Effect of reactive oxygen species on endothelin-1 production by human mesangial cells. *Kidney Int*. 49:181–189.

239. Hou, Y. C.; Janczuk, A.; Wang, P. G. (1999). Current trends in the development of nitric oxide donors. *Curr. Pharm. Design* 5:417–441.

240. Fink, G. D.; Johnson, R. J.; Galligan, J. J. (2000). Mechanisms of increased venous smooth muscle tone in desoxycorticosterone acetate-salt hypertension. *Hypertens* 35:464-469.

241. Johnson, R. J.; Galligan, J. J.; Fink, G. D. (2001). Effect of an ET(B)-selective and a mixed ET(A/B) endothelin receptor antagonist on venomotor tone in deoxycorticosterone-salt hypertension. *J. Hypertens*. 19:431–440.

242. Zicha, J.; Kunes, J.; Lebl, M.; Pohlova, I.; Slaninova, J.; Jelinek, J. (1989). Antidiuretic and pressor actions of vasopressin in age-dependent DOCA-salt hypertension. *Am. J. Physiol. Regul. Integr. Comp. Physiol*. 256:R138–R145.

243. Yu, M.; Gopalakrishnan, V.; McNeill, J. R. (1998). Hemodynamic effects of a selective endothelin-a receptor antagonist in deoxycorticosterone acetate-salt hypertensive rats. *J. Cardiovasc. Pharmacol*. 31:S262–S264.

244. Quehenberger, P.; Bierhaus, A.; Fasching, P.; Muellner, C.; Klevesath, M.; Hong, M.; Stier, G.; Sattler, M.; Schleicher, E.; Speiser, W.; Nawroth, P. P. (2000). Endothelin-1 transcription is controlled by nuclear factor-kB in AGE-stimulated cultured endothelial cells. *Diabetes* 49:1561–1570.

245. Maity, B.; Yadav, S. K.; Patro, B. S.; Bandyopadhyay, S. K.; Chattopadhyay, S. (2012). Molecular mechanism of the anti-inflammatory activity of a natural diarylnonanoid, malabaricone C. *Free Radic. Biol. Med*. 52:1680–1691.

246. Li, L.; Fink, G. D.; Watts, S. W.; Northcott, C. A.; Galligan, J. J.; Pagano, P. J.; Chen, A. F. (2003). Endothelin-1 increases vascular superoxide via endothelin A–NADPH oxidase pathway in low-renin hypertension. *Circulation* 107:1053–1058.

247. Ma, X. L.; Gao, F.; Nelson, A. H.; Lopez, B. L.; Christopher, T. A.; Yue, T. L.; Barone, F. C. (2001). Oxidative inactivation of nitric oxide and endothelial dysfunction in stroke-prone spontaneous hypertensive rats. *J. Pharmacol. Exp. Ther*. 298:879–885.

248. Schiffrin, E. L. (2005). Vascular endothelin in hypertension. *Vascul. Pharmacol*. 43:19–29.

249. Deng, L. Y.; Schiffrin, E. L. (1992). Effects of endothelin on resistance arteries of DOCA-salt hypertensive rats. *Am. J. Physiol*. 262:H1782–1787.

250. Uehara, Y.; Numabe, A.; Hirawa, N.; Ishimitsu, T.; Takada, S.; Sugimoto, T.; Yagi, S. (1988). Alterations to the vascular vasodepressor prostaglandin system in DOCA-salt hypertensive rats and their enzymatic analysis. *J. Hypertens. Suppl*. 6: S392–394.

251. Van de Voorde, J.; Leusen, I. (1986). Endothelium dependent and independent relaxation of aortic rings from hypertensive rats. *Am. J. Physiol*. 250:H711–H717.

252. Perez-Vizcaino, F.; Duarte, J.; Andriantsitohaina, R. (2006). Endothelial function and cardiovascular disease: effects of quercetin and wine polyphenols. *Free Radic. Res*. 40:1054–1065.

253. Diercks, D. B.; Shumaik, G. M.; Harrigan, R. A.; Brady, W. J.; Chan, T. C. (2004). Electrocardiographic manifestations: electrolyte abnormalities. *J. Emergency Medicine* 27:153–160.

254. Perez, V.; Chang, E. T. (2014). Sodium-to-potassium ratio and blood pressure, hypertension, and related factors. *Adv. Nutr*. 5:712–741.

255. Moore, K. L.; Dalley, A. F.; Agur, A. M. (2007). Clinically Oriented Anatomy. 3rd ed.; Lippincott Williams & Wilkins, Baltimore: USA. p.92- 94

256. Capuano, V.; Ruchon, Y.; Antoine, S.; Sant, M. C.; Renaud, J. F. (2002). Ventricular hypertrophy induced by mineralocorticoid treatment or aortic stenosis differentially regulates the expression of cardiac K^+ channels in the rat. *Mol. Cell. Biochem*. 237:1–10.

257. Zhang, G. Q.; Zhang, W. (2009). Heart rate, lifespan, and mortality risk. *Ageing Res. Rev*. 8:52–60.

258. Tomaselli, G. F.; Marban, E. (1999). Electrophysiological remodeling in hypertrophy and heart failure. *Cardiovasc. Res*. 42:270–283.

259. Jalife, J.; Michaels, D. C. (1994). Neural control of sinoatrial pacemaker activity. In: Levy, M. N.; Schwartz, P. J., eds. Vagal Control of the Heart: Experimental Basis and Clinical Implications. Armonk, NY: Futura; 173-205.

260. Reichelt, M. E.; Willems, L.; Hack, B. A.; Peart, J. N.; Headrick, J. P. (2009). Cardiac and coronary function in the Langendorff-perfused mouse heart model. *Exp. Physiol*. 94:54–70.

261. Galderisi, M (2005). Diastolic dysfunction and diastolic heart failure: diagnostic, prognostic and therapeutic aspects. *Cardiovasc. Ultrasound* 3:9 doi:10.1186/1476-7120-3-9.

262. Mohring, J.; Mohring, B.; Naumann, H. J.; Philippi, A.; Homsy, E.; Orth, H, et al. (1975). Salt and water balance and renin activity in renal hypertension of rats. *Am. J. Physiol*. 228:1847–1855.

263. Navarro, C. M.; Montilla, P. M.; Martin, A; Jimenez, J.; Utrilla, P. M. (1993). Free radicals scavenger and antihepatotoxic activity of Rosmarinus. *Plant Med Phytother* 59:312–314.

264. Kwiatkowsha, S.; Piasecka, G.; Zieba, M.; Piotrowski, W.; Nowak, D. (1999) Increased serum concentrations of conjugated diens and malondialdehyde in patients

with pulmonary tuberculosis. *Respir. Med*. 93:272–276.

265. Hernández, N.; Torres, S. H.; de Sanctis, J. B.; Sosa, A. (2000). Metabolic changes in DOCA-salt hypertensive rats. *Res. Commun. Mol. Pathol. Pharmacol*. 108:201–211.
266. Seifi, B.; Kadkhodaee, M.; Karimian, S. M.; Zahmatkesh, M.; Xu, J.; Soleimani, M. (2010). Evaluation of renal oxidative stress in the development of DOCA-salt induced hypertension and its renal damage. *Clin. Exp. Hypertens*. 32:90–97.
267. Mason, R. P.; Kubant, R.; Jacob, R. F.; Walter, M. F.; Boychuk, B.; Malinski, T. (2006). Effect of nebivolol on endothelial nitric oxide and peroxynitrite release in hypertensive animals: Role of antioxidant activity. *J. Cardiovasc. Pharmacol*. 48:862–869.
268. Deoghare, S.; Kantharia, N. D. (2013). Effect of atenolol and enalapril treatment on oxidative stress parameters in patients with essential hypertension. *Int. J. Basic Clin. Pharmacol*. 2:252–256.
269. Kyselovic, J.; Krenek, P.; Wibo, M.; Godfraind, T. (2001). Effects of amlodipine and lacidipine on cardiac remodelling and renin production in salt-loaded stroke-prone hypertensive rats. *Br. J. Pharmacol*. 134:1516–1522.